

Performance Analysis of Cellular Networks with Digital Fixed Relays

By

Huining Hu, B.Eng.

A thesis submitted to

The Faculty of Graduate Studies and Research

In partial fulfillment of

The requirements of the degree of

Master of Applied Science

Ottawa-Carleton Institute for Electrical and Computer Engineering

Department of Systems and Computer Engineering

Carleton University

Ottawa, Ontario

© Copyright 2003, Huining Hu

The undersigned hereby recommends to the Faculty of Graduate Studies and Research
acceptance of the thesis

Performance Analysis of Cellular Networks with Digital Fixed Relays

Submitted by Huining Hu

In partial fulfillment of the requirements for the

Degree of Master of Applied Science

Thesis Supervisor
Dr. Halim Yanikomeroglu

Chair, Department of Systems and Computer Engineering
Dr. Rafik A. Goubran

Carleton University
September 2003

Abstract

The concept of relaying is a promising solution for the challenging throughput and high data rate coverage requirements of future wireless cellular networks. In this thesis we demonstrate that throughput and high data rate coverage can be enhanced significantly in such networks through the use of digital fixed relays operating with rather straightforward protocols which do not incur any capacity penalty (except for some modest signalling overhead); this demonstration is the main contribution of this thesis.

In particular we considered the downlink of a non-CDMA network where 6 digital fixed relays are placed evenly in each cell in a hexagonal layout. A user equipment chooses to receive the transmitted signal either directly (in single hop) from the base station or via one of the relays (in two hops). Distance-, pathloss-, and SINR-based algorithms are studied for the relay selection process. Whenever a relay is used, a second channel is needed as the relays cannot receive and transmit at the same channel. We propose a "pre-configured" relaying channel selection algorithm in which relays further reuse the already used channels in the network; but this reusing is done in a controlled manner in order to prevent the co-channel interference increasing to unacceptable levels. Due to the "pre-configured" nature of this algorithm, the channel selection is fixed (i.e., not dynamic) which incurs minimal overhead; at the same time, the benefits of relaying are achieved without any need for additional bandwidth. The improved links are exploited to yield higher throughput through the use of adaptive modulation and coding. Diversity benefits are also studied whenever the signal is received in two-hops.

We investigated the performance of the proposed algorithms for a number of system variables, including propagation parameters, cell sizes, transmit power levels, relay locations, number of user equipments, and transmission bandwidth, through Monte-Carlo simulations. We consistently observed that the throughput is increased and the outage is decreased (which may be converted to range extension), without any capacity penalty, for the realistic range of values of the parameters investigated. Our overall conclusion is that digital fixed relaying has great potential in providing the envisioned high data rate coverage in future wireless cellular networks.

Acknowledgments

First and most importantly of all, I would like to express my sincerest appreciation to my thesis supervisor, Dr. Halim Yanikomeroglu, for the tremendous time, comprehensive guidance and consistent support he has provided for this research. His profound knowledge and strong interests in this research area, as well as his nice personality have been an impetus to the completion of my study. I feel very proud and very honoured to have him as my thesis supervisor.

Secondly, I am grateful to Dr. David Falconer, as he has taken time to offer me academic support ever since the beginning of this research. My many thanks are extended to my academic advisor, Dr. Ian Marsland, as he has given me kind advice on course selections. I would also like to thank Xiaobin Tang, a member of this research team, in discussing and comparing her research results with mine.

In addition, I would like to take this opportunity to thank Nortel Networks for their financial support to make this research a success. Especially, I thank Dr. Shalini Periyalwar of Nortel Networks for many of her kind recommendations.

Last but not least, my family's support is another catalyst in my research motivation. I bestow my special gratitude upon my parents, my husband and my lovely daughter.

Table of Contents

Abstract	iii
Acknowledgments	iv
Table of Contents	v
List of Figures and Tables	viii
List of Acronyms	xiii
List of Symbols	xiv
Chapter 1 - INTRODUCTION	1
1.1 Nortel Networks Project on Cellular Networks with Relaying	2
1.2 Thesis Motivation	4
1.3 Research Overview	7
1.4 Relevant Literature	9
1.5 Thesis Organization	10
Chapter 2 - RELAYING CHANNEL PARTITION SCHEME AND RELAY SELECTION	12
2.1 Propagation Model	12
2.2 Adaptive Modulation and Coding	13
2.3 Cellular Layout	17
2.4 Relaying Channel Partition Scheme	20
2.5 Relay Selection	27
2.5.1 <i>Distance-based Algorithm</i>	28
2.5.2 <i>Pathloss-based Algorithm</i>	30
2.5.3 <i>SINR-based Algorithm</i>	31

2.6 Diversity	32
2.7 Simulation Model for $N = 1$ Case	33
Chapter 3 - SIMULATION ALGORITHM	34
3.1 Environment and Parameters Assumptions	34
3.2 Simulation Algorithm for $N = 4$ Case	35
3.3 Simulation Algorithm for $N = 1$ Case	41
Chapter 4 - SIMULATION RESULTS, PART I: $N = 4$ CASE	44
4.1 Average Spectral Efficiency for SINR-based Algorithm	44
4.2 Relay Usage	46
4.3 Average Spectral Efficiency for with and without ORB Cases	48
4.4 Average Spectral Efficiency Comparison for Different Relay Selection Algorithms	51
4.5 Average Spectral Efficiency Comparison for with and without Diversity	53
4.6 Effect of Background Noise	55
4.7 Effect of Bandwidth (i.e., Noise Power)	56
4.8 Effect of Pathloss Exponent	57
4.9 Adaptive Modulation and Coding Histograms	60
4.10 Coverage Extension	64
Chapter 5 - SIMULATION RESULTS, PART II: $N = 1$ CASE	67
5.1 Average Spectral Efficiency with respect to Interference Suppression Factor	67
5.2 Coverage at Various <i>SINR</i> Levels with respect to Interference Suppression Factor	69
5.3 Average Spectral Efficiency with respect to Relay Positions	71
5.4 Coverage Extension	74

Chapter 6 – CONCLUSIONS AND DISCUSSIONS.....	76
6.1 Conclusions	76
6.2 Thesis Contributions	77
6.3 Future Research	78
References	80
Appendix A - Geometric Characteristic of Co-channel BSs and Relays for Cluster Size $N = 3$ and $N = 7$ Cases	84
Appendix B - Proof of “the locus is a circle when meeting the condition the ratio of the distances of a moving point to two fixed points is a constant”	86
Appendix C - Diversity Results for Cluster Size $N = 4$ and $N = 1$ Cases.....	92

List of Figures and Tables

Figure 2.1 <i>BER</i> vs. <i>SINR</i> for combinations of various modulations and code rates.....	15
Table 1 Relation of all combinations, required <i>SINR</i> and spectral efficiency that will yield <i>BER</i> of 10^{-5}	16
Figure 2.2 BS and relay positions.....	17
Figure 2.3 Cellular layout ($N = 4$).....	18
Figure 2.4 Evenly distributed BSs and relays without cell boundaries ($N = 4$).....	19
Figure 2.5 One relay reusing a channel from cell D.....	22
Figure 2.6 All relays reusing channels from cell D.....	23
Figure 2.7 Cell layout and relaying channel partition scheme.....	24
Figure 2.8 Geometric characteristic of co-channel BSs and relays ($N = 4$).....	25
Figure 2.9 BS & relay coverage boundary in distance-based algorithm.....	29
Figure 2.10 Simplified BS & relay coverage boundary in distance-based algorithm.....	30
Figure 2.11 Pathloss- and SINR-based algorithms.....	31
Figure 2.12 Diversity algorithm.....	32
Figure 2.13 Cellular layout for cluster size $N = 1$ case.....	33
Figure 3.1 Interference received by UE 2 from other BSs and relays (When UE 2 receives signal from the BS).....	38
Figure 3.2 Interference received by UE 6 from other BSs and relays (When UE 6 receives signal from a relay).....	39
Figure 3.3 Flowchart (when ORB is not taken into account).....	40
Figure 3.4 Flowchart (when ORB is taken into account).....	41

Figure 3.5 Interference sources for cluster size $N = 1$ case (when UE receives signal from a relay).....	42
Figure 3.6 Interference sources for cluster size $N = 1$ case (when UE is receives signal from the BS).....	43
Figure 4.1 Average spectral efficiency (SINR-based relay selection algorithm, $R = 2000$ m, $N = 4$).....	45
Figure 4.2 Average spectral efficiency (SINR-based relay selection algorithm, $R = 1000$ m, $N = 4$).....	45
Figure 4.3 Average spectral efficiency (SINR-based relay selection algorithm, $R = 500$ m, $N = 4$).....	46
Figure 4.4 Percentage of users affected by ORB (SINR-based relay selection algorithm, $N = 4$).....	47
Figure 4.5 Percentage of users communicating with relays (SINR-based relay selection algorithm, $N = 4$).....	48
Figure 4.6 Average spectral efficiency comparison for two cases: with and without ORB incorporated (SINR-based relay selection algorithm, $R = 2000$ m, $N = 4$).....	49
Figure 4.7 Average spectral efficiency comparison for two cases: with and without ORB incorporated (SINR-based relay selection algorithm, $R = 1000$ m, $N = 4$).....	50
Figure 4.8 Average spectral efficiency comparison for two cases: with and without ORB incorporated (SINR-based relay selection algorithm, $R = 500$ m, $N = 4$).....	50
Figure 4.9 Average spectral efficiency comparison for distance-, pathloss- and SINR-based relay selection algorithms ($R = 2000$ m, $N = 4$).....	51
Figure 4.10 Average spectral efficiency comparison for distance-, pathloss- and SINR-based relay selection algorithms ($R = 1000$ m, $N = 4$).....	52
Figure 4.11 Average spectral efficiency comparison for distance-, pathloss- and SINR-based relay selection algorithms ($R = 500$ m, $N = 4$).....	52
Figure 4.12 Average spectral efficiency comparison for with and without diversity (SINR-based relay selection algorithm, $R = 2000$ m, $N = 4$).....	53
Figure 4.13 Average spectral efficiency comparison for with and without diversity	

(SINR-based relay selection algorithm, $R = 1000$ m, $N = 4$).....	54
Figure 4.14 Average spectral efficiency comparison for with and without diversity (SINR-based relay selection algorithm, $R = 500$ m, $N = 4$).....	54
Figure 4.15 Average spectral efficiency comparison for with and without background noise (SINR-based relay selection algorithm, $R = 1000$ m, $N = 4$).....	55
Figure 4.16 Average spectral efficiency for different bandwidth values (SINR-based relay selection algorithm, $P_{rel} = 1$ W, $R = 1000$ m, $N = 4$).....	56
Figure 4.17 Average spectral efficiency for different propagation exponent (n) values (SINR-based relay selection algorithm, $P_{rel} = 1$ W, $R = 2000$ m, $N = 4$).....	58
Figure 4.18 Average spectral efficiency for different propagation exponent (n) values (SINR-based relay selection algorithm, $P_{rel} = 1$ W, $R = 1000$ m, $N = 4$).....	59
Figure 4.19 Average spectral efficiency for different propagation exponent (n) values (SINR-based relay selection algorithm, $P_{rel} = 1$ W, $R = 500$ m, $N = 4$).....	59
Table 2 Coverage results.....	60
Table 3 Outage results.....	61
Figure 4.20 Percentage of time using a combination of modulation and coding (without relaying, SINR-based relay selection algorithm, $R = 2000$ m, $N = 4$).....	61
Figure 4.21 Percentage of time using a combination of modulation and coding (with relaying, $P_{rel} = 1$ W, SINR-based relay selection algorithm, $R = 2000$ m, $N = 4$).....	62
Figure 4.22 Percentage of time using a combination of modulation and coding (without relaying, SINR-based relay selection algorithm, $R = 1000$ m, $N = 4$).....	62
Figure 4.23 Percentage of time using a combination of modulation and coding (with relaying, $P_{rel} = 1$ W, SINR-based relay selection algorithm, $R = 1000$ m, $N = 4$).....	63
Figure 4.24 Percentage of time using a combination of modulation and coding	

(without relaying, SINR-based relay selection algorithm, $R = 500$ m, $N = 4$).....	63
Figure 4.25 Percentage of time using a combination of modulation and coding (with relaying, $P_{rel} = 1$ W, SINR-based relay selection algorithm, $R = 500$ m, $N = 4$).....	64
Figure 4.26 Average spectral efficiency for different cell sizes (SINR-based relay selection algorithm, $P_{rel} = 1$ W, $N = 4$).....	65
Figure 4.27 Outage results for different cell sizes (SINR-based relay selection algorithm, $P_{rel} = 1$ W, $N = 4$).....	66
Figure 5.1 Average spectral efficiency with respect to interference suppression factor (SINR-based algorithm, $P_{rel} = 1$ W, $R = 2000$ m, $N = 1$, no diversity).....	68
Figure 5.2 Average spectral efficiency with respect to interference suppression factor (SINR-based algorithm, $P_{rel} = 1$ W, $R = 1000$ m, $N = 1$, no diversity).....	68
Figure 5.3 Average spectral efficiency with respect to interference suppression factor (SINR-based algorithm, $P_{rel} = 1$ W, $R = 500$ m, $N = 1$, no diversity).....	69
Figure 5.4 Coverage at various <i>SINR</i> levels with respect to interference suppression factor (SINR-based algorithm, $P_{rel} = 1$ W, $R = 2000$ m, $N = 1$, no diversity).....	70
Figure 5.5 Coverage at various <i>SINR</i> levels with respect to interference suppression factor (SINR-based algorithm, $P_{rel} = 1$ W, $R = 1000$ m, $N = 1$, no diversity).....	70
Figure 5.6 Coverage at various <i>SINR</i> levels with respect to interference suppression factor (SINR-based algorithm, $P_{rel} = 1$ W, $R = 500$ m, $N = 1$, no diversity).....	71
Figure 5.7 Relay position.....	72
Figure 5.8 Average spectral efficiency with respect to relay positions (SINR-based relay selection algorithm, with relay, $P_{rel} = 1$ W, $N = 1$, $ISF = 0.2$)	72
Figure 5.9 Percentage of users affected by Optimal-Route-Blockage (SINR-based relay selection algorithm, $R = 1000$ m, $ISF = 0.2$, $P_{rel} = 1$ W, $N = 1$)	73
Figure 5.10 Percentage of users communicating with relays (SINR-based	

relay selection algorithm, $R = 1000$ m, $ISF = 0.2$, $P_{rel} = 1$ W, $N = 1$).....	74
Figure 5.11 Average spectral efficiency for different cell sizes (SINR-based relay selection algorithm, $P_{rel} = 1$ W, $N = 1$).....	75
Figure 5.12 Outage results for different cell sizes (SINR-based relay selection algorithm, $P_{rel} = 1$ W, $N = 1$).....	75
Figure A.1 Cluster size $N = 3$ case.....	84
Figure A.2 Cluster size $N = 7$ case.....	85
Table B.1 Locus information based on various P_{rel} values ($R = 1000$ m)	88
Figure B.1 Distance-based relay selection in various relay transmit power settings, $R = 1000$ m.....	90
Figure B.1 Distance-based relay selection in various relay transmit power settings, $R = 1000$ m (Continued).....	91
Figure C.1 Percentage of time using a combination of modulation and coding (with relaying, $P_{rel} = 1$ W, SINR-based relay selection algorithm, with diversity, $R = 2000$ m, $N = 4$).....	92
Figure C.2 Percentage of time using a combination of modulation and coding (with relaying, $P_{rel} = 1$ W, SINR-based relay selection algorithm, with diversity, $R = 1000$ m, $N = 4$).....	93
Figure C.3 Percentage of time using a combination of modulation and coding (with relaying, $P_{rel} = 1$ W, SINR-based relay selection algorithm, with diversity, $R = 500$ m, $N = 4$).....	93
Figure C.4 Coverage at various $SINR$ levels with respect to interference suppression factor (SINR-based algorithm, $P_{rel} = 1$ W, $R = 2000$ m, $N = 1$, with diversity).....	94
Figure C.5 Coverage at various $SINR$ levels with respect to interference suppression factor (SINR-based algorithm, $P_{rel} = 1$ W, $R = 1000$ m, $N = 1$, with diversity).....	94
Figure C.6 Coverage at various $SINR$ levels with respect to interference suppression factor (SINR-based algorithm, $P_{rel} = 1$ W, $R = 500$ m, $N = 1$, with diversity).....	95

List of Acronyms

AMC	Adaptive Modulation and Coding
AWGN	Additive White Gaussian Noise
BER	Bit Error Rate
BICM	Bit-Interleaved Coded Modulation
BS	Base Station
CDMA	Code Division Multiple Access
EIRP	Effective Isotropic Radiated Power
GPS	Global Positioning System
LOS	Line-of-Sight
MIMO	Multi-Input-Multi-Output
MRC	Maximal Ratio Combining
OFDM	Orthogonal Frequency Division Multiplexing
ORB	Optimal Route Blockage
QAM	Quadrature Amplitude Modulation
QPSK	Quadrature Phase Shift Keying
SINR	Signal to Interference and Noise Ratio
TDMA	Time Division Multiple Access
UE	User Equipment
WLAN	Wireless Local Area Network

List of Symbols

a	Distance between BS and relay
c	Speed of light
d	Distance between transmitter and receiver
d_0	Reference distance
d_1	Distance between BS and UE
d_2	Distance between relay and UE
f	Carrier frequency
F	Noise figure
G_r	Antenna gain of receiver
G_t	Antenna gain of transmitter
ISF	Interference suppression factor
k	Constant
K_b	Boltzmann's constant
m	Distance ratio of BS to relay and BS to one corner of cell
n	Propagation exponent
n_s	Selected node (BS or relay) for transmitting signals to UE
N	Cluster size
P_{BS}	BS transmit power
P_I	Received interference power
P_N	Received noise power
P_r	Received power

P_{r1}	Received signal power at UE from BS
P_{r2}	Received signal power at UE from relay
P_{rel}	Relay transmit power
P_S	Received signal power
P_t	Transmitted power
PL	Average pathloss
PL_{BS}	Pathloss between BS and UE
PL_{R1}	Pathloss between relay 1 and UE
PL_{R2}	Pathloss between relay 2 and UE
R	Cell radius
S	Number of UEs per cell
$SINR_{BS}$	SINR received at UE from BS
$SINR_{R1}$	SINR received at UE from relay 1
$SINR_{R2}$	SINR received at UE from relay 2
T	System temperature
W	Transmission bandwidth
X_1, X_2	Two independent Gaussian random variables
X_σ	A lognormally distributed random variable with stand deviation σ
Y	An exponential random variable
β	Pathloss adjustment coefficient

Chapter 1 Introduction

Modern cellular networks not only need to provide high quality voice for customers, but a large amount of data transfer service as well, such as wireless internet, multimedia, file transfer and downloading. These concerns lead to the new demand to enhance the throughput and high data rate coverage for future cellular networks. However, conventional cellular networks cannot offer the Signal to Interference and Noise Ratio (*SINR*) that is high enough to meet the new requests. Theoretical difficulties will be encountered if the future 4G networks are constructed purely based on conventional network architecture. First, the transmission rate for the future 4G networks is much higher than that of 3G networks, which will adversely affect the *SINR* at the receiving end, since *SINR* is in inverse proportion to the transmission rate*. Second, the spectrum allocated for 4G networks could be well above 2 GHz used by 3G networks. Under the operation of such a high band, the received signal will decrease tremendously according to the radio propagation model detailed in Section 2.1 and formulas (1) and (2) [5, 29].

We can resort to applying interference cancellation algorithms or smart antenna technologies, such as MIMO or adaptive antennas to distribute and collect signals more efficiently, but these technologies can only solve the problem to a certain extent, since even the most advanced antenna does not work well with the existence of heavy shadowing in the network, plus applying complicated antenna techniques on UEs may be unrealistic [5].

* When the transmit power is a constant, and if the transmit rate increases, then the bit energy E_b decreases. Since noise spectral density N_0 is a constant, E_b/N_0 decreases, so *SINR* decreases.

Another way to get stronger SINR values at the receiving end is to shorten the communication links between the BS and UEs. Employing more BSs can lead to shorter communication links. Pico-cell or micro-cell infrastructures are examples of denser BS deployment. However, none of these are ideal solutions due to the high deployment costs.

A novel solution to shorten the communication links is multi-hop or relaying technology. This is a cost effective approach since relays are functionally much simpler than BSs, which is explained in Section 1.2. The concept of relaying is that “relays” are new network elements in a cell and they act as the intermediate signal forwarding points between the BS and UEs. Their signal relaying mechanism is two-way: from BS to UE and from UE to BS. This greatly aids the signal transmission between the BS and UEs and guarantees stronger and more stable receiving signals, especially for the UEs near the edge of the cell, thereby improving the overall system throughput.

1.1 Nortel Networks Project on Cellular Networks with Relaying

Today’s cellular mobile networks are mainly “single hop”, meaning there is only one hop involved for a BS and a UE to exchange information. Some cellular networks use analog repeaters to provide service to coverage holes (such as subway stations). Lately, the potential of cellular multi-hop networks in the provision of ubiquitous high data rate coverage has been discovered, and currently there is great interest on this concept both in academia and in industry [1,2,3].

This entire Nortel Networks-funded research studies from various perspectives how multi-hop relaying technology can improve system throughput and high data rate coverage in cellular networks. It is an on-going research and is carried out in phases.

The research work in Phase I concerns digital peer-to-peer relaying [4, 8, 29-31], which is summarized in this paragraph. In peer-to-peer relaying, any UE with adequate received signals from the BS can relay signals for other UEs with poor received signals from the BS. In that research, relaying channels (for relays to forward signals to UEs) are acquired via reusing already used channels in the neighboring cells in the same cluster. A loaded cellular TDMA system with square cells and omni-directional antennas is considered as the network environment. More specifically, two types of systems, noise-limited and interference-limited systems, are investigated. In an attempt to have better radio resource management, multiple relay selection schemes, relaying channel selection schemes and relaying power selection and control schemes are studied. Overall, the simulation results show that better performance returns can be achieved through this type of mobile digital relaying, as opposed to the without-relaying scenario. Peer-to-peer relaying is able to provide better performance results when the number of UEs in a cell increases. Moreover, a network with peer-to-peer relaying is quite sensitive to relay selection scheme, but insensitive to relaying channel selection scheme. Different relay selection criteria can make a big difference on system performance; on the contrary, the performance differences among relaying channel selection criteria are not significant provided that the relays are selected appropriately. Additionally, the simulations indicate that power control can further enhance the performance returns, especially for small-size cells. In large cells, a better system performance can be achieved with higher relay transmit power levels; in small cells, on the other hand, most of the performance returns can be achieved with relatively low relay transmit power levels. One important

conclusion of Phase I research suggested that peer-to-peer relaying can be realized without much stress on the batteries of the UEs.

This current Phase II study concentrates on “fixed” relaying technologies. More specifically, two types of relaying are investigated in Phase II: analog fixed relaying and digital fixed relaying. The main difference between analog relaying and digital relaying is that the analog relay simply amplifies the entire signal it receives and re-transmits it, while the digital relay performs decoding and re-encoding of the receiving signal before re-transmitting it to ensure it only forwards the signal, not the noise.

Please refer to [10] for a detailed study of coverage performance through on-channel analog fixed relaying technology. Two types of analog relays are studied in [10]: non-selective and selective types. The non-selective analog fixed relays amplify and transmit all the signals they receive; i.e., relaying is always performed without checking whether a UE needs relaying or not. In the case of selective analog fixed relays, on the other hand, the UE is able to select the best link from the BS and all the relays to receive signal. The main results obtained from these two scenarios are: a) analog fixed relaying only works when there is strict isolation between the relay transmit and receive antennas; b) the selective analog fixed relaying with directional antenna between the BS and relay can significantly improve the system coverage.

1.2 Thesis Motivation

This thesis is on digital fixed relaying. In this type of relaying, all the techniques applied in modern digital wireless communications, such as diversity, adaptive

modulation and coding, etc., can be incorporated to further increase the system performance.

The reasons for bringing in the idea of “fixed” relay are that the peer-to-peer relaying has the following implementation difficulties:

- Since all the UEs in a cell need to act as relays whenever necessary, some additional hardware and software will be needed for a UE, and thus its cost will be higher than that of a conventional UE [5].
- When the UE density is low, it may be hard to find a mobile relay, so the performance improvement will be limited in such situations [5].
- Since the relay is mobile, the channel between it and the BS is subject to changes, which will result in a high number of inter-relay handoffs.
- The UE acting as relays might be “reluctant” to offer relaying assistance to fellow UEs with poor received signals, because by doing so, their batteries would be used.
- There could be billing and security issues that cannot be neglected.

Fixed relaying is an alternative approach. By adding a modest number of fixed relays in a cell, the above shortcomings can be addressed.

- Since only the fixed relays are responsible for relaying signals for all the UEs, there will be no need to complicate the UEs.*
- Since fixed relays are spread evenly in a cell, any UE can find a proper relay, even if the cell density is low.

* When distance-based relay selection algorithm is adopted, the aid of GPS (Global Positioning System) technology is needed; however, this is only for the BS, not for the UEs.

- Fixed relays can be placed in positions with good receiving signals from the BS, therefore the channel is stable and no extra handoffs.
- Since fixed relays will take the whole relaying responsibility, there will be no battery consumption issues among UEs.
- And since relays are network elements, billing and security issues can be handled more effectively.

The primary responsibility of fixed relays is to receive and re-transmit signals between the BS and UE. Thus they are relatively simple equipment compared to the BS, and only a little more complex than UEs. This makes them easier to build and requires shorter deployment time, compared to the methods currently used to increase system throughput and coverage, such as adding new cell sites or sectorizing antennas.

Digital fixed relays are anticipated to have the following features:

- 1) They are AC power operated and can be directly plugged to the power line, so there is no need for batteries, and thereby there is no energy limitation for them to operate. This is a great advantage over peer-to-peer relaying which certainly needs additional battery power for mobile relays.
- 2) They do not require wireline to connect to the internet, which is an advantage over BS and WLAN technology which need wiring to the internet, since constant internet wire line connection is expensive and cannot be overlooked by wireless operators when budgeting their operating costs.
- 3) It is well known that the cost increases rapidly with the increase of transmission power. Unlike the BS which is capable of emitting large amounts of power, the

transmit power of a relay is comparable to a UE, which makes the relay a low-cost device.

- 4) The placement of a relay can be lower than the BS, or it can be flexibly placed on mountaintops or lampposts. Hence there is no need to build a tower for relays.
- 5) The relay is a rugged device designed for durable usage. It can withstand severe weather if weather-insulated work has been done for it.

In the fourth generation cellular networks, high data rate coverage and throughput provision is essential [6, 20]. Not only do UEs need to send and receive voice, but large data packets (such as accessing the internet and file downloading) as well, which has a very high demand on system throughput. This is why throughput (average spectral efficiency) is used in this thesis as one of the major metrics for system performance. In order to achieve better throughput results, it is assumed that the network can track the channel variation, so that adaptive modulation and coding scheme can be applied. It shows in [6], the above adaptive scheme can improve the throughput of cellular systems.

1.3 Research Overview

This research concentrates on digital fixed relaying technology in cellular networks, in an effort to attest that it is an effective way to improve system throughput and coverage. A non-CDMA cellular network is used as an overall wireless environment. In this research, a novel and simple digital cellular infrastructure is proposed. In conventional cellular networks, the whole service area is divided into multiple cells with a BS in each cell. In the new network architecture, with the BS position unchanged, several digital

fixed relays are placed in strategic locations in each cell to assist the BS with system throughput and coverage. The maximum transmit power of these relays is 1W.

After establishing the new cellular layout, we introduce the relay selection schemes, used by the UE to choose which node (BS or relay) it will receive signal from. Three relay selection schemes, namely pathloss-based, SINR-based and distance-based schemes are introduced and compared with one another. Each scheme has its strengths and shortcomings that are to be detailed in the main body of the thesis.

Another contribution of this research is an original preset relaying channel partition scheme. In this scheme, the relaying channel required by relays to extend signal to UEs is obtained by reusing the existing channels in the network, so that it can provide relaying channels for all UEs that need relaying assistance without requesting any extra bandwidth. Further, it does not need control signaling due to its preset feature. Whenever a relay requires a relaying channel, it simply uses a channel from a set of channels allocated to it.

In addition, because of the adaptation techniques adopted in this research, there is no need for transmit power control in this new network. Nevertheless, there is still some control signaling needed in the system for the AMC.

Simulation results show that with the implementation of digital fixed relays, the SINR value is increased in the network. Furthermore, with the adoption of AMC scheme, the system throughput is greatly improved, and the ubiquitous high data rate coverage can ultimately be realized.

Diversity technology is investigated in this research. Moreover, for the purpose of testing the sensitivity of the new relaying network, several system parameters are

adjusted with different values in the simulation, such as the pathloss exponent, the transmission bandwidth and the background noise.

1.4 Relevant Literature

Due to the improvement that relaying technology is capable of offering in terms of the throughput and coverage in cellular mobile networks, recently there has been increased interest in studying and investigating relaying. This section first catalogues relevant literature on relaying-related subjects.

As an overview of the concept of relaying, [5] is a good document to start with. It features what has been achieved and what conclusion has been drawn so far in this research area, as well as what further investigation is suggested in what subject. Another important feature of relaying --- load balancing is described in [11]. The basic idea is to place a number of mobile relay stations within each cell to divert traffic from one cell to another. The simulation illustrates that relaying is able to balance the traffic well among cells. Furthermore, the throughput gained by using the multihop approach is investigated in [17]. A specific analysis of theoretical characterizations for the physical layer of multihop wireless communications channels is described in [18, 22-24]. Four channel models are investigated: decoded / amplified relaying multihop channel with / without diversity. The analyses and simulations indicate that all four multihop channels outperform the singlehop channel. The multihop channels with diversity outperform the ones without diversity. The performance gains of the amplified relaying multihop diversity channel are much greater than those of the decoded relaying multihop diversity channel. A new form of spatial diversity, in which diversity gains are achieved via the cooperation of mobile users is proposed in [21]. Results indicate that user cooperation is

beneficial and can result in substantial gains over a non-cooperative strategy. Using multihop selection combining or multihop maximal ratio combining, a novel routing algorithm, which factors diversity in route selection, is presented in [19,32]. Results show that significant system throughput increase and reduced outage can be realized without additional time slots.

Because adaptive modulation and coding scheme has been adopted in this research, a number of publications related to adaptation techniques are worth viewing. A procedure of data rate adaptation to achieve higher data rates for major cellular standards is described in [25]. In [26], coset codes are combined with not only a general class of adaptive modulation techniques, but also with a spectrally efficient technique: MQAM. Both coding gains and power savings can be achieved via such technology.

Documents on the subject of SINR measurements are also recommended. A technique to measure SINR over fading channels is proposed in [27]. This SINR estimate is also used for data rate adaptation and power control. In [28], a new algorithm is developed to estimate the SINR in a TDMA system. This new estimation technique is computationally simple and accurate, but with a significantly reduced computational complexity.

1.5 Thesis Organization

This thesis is structured as follows: Chapter 2 presents the cellular layout, relay selection algorithms and relaying channel partition scheme. Cell layout introduces the geometric locations of the BSs and relays in cluster size $N = 4$ and $N = 1$ cases. Three relay selection algorithms are introduced: Pathloss-based, distance-based and SINR-based algorithms. A pre-configured relaying channel partition scheme is then introduced. The last part of this chapter elaborates on the AMC scheme implemented in this research.

Chapter 3 describes the simulation models and algorithms for both cluster size $N = 4$ and $N = 1$ cases. The environmental parameters as well as how throughput is figured out are introduced. Furthermore, the overall simulation flowcharts are detailed. Chapter 4 demonstrates the simulation results for the case of cluster size $N = 4$, including the performance enhancement offered by digital fixed relays, the throughput increase that adaptive modulation and coding can offer, result comparison among three relay selection algorithms, result comparison between with and without diversity, the effect of background noise on system performance, as well as the impact of various system parameters (such as bandwidth and pathloss exponent) on system performance. Similarly, Chapter 5 provides the simulation results for the case of cluster size $N = 1$. Overall, Chapters 4 and 5 provide quantitative results on the performance improvement of the system when using digital fixed relays. Finally, in Chapter 6 the conclusions from this work are presented and some suggestions are made on possible future research in this area.

Chapter 2 Relaying Channel Partition Scheme and Relay Selection

In this chapter, the pathloss model is firstly introduced, where distance attenuation, lognormal shadowing and Rayleigh fading are considered. Adaptive modulation and coding scheme, as an important feature of the future cellular wireless systems, is considered in this research and elaborated. Then the cellular layout and relaying channel partition scheme are established. The positions of BSs and relays are detailed in the cell layout, and how relaying channels are allocated among relays are elaborated in the relaying channel partition scheme, which constitutes one of the most important contributions in this thesis. Afterwards three relay selection algorithms are discussed: distance-, pathloss-, and SINR-based algorithms. The diversity technique adopted in our simulation to get better system performance is discussed in the last portion of this chapter.

2.1 Propagation Model

In wireless communication environments, radio channels are randomly changing and are typically analyzed in a statistical way. First of all, the received signal power is inversely proportional to the distance between the transmitter and the receiver. Also, there exist both large-scale variations and small-scale variations that can be described as lognormal shadowing and multipath fading respectively [9]. Taking all the above into consideration, we use the following formula to determine the received power in this research:

$$P_r = P_t \frac{G_t G_r}{PL} X_\sigma Y, \quad (1)$$

where P_t is the transmitted power and P_r is the received power, G_t and G_r are the antenna gains of transmitter and receiver, respectively (which are set to 1 in this research), PL , the average pathloss, is described in formula (2), X_σ is a lognormally distributed random variable capturing shadowing effects with zero mean and standard deviation σ , and Y is an exponential random variable with unity mean which captures the effects of multipath fading. Y can be generated as follows:

$$Y = \frac{X_1^2 + X_2^2}{2},$$

where X_1 and X_2 are two independent Gaussian random variables with zero mean and a standard deviation of 1. It is easy to verify that $E[Y] = 1$.

PL , the average pathloss, can be calculated as:

$$PL = \left(\frac{4\pi d_0 f}{c}\right)^2 \left(\frac{d}{d_0}\right)^n, \quad (2)$$

where d_0 is the reference distance and is set to 10 m, f is the carrier frequency, c is the speed of light, d is the distance between the transmitter and the receiver, n is the propagation exponent. In this research n is set to 4 unless otherwise stated. We also investigate the effects of changing n to other values (2.5, 3, 3.5, 4.5, 5) in one case.

2.2 Adaptive Modulation and Coding

In order to increase the throughput and further provide the high data rate coverage, adaptive modulation and coding [6] are employed in this study. The basic concept for

adaptive modulation and coding is to apply different combinations of constellation sizes and code rates based on the channel conditions (or received *SINR* values).

Due to its bandwidth-efficient nature, BICM (Bit-Interleaved Coded Modulation) [7,14] is applied in this study as a coding scheme. BICM is basically composed of binary error-correcting coding, bit-by-bit interleaving and high order modulation [15]. The basic manner of BICM is to interleave and encode the bits to be modulated, and then map them to a certain constellation via Gray or quasi-Gray mapping. At the stage of decoding, a binary decoder is employed after de-interleaving. BICM has a high performance in cases of high data rates and fading channels, mainly due to a bit-wise interleaving mechanism at the transmitting end and a soft-decision metric process at the receiving end. BICM has proven to be a simple yet powerful modulation technique especially for optimal BER (bit-error rate) performance.

The combinations of three modulation schemes (QPSK, 16-QAM, 64-QAM) and five code rates (1/2, 2/3, 3/4, 7/8 and 1) are considered in this research. Figure 2.1 shows *BER* vs. *SINR* for all the fifteen combinations. The targeted *BER* is 10^{-5} . The received *SINR* value determines which combination to use. For example, if the received *SINR* is greater than 21 dB, the threshold of combination of “64-QAM, rate-7/8”, but less than 26 dB, the threshold of combination of “64-QAM, rate-1”, the former combination will be employed.

Note that the data used to generate Figure 2.1 assume the system channel to be an AWGN (additive white Gaussian noise) channel, namely it is assumed that the noise and the interference have Gaussian distribution. However, shadowing and Rayleigh fading in the channel are considered in our simulation model. Since we use a Monte Carlo type of

simulation, all the data are averaged by $N \times S \times 1000$ times (N = cluster size; S = number of UEs per cell; 1000 is the number of repeating times). After so many times of averaging, the randomness caused by shadowing and fading is averaged out, therefore we can still use this figure to further calculate the throughput after we get the $SINR$ value.

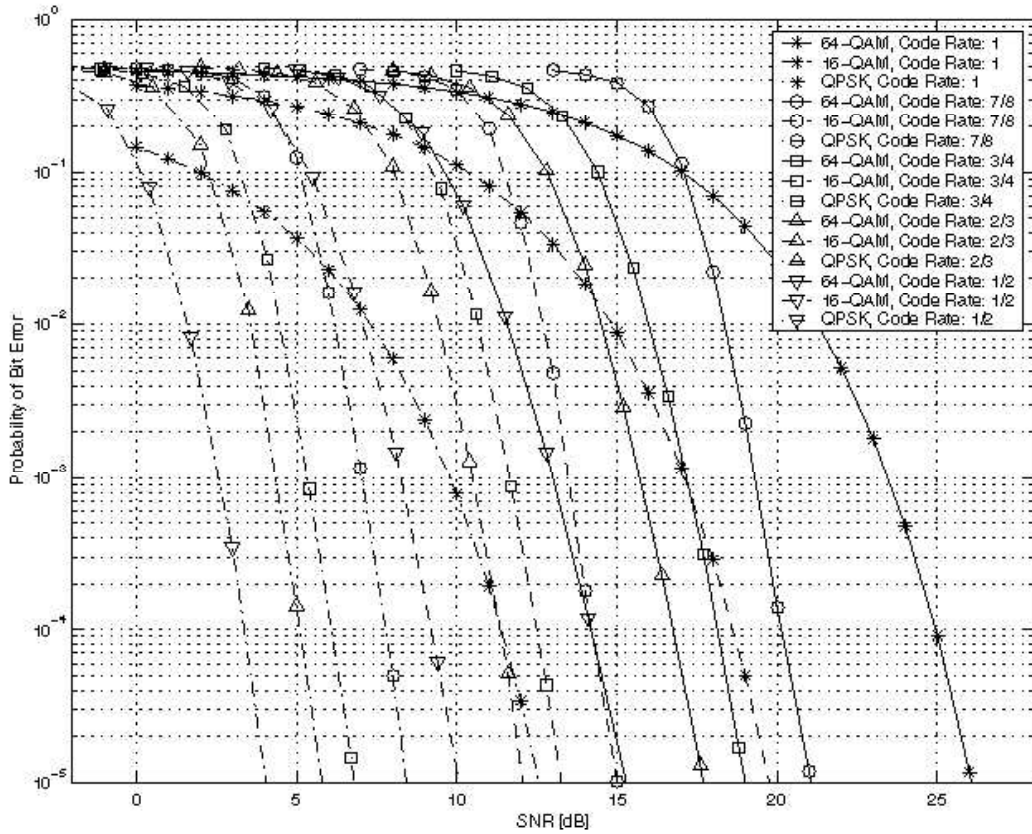


Figure 2.1: *BER* vs. *SINR* for combinations of various modulations and code rates*.

* The data used to produce this figure are provided by Dr. Sirikiat Lek Ariyavisitakul.

Table 1 depicts the relation between the received *SINR* value and the spectral efficiency. By looking up this table, we can find the system throughput based on the *SINR* value obtained from the simulation. Note in Table 1 that three combinations are not used, because in these three cases, higher *SINR* values are required, but only less throughput is achieved in comparison to some other combinations.

Table 1: Relation of all combinations, required *SINR* and spectral efficiency that will yield *BER* of 10^{-5}

Combinations of modulation and code rates	Minimum Required <i>SINR</i> [dB]	Spectral Efficiency [bits/sec/Hz]
QPSK, rate: 1/2	4	1
QPSK, rate: 2/3	6	1.33
QPSK, rate: 3/4	6.8	1.5
QPSK, rate: 7/8	7.8	1.75
16-QAM, rate: 1/2	10	2
16-QAM, rate: 2/3	12	2.67
QPSK, rate: 1 (not used)	12.5	2
16-QAM, rate: 3/4	13	3
16-QAM, rate: 7/8	15	3.5
64-QAM, rate: 1/2 (not used)	15.1	3
64-QAM, rate: 2/3	17.7	4
64-QAM, rate: 3/4	19	4.5
16-QAM, rate: 1 (not used)	19.7	4
64-QAM, rate: 7/8	21	5.25
64-QAM, rate: 1	26	6

2.3 Cellular Layout

Two different values for the cluster size (N) are considered: $N = 4$ and $N = 1$ cases. Sections 2.3-2.5 describes the $N = 4$ case and Section 2.7 discusses the $N = 1$ case. Cells with different sizes are investigated. The cell radii are 2000 m, 1000 m, and 500 m, for large, medium, and small cells, respectively.

Hexagonal cells are studied in this research. Similar to current cellular networks, the BS is located in the centre of the hexagonal cell. Six fixed relays are placed in each cell as new network elements different from current cellular infrastructure. Each relay is located on the line that connects the centre of the cell to one of the six cell vertices, and it is $2/3$ away from the centre (BS). Figure 2.2 shows the BS and relay positions in one cell. The square in the center of the cell represents BS and the circles close to the cell boundary represent relays. With this relay position design, the BSs and relays are spread out evenly across the hexagonal layout. Figure 2.3 shows the cellular layout for $N = 4$ case. In this case, seven clusters with four cells in each cluster are investigated. Figure 2.4 shows the cellular layout without cell boundaries, which demonstrates that the BSs and relays are evenly distributed in the network.

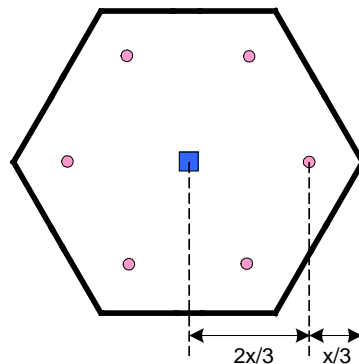


Figure 2.2: BS and relay positions.

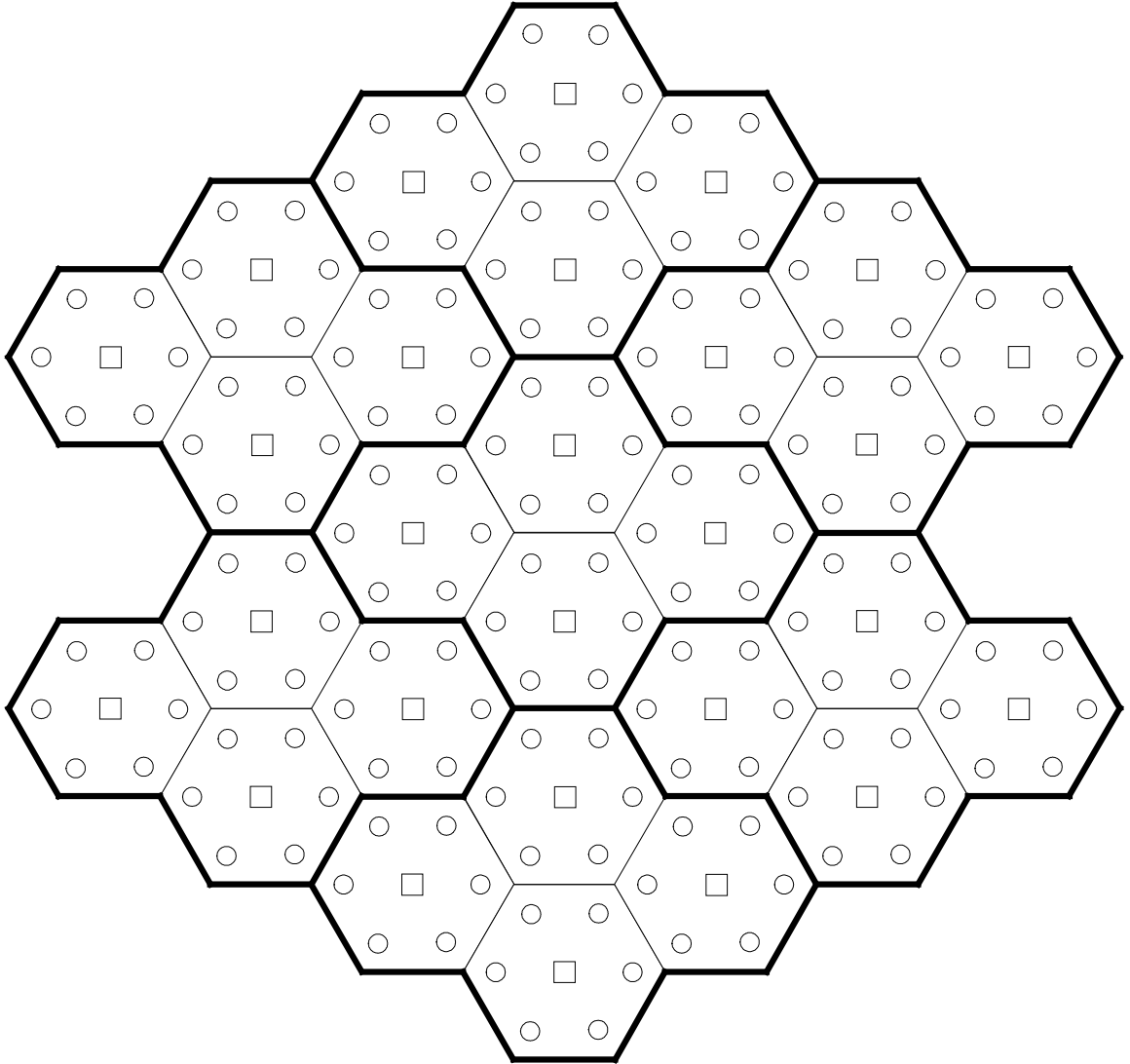


Figure 2.3: Cellular layout ($N = 4$).

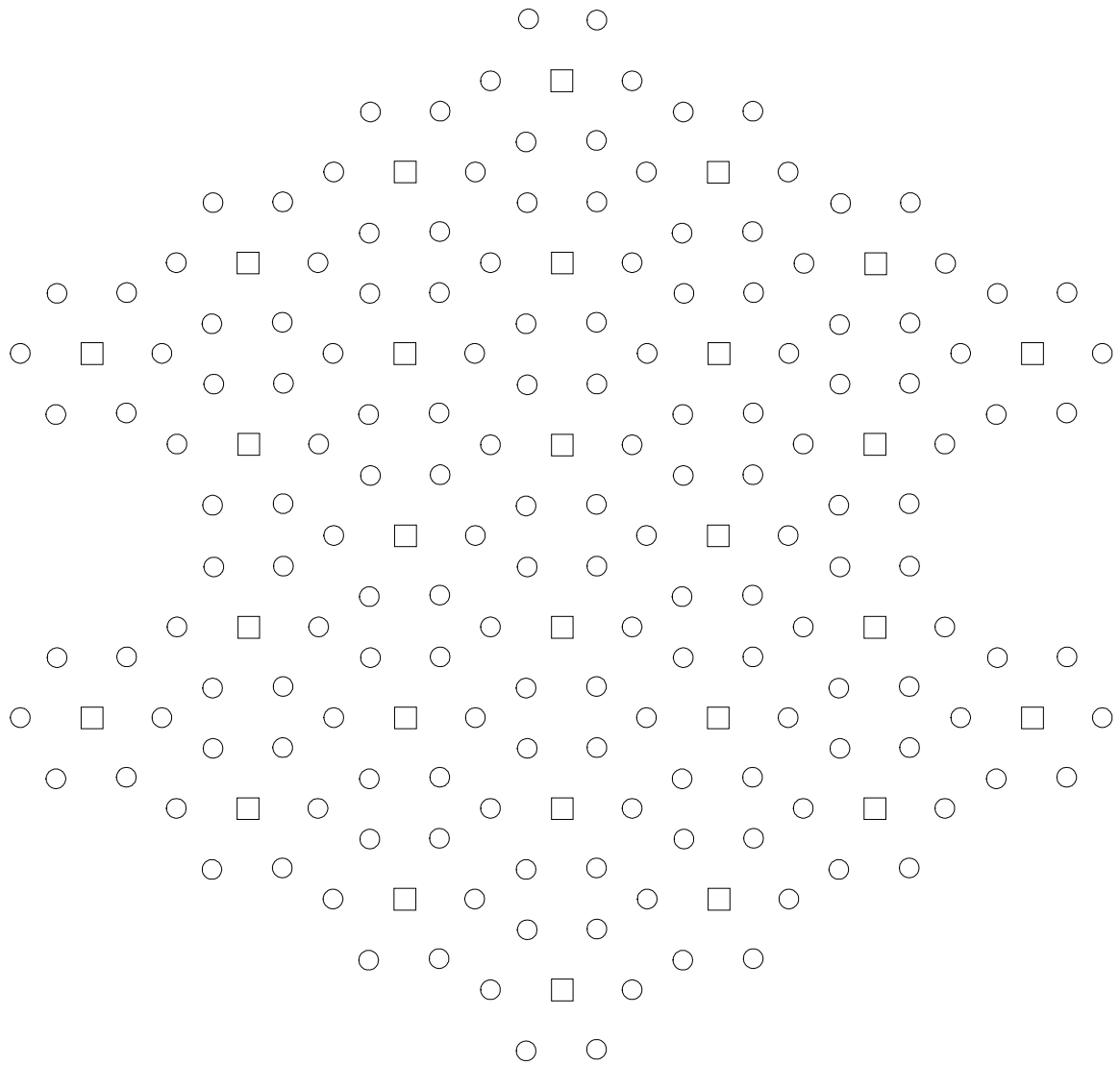


Figure 2.4: Evenly distributed BSs and relays without cell boundaries ($N = 4$).

2.4 Relaying Channel Partition Scheme

The terminology “channel” may have different meanings in different wireless systems. In this research we consider a non-CDMA system, which can be a TDMA or an OFDM type. In a TDMA system, “channel” is a time slot, while in an OFDM system, “channel” corresponds to frequency and/or time slot.

In a relaying network, an extra channel, relaying channel (between relay and UE), is needed by a relay to forward the signal to a UE [4,29]. In analog relaying, this relaying channel can be the same channel between the BS and relay, called by some researchers as “on-channel relaying” [10]. Due to the mechanism of on-channel relaying, the feedback from the transmitter to the receiver of a relay is expected. This feedback problem must be dealt with before the on-channel relaying technology can be implemented.

In the meanwhile, we may turn to other sources for relaying channels. The unlicensed band is one of the appealing considerations due to the reasons that 1) unlicensed bands are much more inexpensive than licensed bands and 2) any error occurred in the course of relaying will only affect those UEs who need relaying, not the rest who receive signals directly from the BS and use the licensed band. The side effect of utilizing unlicensed bands is that it will complicate the structure and function of the UE and relay, since they need to operate in the dual-band mode (licensed bands and unlicensed bands). [16] is a detailed study of using the unlicensed bands for relaying in cellular CDMA networks.

Also, some channels can be exclusively reserved for relaying purpose. However since the spectrum is a limited resource, this channel reservation approach is not desirable.

Instead of reserving, searching for any vacant channels for relaying might also be an idea. However obviously this approach limits the opportunities for UEs to obtain relaying

assistance, since only when there are vacant channels available in the network can relaying be implemented.

In this research we have the following pessimistic assumptions: 1) The investigated cellular mobile network is fully loaded and no channels are to be reserved for relaying purposes. 2) In each cell the number of channels equals the number of UEs. Therefore, all relaying channels must be obtained via further reusing channels from the system. This is an aggressive strategy, but it will be the most desired one if it works well, because no extra radio resources are consumed while improving poor radio links. However, as can be imagined, the assumptions made above will cause denser channel reuse and will result in increased co-channel interference. In an effort to minimize these shortcomings and seek a suitable approach for relaying channel acquisition, we have found a relaying channel partition scheme with only controlled co-channel interference and least computational overhead and it is detailed below. Note that only the downlink scenario is considered in this relaying channel partition scheme.

The relaying channel partition scheme is based on the following: First, to avoid self-interference, a relay is not allowed to reuse any channel in the same cell. For example, in Figure 2.5, all the relays in cell C must reuse channels from cells A, B, or D as relaying channels. Second, because a cell farthest from a relay most probably has the least co-channel interference to this relay, we decide to let a relay reuse the channel from the cell farthest from it. For example, in Figure 2.5, the relay in the low left corner of cell C in the center cluster is marked “D”, meaning it reuses one channel from cell D, the farthest away cell from this relay.

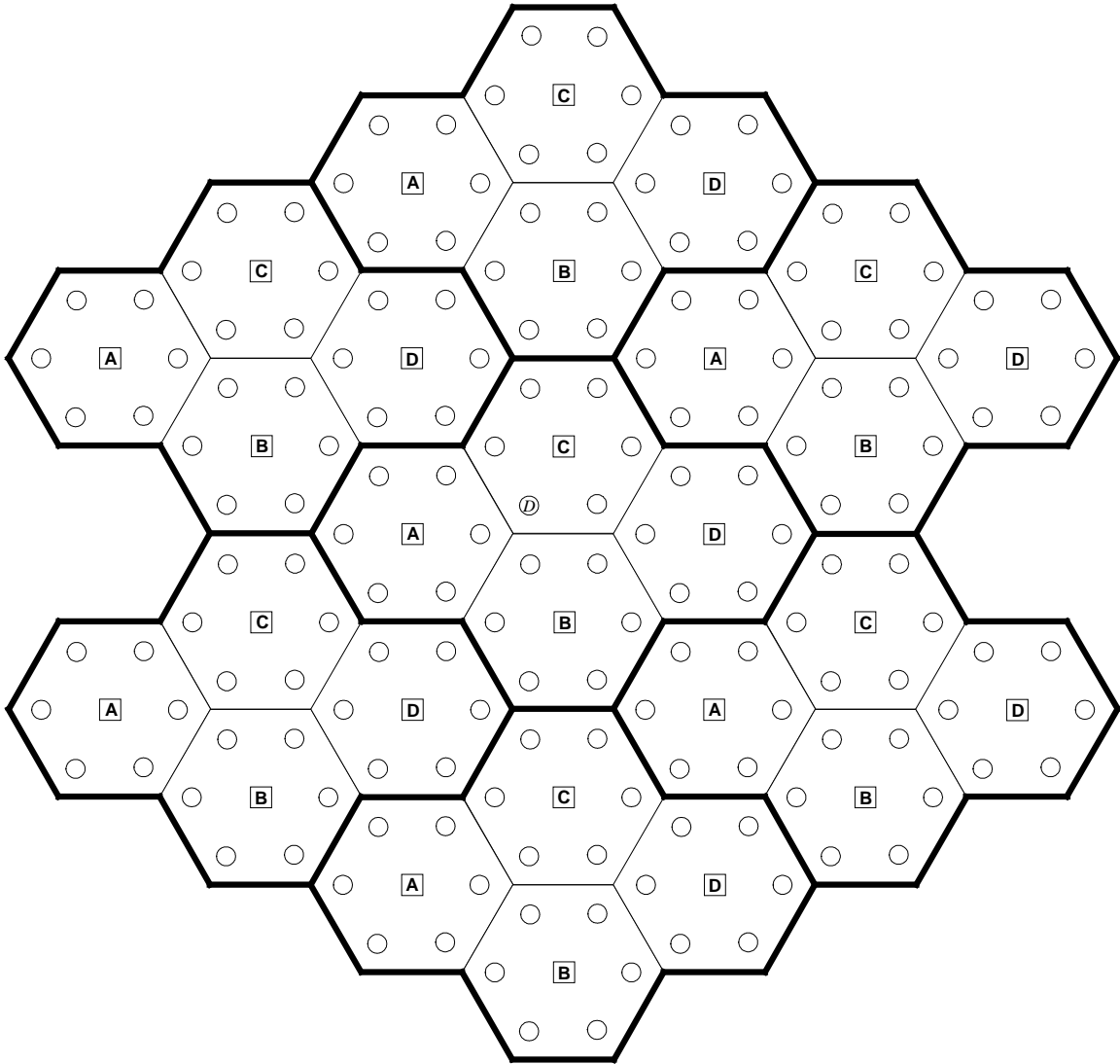


Figure 2.5: One relay reusing a channel from cell D.

In Figure 2.6, all the relays reusing channels from cell D are marked out. It can be seen that in each cluster, six relays will reuse channels from cell D as relaying channels. In order to avoid these six relays reusing the same channel, all channels belonging to cell D are divided into six disjoint groups with equal numbers of channels, and each relay reuses one group of them. For example, if there are 48 channels per cell, each relay will be assigned 8 channels. In Figure 2.6, a relay marked “ D_3 ” means it reuses the third group of channels from cell D.

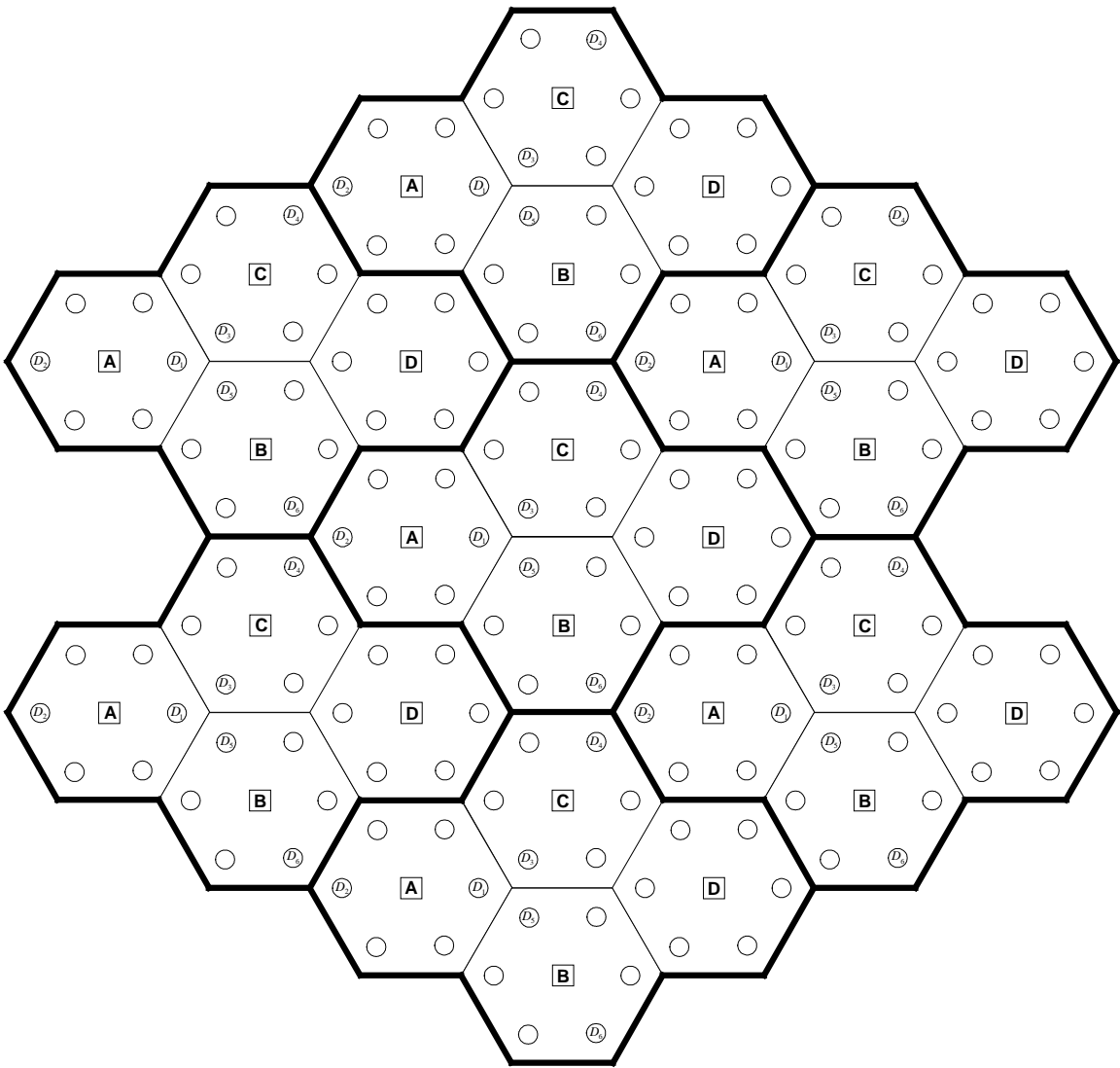


Figure 2.6: All relays reusing channels from cell D.

Figure 2.7 shows the overall channel partition scheme with the aforementioned channel-reusing criterion applied to all relays. Note that in this relaying channel partition scheme, no two relays in a cluster will choose the same relaying channel based on our design.

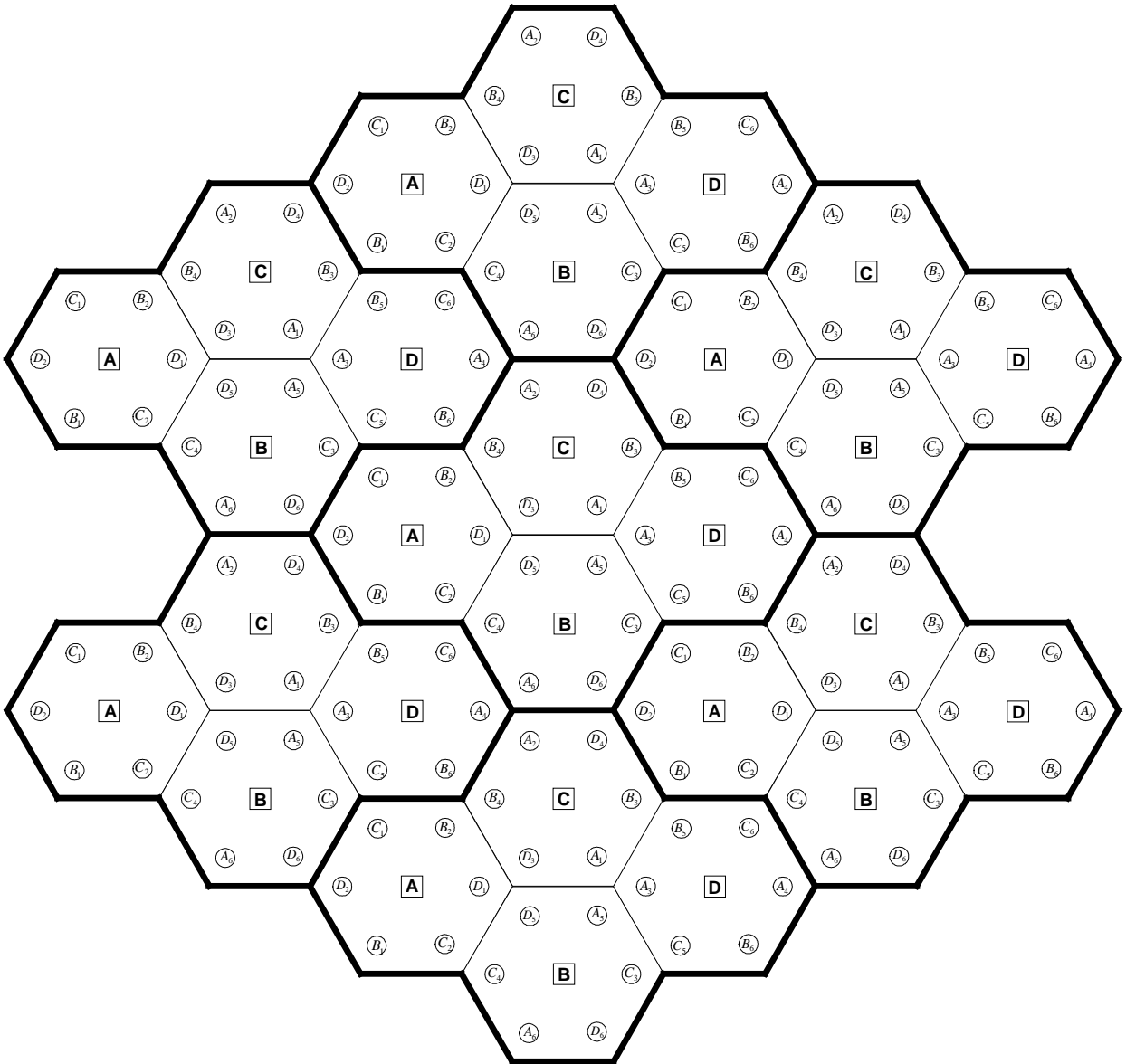


Figure 2.7: Cell layout and relaying channel partition scheme.

Another observation is that the geometric locations of all the co-channel relays reusing channels from the same cell (e.g. cell D) have a common characteristic. They are all located on circles whose centers are exactly the co-channel BSs these relays are reusing channels from. Figure 2.8 shows this geometric characteristic. All these co-channel BSs and relays are shaded.

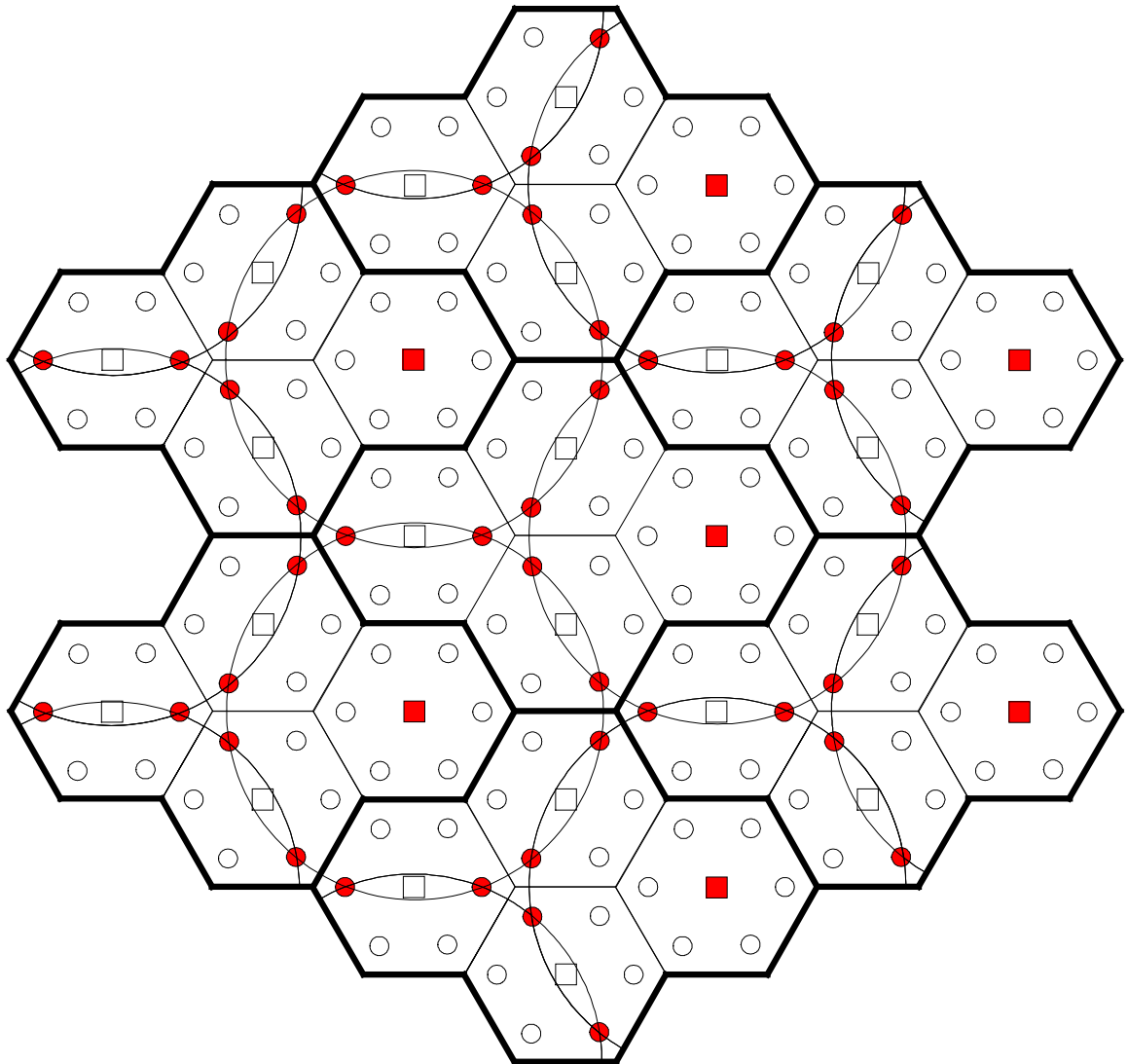


Figure 2.8: Geometric characteristic of co-channel BSs and relays ($N = 4$).

The aforementioned fixed relaying channel selection scheme not only applies to the cluster size $N = 4$ case, but works well for any cluster size. $N = 1$ case is a special one and it is discussed in Section 3.3. The same geometric characteristic exists for all N values as well. Appendix A shows the above described geometric characteristic for $N = 3$ and $N = 7$ cases.

The fixed relay position makes this relaying channel partition scheme a reality. The main advantage of this scheme is the fact that it is a “preset” way of channel partition; there are no need for the complicated channel selection schemes and complicated channel measuring schemes, and there is no overhead calculation. Whenever a relay requires a relaying channel, it simply uses a channel from a set of channels allocated to it.

This relaying channel partition scheme is “sub-optimum” due to the fact that this is a fixed channel assignment, not a dynamic channel assignment based on the instantaneous state of all the channels. In other words, only the distances between the BSs and relays are considered when relaying channel partition scheme is defined. Shadowing and multi-path fading are not taken into account. However, a significant amount of signalling overhead will be inevitable if applying a dynamic channel selection, which might not be feasible for a large cellular system.

Sometimes a UE requiring relaying finds an appropriate relay, but all the channels the relay has are used at the moment. In this case, the relay denies the relaying service for this UE. Then the UE has to go through a “sub-optimal route”; i.e., the UE turns to the next relay or BS whichever is the second best, based on the relay selection schemes explained in Section 2.5 (See (3) and (4)). We refer to this situation as “Optimal-Route-Blockage (ORB)”.

2.5 Relay Selection*

Number of relays and how they are placed in a cell are specified in Section 2.3. A UE then has two choices to receive signals: either from the BS or from one of the six relays. This section describes the three algorithms used to determine from which node (BS or relays) a UE will receive its signal. The algorithms are based on the following three criteria: distance, pathloss and SINR. These three criteria have their own advantages and disadvantages, for instance, the distance-based algorithm is the simplest to implement with the assistance of GPS (Global Positioning System) technology [12,13], but the performance enhancement it introduces is the least among the three algorithms. The SINR-based algorithm produces the greatest performance improvement; conversely, it involves more signalling overhead.

In all the three relay selection algorithms, we assume all six fixed relays are placed in strategic locations with good receiving signals from the BS. The AMC mode will be decided based on the *SINR* level between the relay and UE. The BS-relay link is assumed to be good enough to support this mode of operation. In other words, the links between the BS and the relays are assumed to be good enough to support the highest AMC mode with negligible errors, though it will actually use the level that relay-UE link is using. This assumption is not an unrealistic one, but made in order to simplify the system model. In fact, it can be easily accomplished by placing the relays at high place above any obstructions to ensure that there exists a Line of Sight path between the relays and the BS. Also directional antennas and MIMO antennas can be used to guarantee a strong signal between the BS and the relays.

* A UE can actually use the relay selection algorithms to select either a BS or a relay.

2.5.1 Distance-based Algorithm

This algorithm is solely based on the distances between the UE and BS and six relays.

Let us find the boundary (locus) on which the receiving signal P_{r1} from the BS and the receiving signal P_{r2} from the relay are identical when shadowing and multipath fading are averaged out. Since

$$P_{r1} = \frac{kP_{BS}}{d_1^4}, \quad P_{r2} = \frac{kP_{rel}}{d_2^4},$$

where k is a constant, setting $P_{r1} = P_{r2}$ yields

$$\frac{P_{BS}}{d_1^4} = \frac{P_{rel}}{d_2^4}.$$

In the above P_{BS} is the BS transmit power, P_{rel} is the relay transmit power, d_1 is the distance between the BS and the UE, and d_2 is the distance between the relay and the UE.

Since P_{BS} and P_{rel} are usually constants,

$$\frac{d_1^4}{d_2^4} = \frac{P_{BS}}{P_{rel}} = \text{constant};$$

therefore, d_1 / d_2 is a constant as well. It can be shown that if the ratio of the distances of a moving point to two fixed points is a constant, the locus meeting this requirement is a circle. For the proof of this, refer to Appendix B. This circle is exactly the boundary that we are trying to figure out. By applying different values to P_{BS} and P_{rel} , we can get the location of the centre of the circle and its radius.

Figure 2.9 shows the coverage boundary of the BS and six relays in a hexagonal cell with $P_{BS} = 10$ W and $P_{rel} = 1$ W.

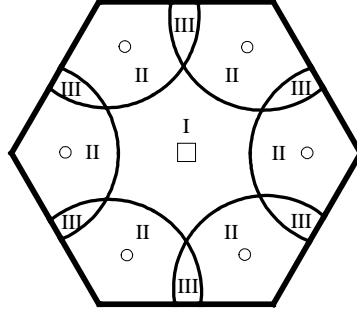


Figure 2.9: BS & relay coverage boundary in distance-based algorithm.

The six arcs (we have omitted the areas of the circle outside the hexagon, so only arcs are shown) are the boundaries where a UE's receiving signals from the BS and from the relay are identical. Therefore, we can mark the entire hexagonal area into three regions: I, II and III. Region I is outside the arcs, where the receiving signal from the BS is greater than that from the relay; region II and III, on the contrary, are inside the arcs, where the receiving signal from the relay is greater than that from the BS.

When not taking Optimal-Route-Blockage (ORB) into account, we can come to the conclusion that 1) if a UE is in region I, it will receive signal from the BS; 2) if it is in region II and III, it will receive signal from the closest relay. Figure 2.10 shows the simplified boundary of this case.

When taking ORB into account, and if the relay happens to not have any channel left for a UE requiring relaying assistance at the moment, then depending on the location of the UE, it will either turn to the second closest relay or the BS.

- 1) If it is in region II, it will communicate with the BS.
- 2) If it is in region III, it will communicate with the second closest relay.

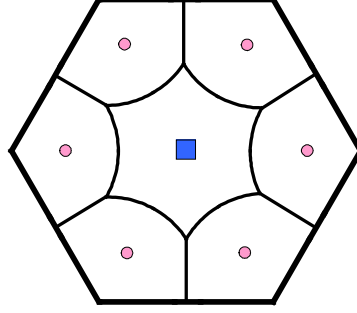


Figure 2.10: Simplified BS & relay coverage boundary in distance-based algorithm.

2.5.2 Pathloss-based Algorithm

Pathloss-based algorithm is supposed to have better throughput results than a distance-based one, because in this algorithm, we take into consideration lognormal shadowing in addition to distance-based attenuation.

As mentioned above, we assume the link between the relays and the BSs are good enough to support the highest AMC mode with negligible errors. Therefore, only the pathloss of the second hop is taken into account when selecting a relay. The pathloss algorithm has two steps:

- 1) Out of the six relays in the cell in which the UE resides, select two that are the closest to the user (R1, R2); please refer to Figure 2.11.
- 2) Compute the pathloss between the two closest relays and the UE, and between the BS and the UE. The node (relay or BS) with the least pathloss will be responsible for transmitting signals for that UE.

$$n_s = \arg \min \{ PL_{R1}, PL_{R2}, PL_{BS} - \beta \}, \quad n_s: \text{Selected node} \quad (3)$$

where $\beta = 10 \log_{10} \left(\frac{P_{BS}}{P_{rel}} \right)$. We always use a P_{BS} value of 10 W. Then, a P_{rel} value of 1 W

will result in $\beta = 10$.

2.5.3 SINR-based Algorithm

This algorithm is expected to yield an enhanced performance in comparison to the other two algorithms (distance and pathloss). Similar to the pathloss-based type, SINR-based algorithm has two steps:

- 1) Out of the six relays in the cell in which the UE resides, select two that are the closest to the UE (R1, R2); please refer to Figure 2.11.
- 2) Compute the $SINR$ between the two closest relays and the UE, and between the BS and the UE. The node (relay or BS) with the maximum $SINR$ will be responsible for transmitting signals for the UE.

$$n_s = \arg \max \{ SINR_{R_1}, SINR_{R_2}, SINR_{BS} \}, \quad n_s: \text{Selected node} \quad (4)$$

Figure 2.11 shows that a UE only listens to the two closest relays and the BS in pathloss- and SINR-based algorithms. The relay selection is made among these three candidates. In the figure the asterisk sign represents a UE.

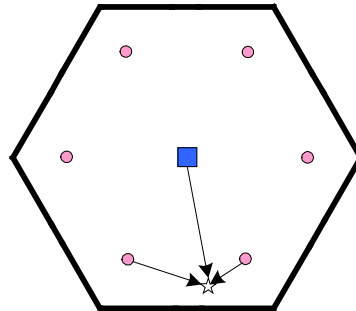


Figure 2.11: Pathloss- and SINR-based algorithms.

2.6 Diversity

Diversity is proposed in this study to attain higher system throughput. Particularly, the two-path diversity is employed in our algorithm. The two-path diversity occurs when a UE needs relay assistance, its receiving signal is a combination from both the BS and the relay. Because there are signals from the BS to the UE anyway, this diversity does not need any extra resource costs, such as transmit power and bandwidth costs. Refer to Figure 2.12 showing the receiving signal of a UE is combined from the BS and the relay with the implementation of two-path diversity. Note that the diversity algorithm discussed here is analogous to macroscopic diversity, rather than microscopic diversity.

Any diversity combining scheme can be used in principle, such as selection combining, equal-gain combining, maximal ratio combining (MRC), and optimal combining. The MRC diversity scheme is employed in our simulation.

Due to the nature of digital relay, additional processing delay is unavoidable because the relay needs to decode and re-encode the signal it receives. Depending on whether the error control coding is applied in the network, this additional processing delay may be up to one frame. Owing to the delay in the relay, another one frame of buffering is necessary to be added.

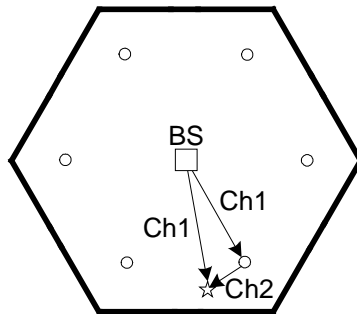


Figure 2.12: Diversity algorithm.

2.7 Simulation Model for $N = 1$ Case

In this section, we consider a cellular system with cluster size one; i.e., $N = 1$. In this case, a single hexagonal cell constitutes one cluster. The relays are placed at the same positions as the $N = 4$ case. The relay selection algorithms are the same as the $N = 4$ case, i.e., it could be distance-, pathloss- and SINR-based, but only the SINR-based one is simulated as an example in this research. The relaying channel partition scheme is still fixed. All the available channels (i.e., available channels for one cell as $N = 1$) are divided into six disjoint groups with equal number of channels. Each relay will reuse one group of them. Once the relay is selected, it knows which channel it should use. Refer to Figure 2.13 for the cell layout for the $N = 1$ case.

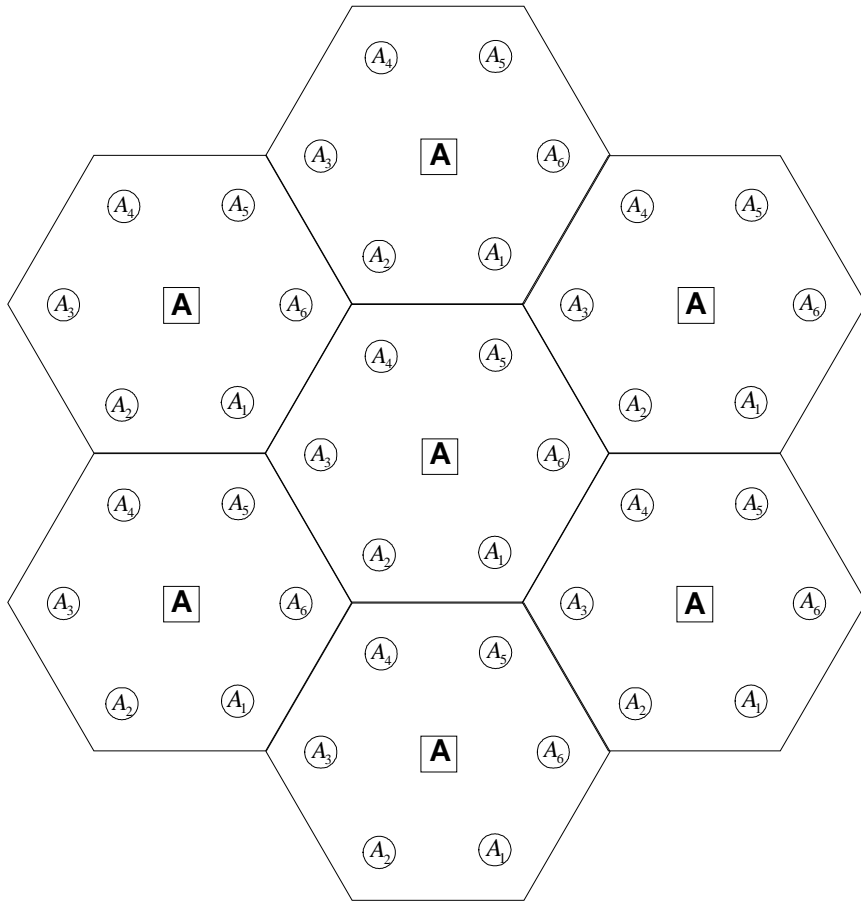


Figure 2.13 Cellular layout for cluster size $N = 1$ case.

Chapter 3 Simulation Algorithm

This chapter primarily concerns the simulation algorithms. First, the environmental parameters used in the simulation are specified. Then, the simulation algorithm is described.

3.1 Environment and Parameters Assumptions

Below is a list of parameters used in the simulation algorithms. They are typical data widely used in simulating cellular networks. They were approved by the research sponsor, Nortel Networks, prior to be used in the simulation.

- Pathloss propagation exponent: $n = 4$
- Lognormal shadowing with a standard deviation: $\sigma = 8$ dB
- Flat Rayleigh fading
- Slow fading: since we aim at achieving high data rate coverage. Fast fading only happens for very low data rate applications [9].
- Doppler effects are ignored: since the effects due to Doppler spread are negligible for slow fading channels [9].
- Simulation area: hexagonal cells with the cell radius $R = 2000$ m, 1000 m or 500 m, 4-cell and 1-cell clusters. Seven clusters are investigated, i.e., the first tier co-channel interference is considered in our simulation.
- RF carrier = 2 GHz
- Transmission bandwidth: $W = 5$ MHz
- Thermal noise with a noise figure: $F = 8$ dB

- Isotropic antennas (with unit gain) for the BS, fixed relay and UE
- No power control: when adaptive modulation and coding scheme is used, power control does not contribute much towards the throughput increase [6].
- Base station transmit power: $P_{BS} = 10$ W
- Fixed relay transmit power: $P_{rel} = 0.1$ W, 0.3 W, 1 W
- Downlink scenario only: since the requested data rate from this direction is likely to be higher than the uplink case.

Note that the channel model elaborated above as well as the omni-directional antenna assumption is valid for the BS-to-UE and relay-to-UE links. As mentioned in Section 2.2, the BS-to-relay link is assumed to be effective enough to support the highest AMC mode with negligible errors.

3.2 Simulation Algorithm for $N = 4$ Case

In this simulation, we compare the system performances of the with-relaying and without-relaying cases.

The UEs are placed randomly across the cluster (4 cells / cluster or 1 cell / cluster) with S UEs per cell. We have chosen six values for S : $S = 12, 24, 36, 48, 60$ or 72 .

For the without-relaying case, all UEs will receive signals from the BS. Let P_S denote the received signal power.

The formula to calculate the interference power is as follows:

$$P_I = P_1 + P_2 + \dots + P_6 ,$$

where P_1, \dots, P_6 are the interference powers from the co-channel BSs.

The noise power is calculated according to the following formula:

$$P_N = K_b \times T \times W \times F = 1.306 \times 10^{-13} \text{ watts,}$$

where K_b is the Boltzmann's constant (1.38×10^{-23} Joules/Kelvin), T is the system temperature (300 K), W is the transmission bandwidth (5 MHz), and F is the noise figure ($6.31 = 8\text{dB}$).

Now SINR can be calculated as:

$$SINR = \frac{P_S}{P_N + P_I}. \quad (3.1)$$

For the with-relaying case, as described before, six relays are placed in each cell. First a node (BS or relay) is selected according to the relay selection schemes described in Chapter 2, i.e. distance-, pathloss- or SINR-based algorithms. The received signal can be either from the BS or from the relay depending on which node the UE is communicating with. The interference power is different from the without-relaying case, because we need to consider the interference from other relays using the same channel in addition to the interference generated by co-channel BSs.

The formula below shows how to calculate the total interference power:

$$P_I = P_1 + P_2 + \dots + P_{13},$$

where if the received signal is from the BS, P_1, \dots, P_6 are the interference powers from the co-channel BSs and P_7, \dots, P_{13} are the interference powers from the relays using the same channel. If the received signal is from the relay, P_1, \dots, P_7 are the interference powers from the co-channel BSs and P_8, \dots, P_{13} are the interference powers from the relays using the same channel. Here the worst case scenario in calculating the interference is considered; in other words, we assume all the relays are using all channels allocated to them to transmit signals, though in fact sometimes some channels will not be used.

Figures 3.1 and 3.2 show the interference sources for the above two cases, respectively. UE 2 and UE 6 are two randomly selected UE positions. In the case of no relays, both of these two UEs receive signals from the BS. After all the relays are in place, due to their different locations, UE 2 still communicates with the BS, while UE 6 chooses a relay. So the interference sources for these two UEs are different, hence the ways to calculate the interference are different. They are depicted in the above paragraph and shown in these two figures. In the figures, solid lines indicate the interference received by a UE from the co-channel BSs, while dotted lines indicate the interference received by a UE from the relays in other clusters using the same channel. The asterisk sign in the figures represents a UE.

Once the interference sources are determined for a UE, $SINR$ can be recalculated using (3.1).

After obtaining the $SINR$ for both without-relay and with-relay cases for each UE, Table 1 is used to find out the throughput (spectral efficiency) for that UE. Then, the throughput values of all the UEs in the innermost cluster are summed up and subsequently divided with the total numbers of UEs in one cluster, which is equal to the number of UEs per cell (S) times the cluster size (N). The above steps are repeated for a total of 1000 times to calculate the sum and average throughput.

Please refer to Figures 3.3 and 3.4 for the flowcharts of distance-, pathloss- and $SINR$ -based algorithms. Figure 3.3 shows the case when ORB (explained in Chapter 2) is not taken into account; Figure 3.4 shows the case when ORB is taken into account.

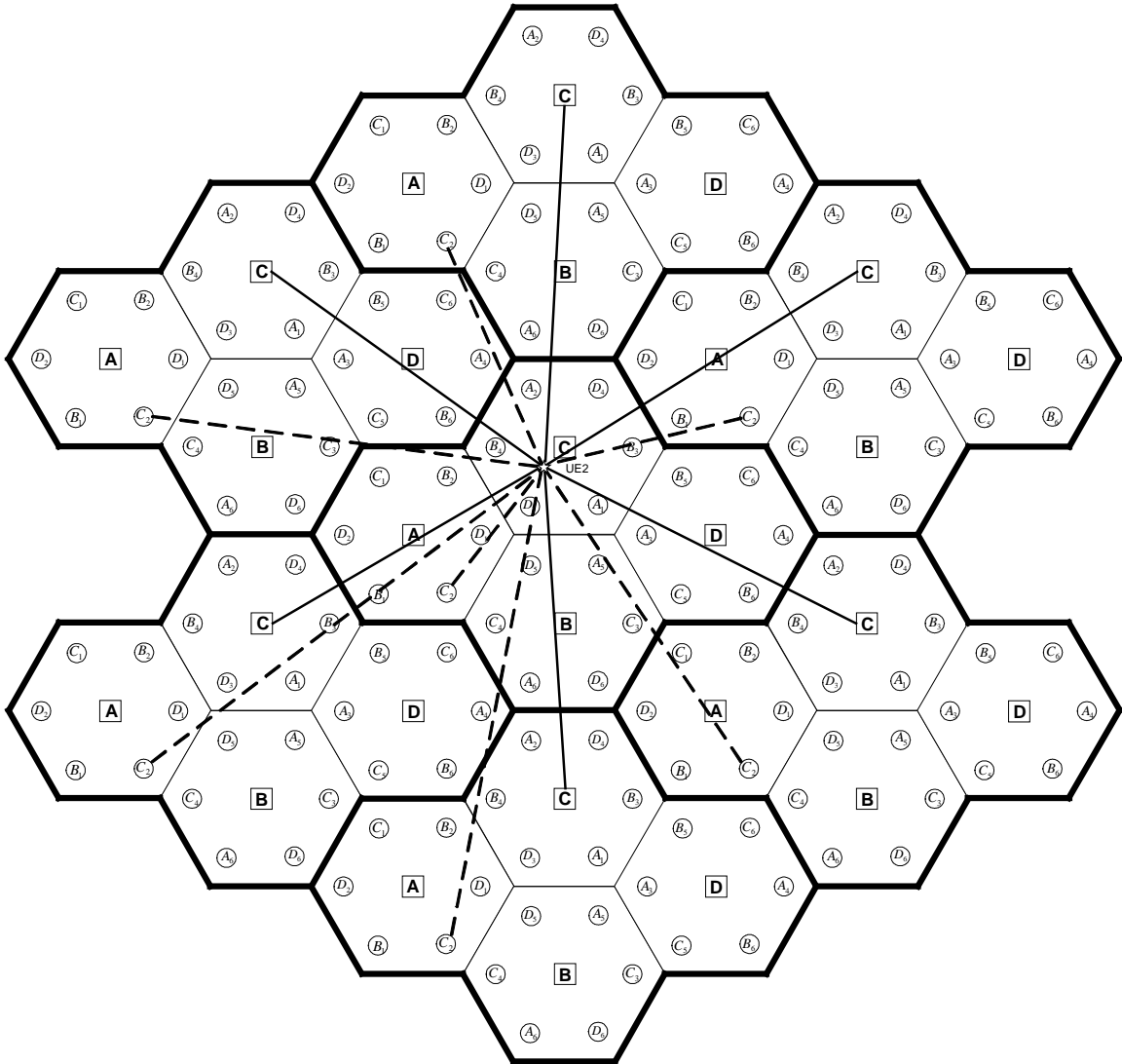


Figure 3.1: Interference received by UE 2 from other BSs and relays (When UE 2 receives signal from the BS).

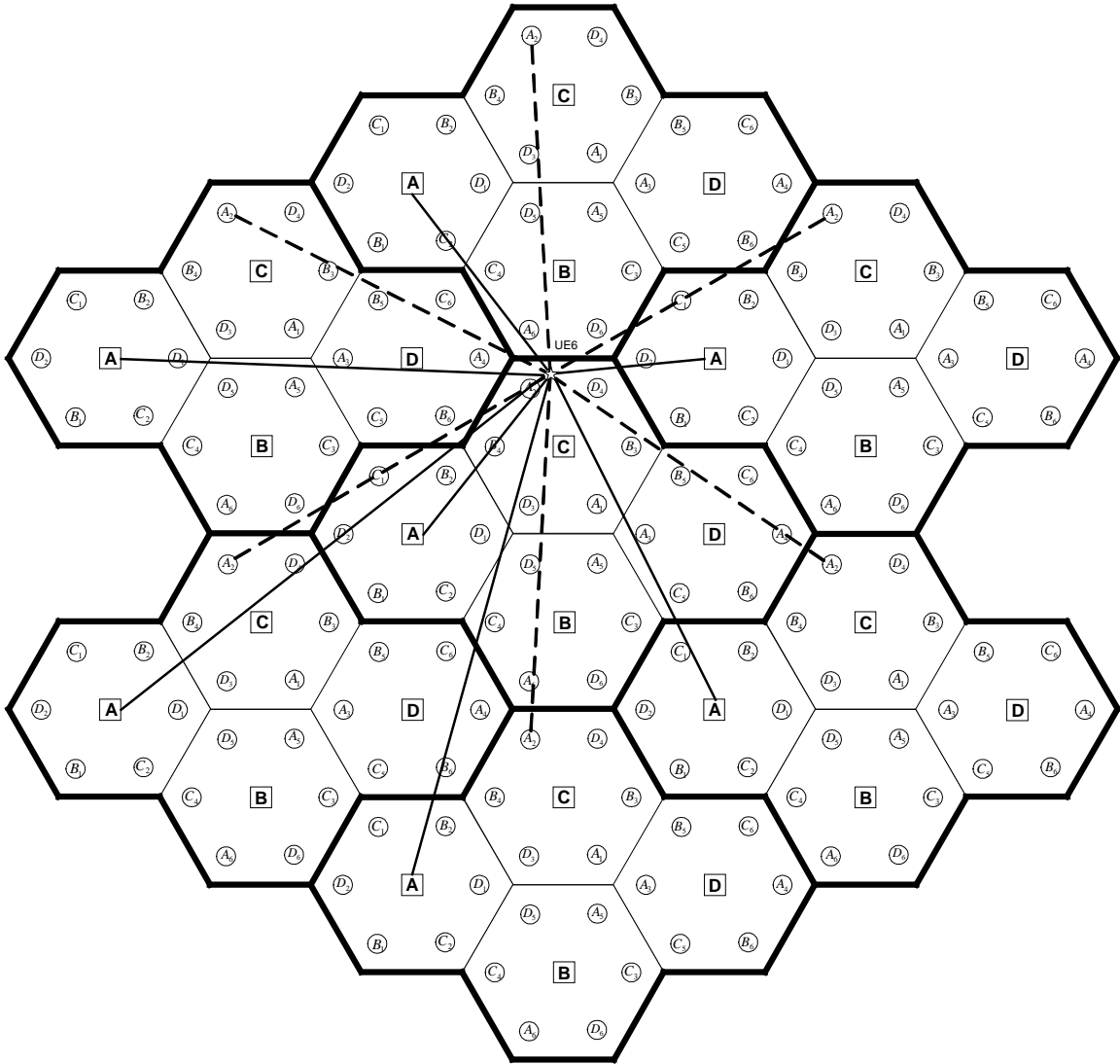


Figure 3.2: Interference received by UE 6 from other BSs and relays (When UE 6 receives signal from a relay).

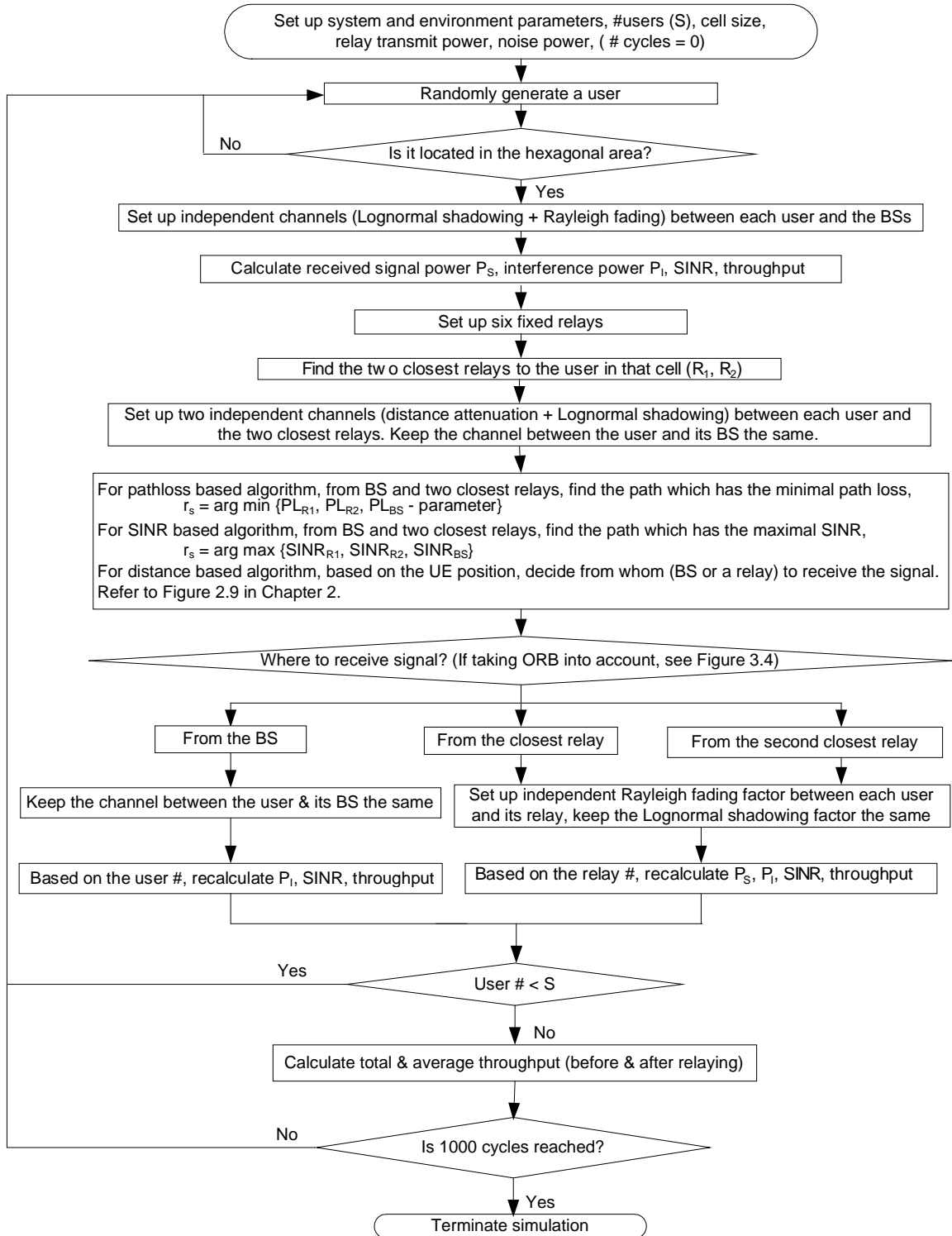


Figure 3.3: Flowchart (when ORB is not taken into account).

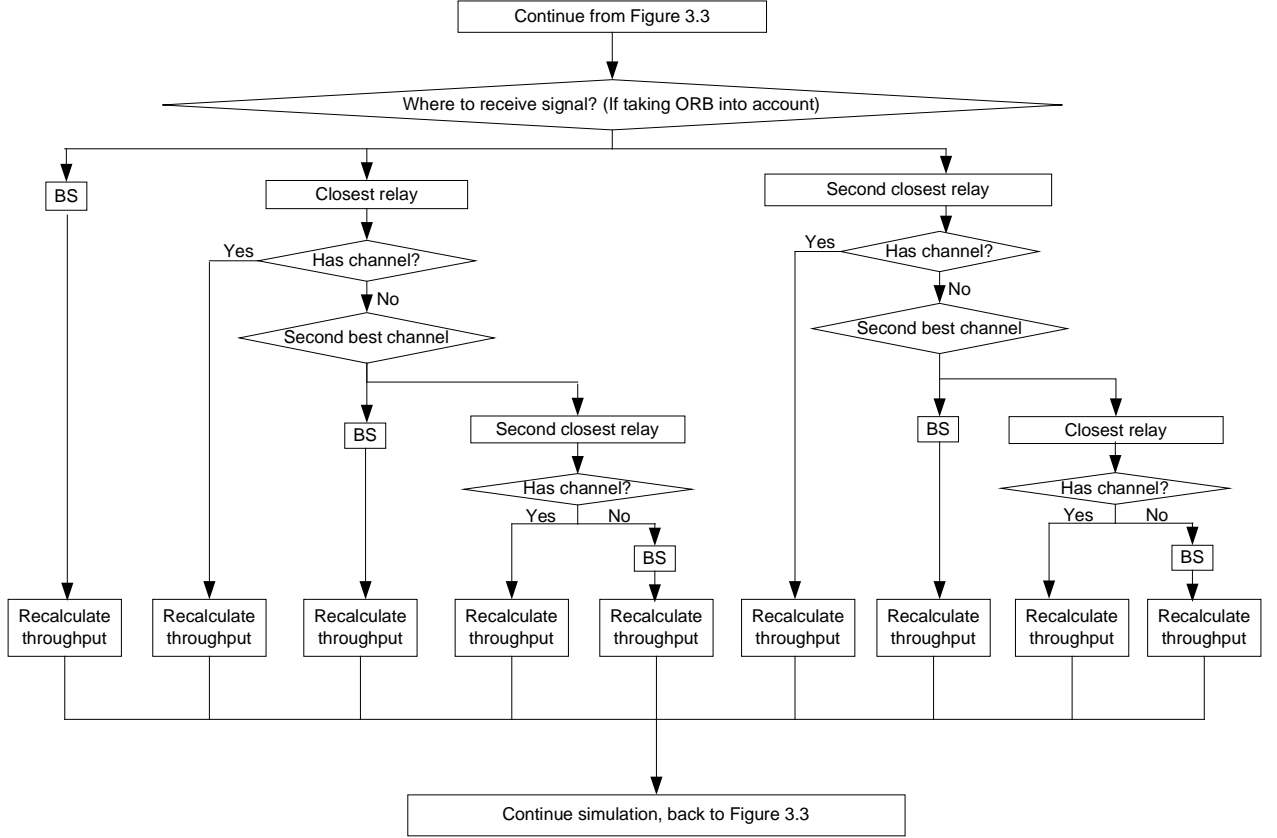


Figure 3.4: Flowchart (when ORB is taken into account).

3.3 Simulation Algorithm for $N = 1$ Case

The simulation algorithm for $N = 1$ case is almost the same as described in section 3.2, except this time we use the following formula for the interference calculation.

$$SINR = \frac{P_s}{ISF \times P_i + P_N},$$

Here ISF is the interference suppression factor. Its value ranges from 0 to 1. When the frequency reuse factor is one, the aggregate interference will be too high and the system will not be able to work properly without some interference mitigation scheme. The parameter ISF indicates the extent of how much an interference cancellation scheme

could reduce the interference. As we can see from the equation, $ISF = 0$ means all the interference is suppressed, so there is no interference from co-channel interferers. Only the noise adversely influences the system performance. $ISF = 1$ means there is no interference suppression. Similar to the $N = 4$ case, Figures 3.5 and 3.6 provide the interference received by the UE for two typical cases. Again, the solid lines represent the interference powers from other BSs using the same channel, and the dotted lines represent the interference powers from relays in other clusters using the same channel.

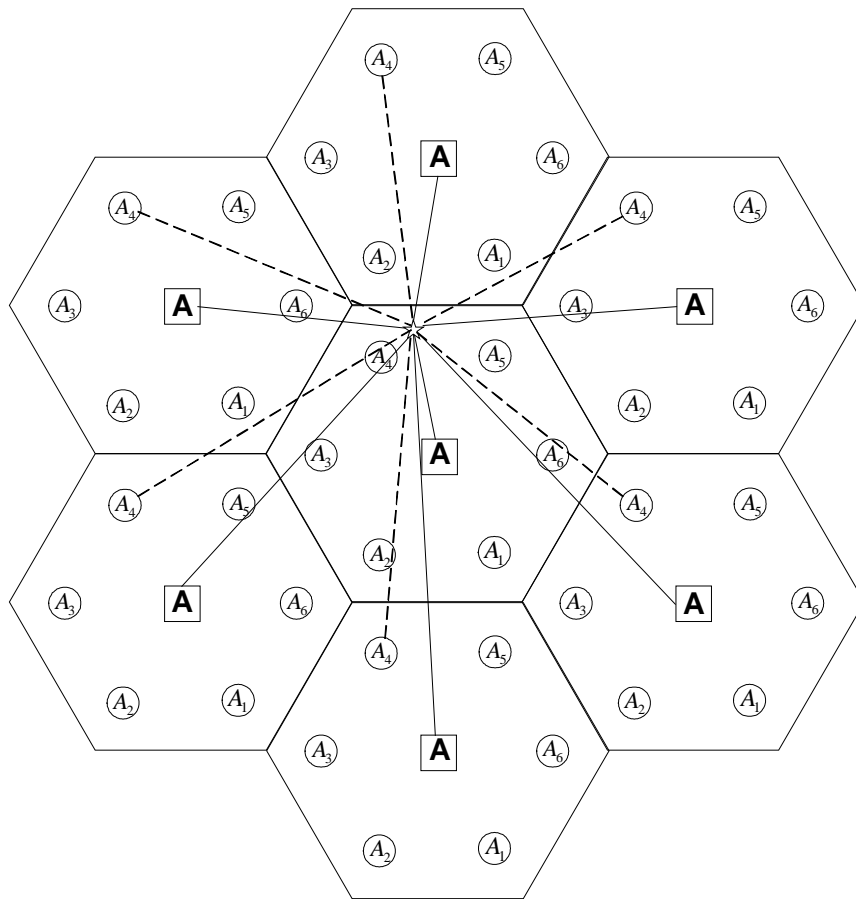


Figure 3.5: Interference sources for cluster size $N = 1$ case (when UE receives signal from a relay).

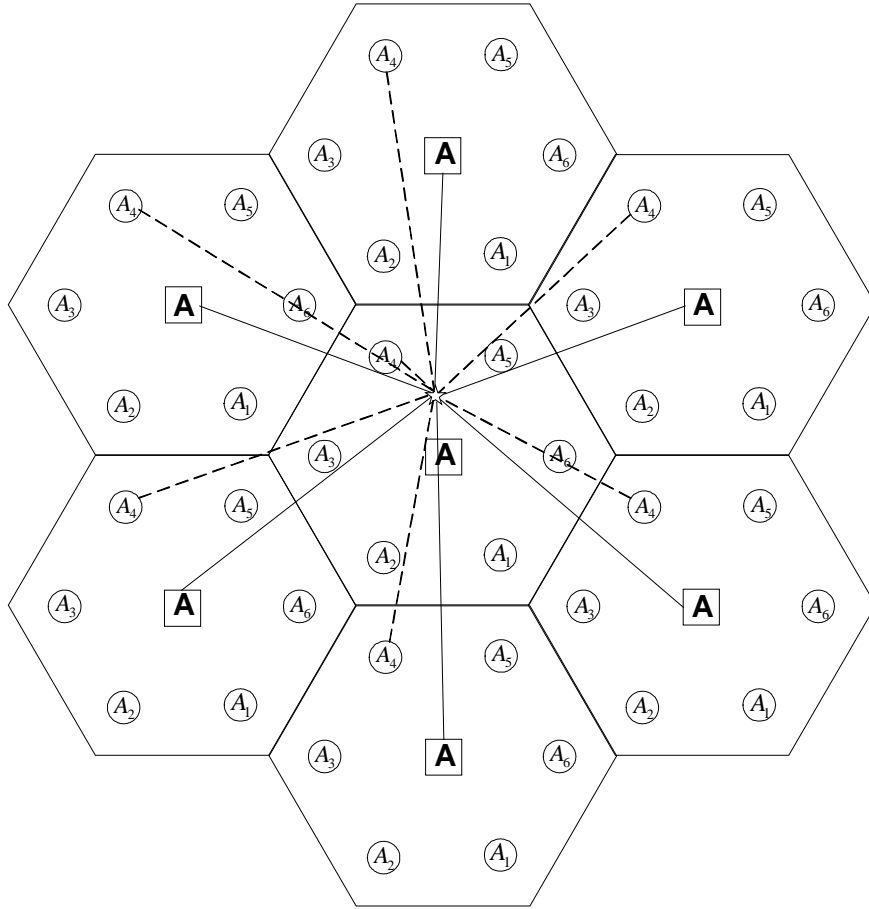


Figure 3.6: Interference sources for cluster size $N = 1$ case (when UE is receives signal from the BS).

Chapter 4 Simulation Results, Part I: $N = 4$ Case

This chapter and the following one present the simulation results. This chapter is focused on the results for the cluster size $N = 4$ case and the following chapter is focused on $N = 1$ case.

The results shown in this and the following chapter are mainly based on SINR-based algorithm, which yields the best output, though the average throughput improvement for the three different relay selection algorithms demonstrated in Section 2.5 is given in Section 4.4. This chapter also investigates the following points: the average throughput improvement, the relay usage, the impact of ORB on system performance, the throughput increase provided by diversity, the system sensitivity to the background noise, the transmission bandwidth and the pathloss exponent. How often each combination of modulation and coding is used is described in the latter portion of this chapter.

4.1 Average Spectral Efficiency of SINR-based Algorithm

Figures 4.1, 4.2 and 4.3 show the average throughput where cell radius is 2000 m, 1000 m and 500 m, respectively. From these three figures we can see that when using relays in a cell, the throughput is greatly increased in all the three cases, comparing to that of the no relaying case.

When the relay transmit power is increased, we get higher throughput. For example in Figure 4.3 where $R = 500$ m, when user density is 72 and $P_{rel} = 0.1$ W, the throughput improvement is 0.7 bits/sec/Hz corresponding to a 22% increase ($3.22 \rightarrow 3.92$). When we increase P_{rel} to 1 W, the throughput is increased by 42% ($3.22 \rightarrow 4.6$).

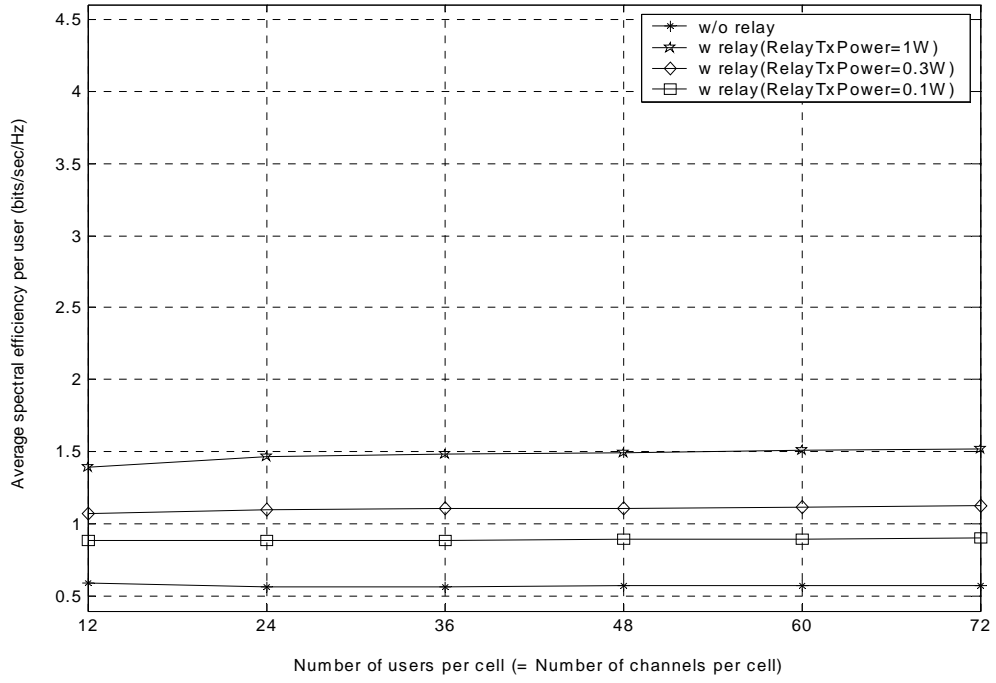


Figure 4.1: Average spectral efficiency (SINR-based relay selection algorithm, $R = 2000$ m , $N = 4$).

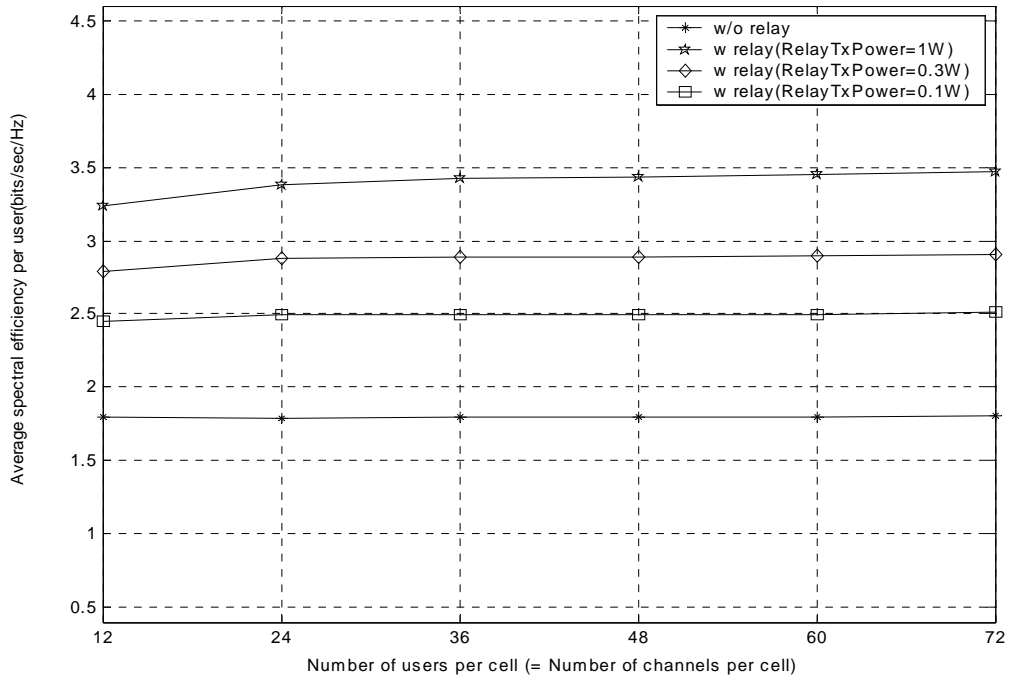


Figure 4.2: Average spectral efficiency (SINR-based relay selection algorithm, $R = 1000$ m , $N = 4$).

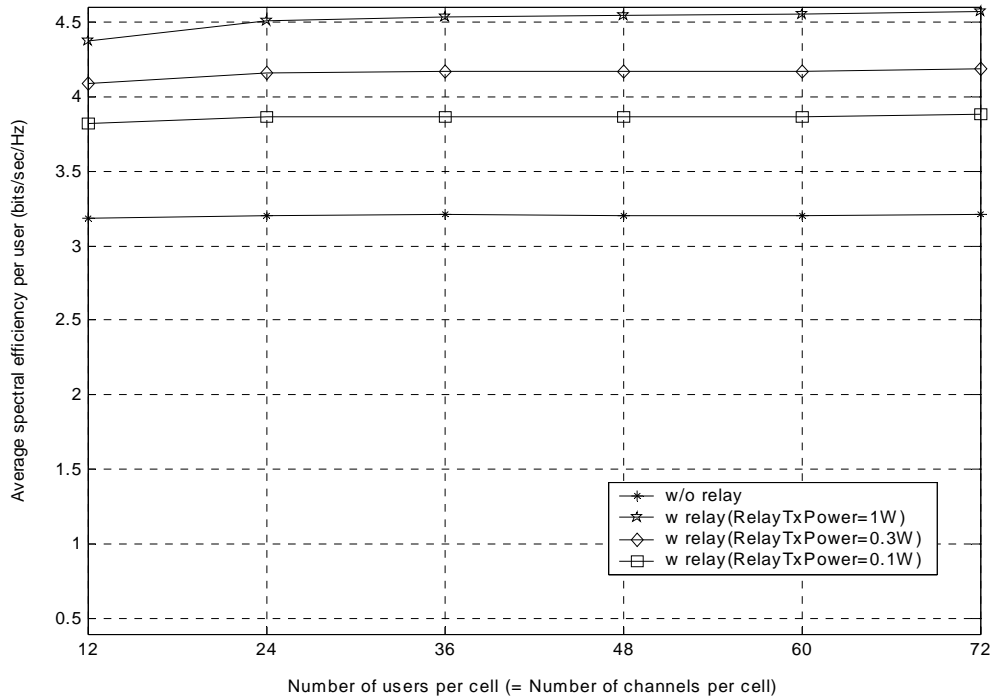


Figure 4.3: Average spectral efficiency (SINR-based relay selection algorithm, $R = 500$ m, $N = 4$).

4.2 Relay Usage

As mentioned in Section 2.4, if too many UEs try to connect to the same relay, Optimal-Route-Blockage (ORB) occurs. Figure 4.4 shows the percentage of users affected by Optimal-Route-Blockage (ORB) when $R = 2000$ m, 1000 m and 500 m. 1) According to the traffic engineering theory, when the user density is lower, e.g., $S = 12$, the probability of being affected by ORB is higher due to the loss of trunking efficiency. 2) Optimal-Route-Blockage does not happen often in any of the cases considered (different relay selection algorithms, different cell sizes, etc.). For example, when the P_{rel} is 1 W and the number of UEs per cell is 12 , the blockage is 9.5% at the most. If the number of UEs per cell is 72 , the blockage is less than 1% . This means if a UE needs relaying assistance, the probability that a relay has a relaying channel and provides

relaying service to this terminal is very high. It can be concluded as well that the relaying channel partition scheme implemented in this research does not cause significant blockage.

Figure 4.5 shows the percentage of users communicating with relays when $R = 2000$ m, 1000 m and 500 m. A joint conclusion can be drawn from Figures 4.4 and 4.5 that the higher the relay transmit power is, the higher percentage of users will communicate with relays, and the higher probability of being affected by Optimal-Route-Blockage will be.

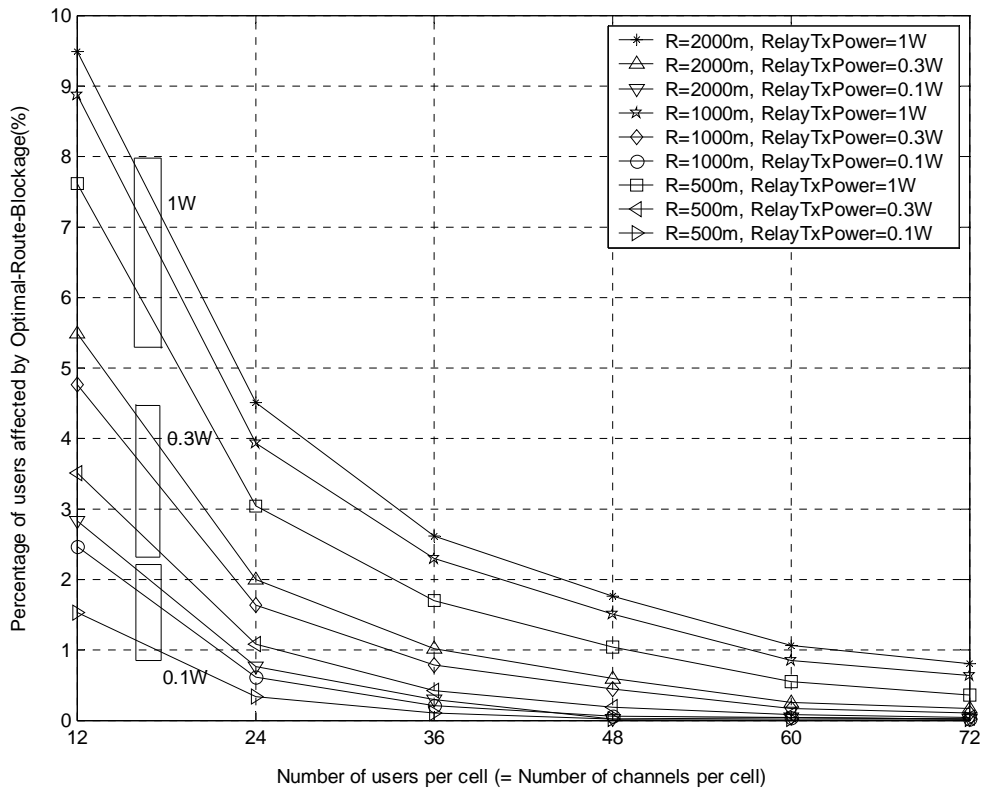


Figure 4.4: Percentage of users affected by ORB (SINR-based relay selection algorithm, $N = 4$).

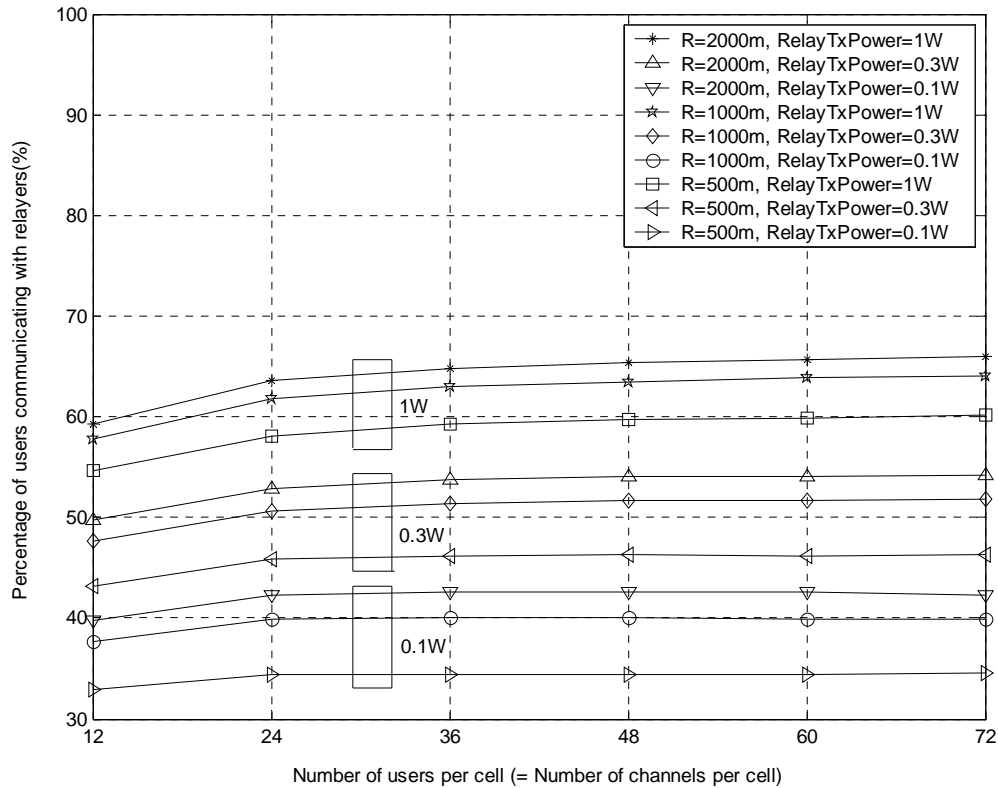


Figure 4.5: Percentage of users communicating with relays (SINR-based relay selection algorithm, $N = 4$).

4.3 Average Spectral Efficiency for with and without ORB Cases

Figures 4.6, 4.7 and 4.8 compare with and without Optimal-Route-Blockage (ORB) cases when $R = 500$ m, 1000 m and 2000 m. For a “without ORB” case, it is assumed that a relay can always offer a relaying channel for a UE, whether the channel is actually available or not. These three figures show that if ORB is not taken into account, the throughput is slightly higher and does not fluctuate with the increase of number of users per cell; if taking ORB into account, the performance slightly decreases, comparing to the opposite case. We can come to a common conclusion from Figure 4.4 and these three figures that the higher number of users per cell, the lower percentage of users being

affected by ORB, the higher throughput we will get, which better reaches the without ORB scenario.

In all the curves except those given in this section, ORB is indeed taken into account. Since the adverse effect of ORB is not significant, especially for higher S values, starting from the next section, only the results for high UE density ($S = 72$) are given out.

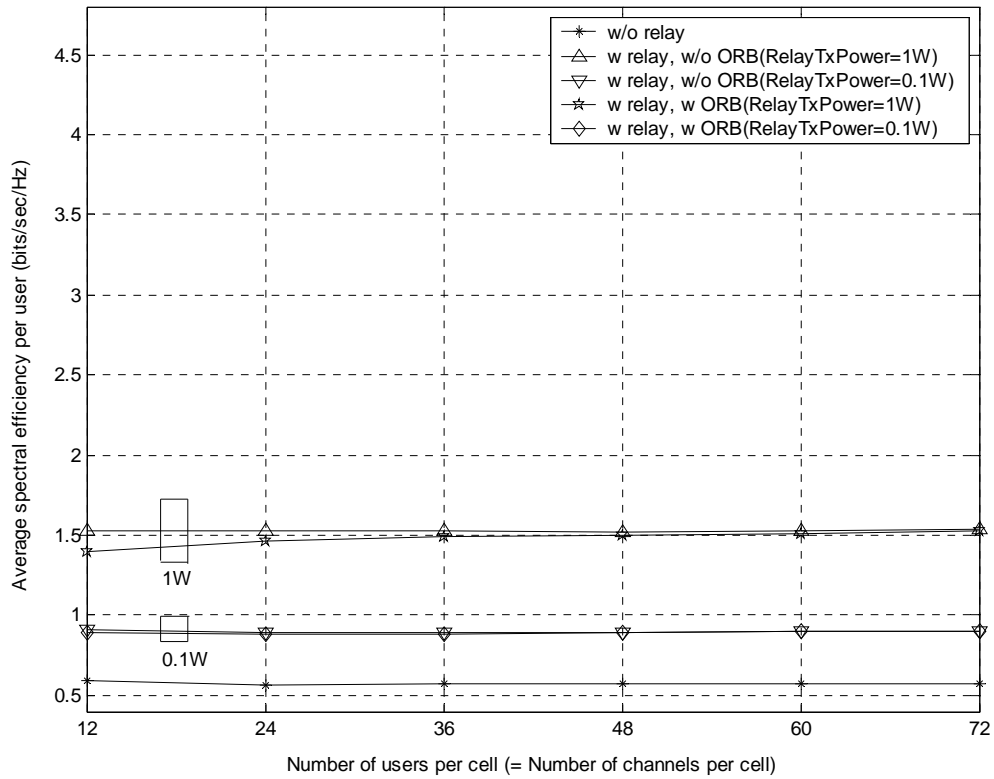


Figure 4.6: Average spectral efficiency comparison for two cases: With and without ORB incorporated (SINR-based relay selection algorithm, $R = 2000$ m, $N = 4$).

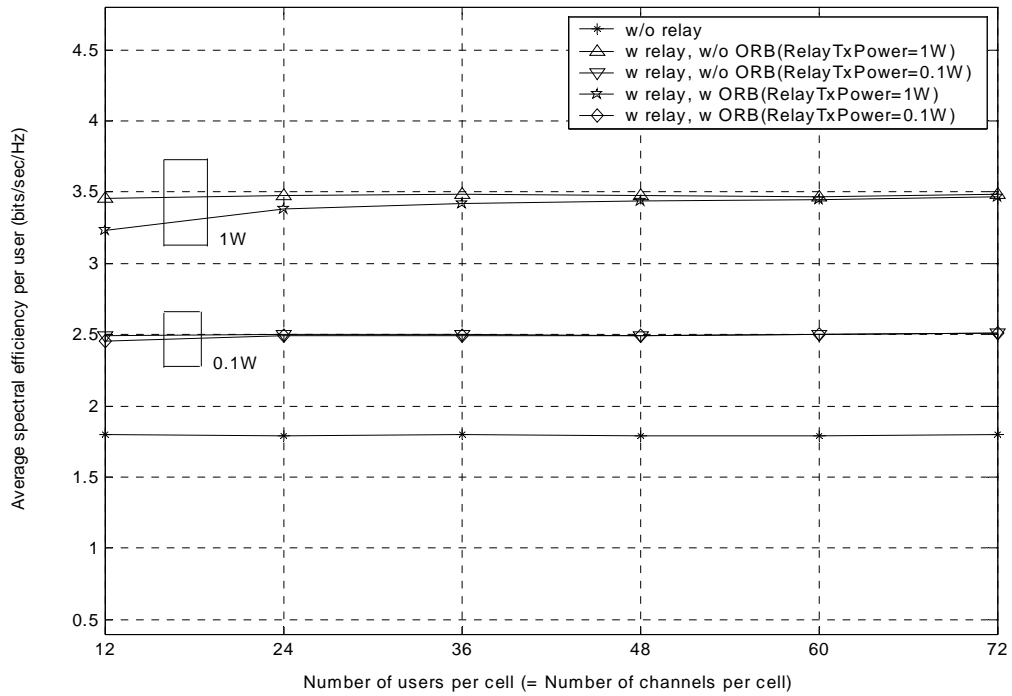


Figure 4.7: Average spectral efficiency comparison for two cases: With and without ORB incorporated (SINR-based relay selection algorithm, $R = 1000$ m, $N = 4$).

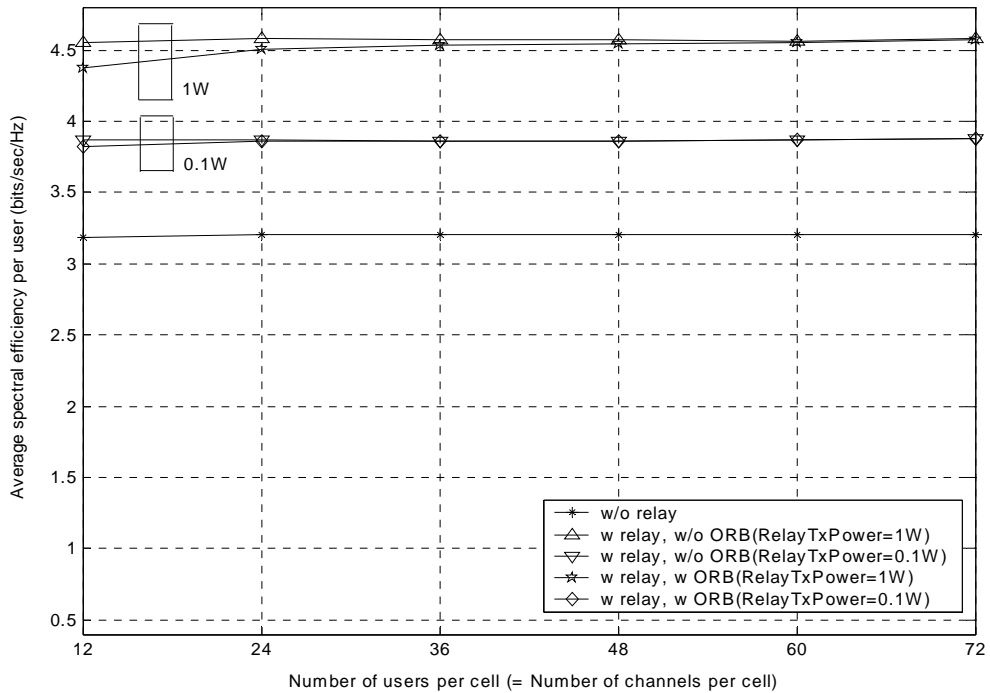


Figure 4.8: Average spectral efficiency comparison for two cases: With and without ORB incorporated (SINR-based relay selection algorithm, $R = 500$ m, $N = 4$).

4.4 Average Spectral Efficiency Comparison for Different Relay Selection Algorithms

Figures 4.9, 4.10 and 4.11 compare the average throughput for the three relay selection algorithms, distance, pathloss and SINR, when $R = 2000$ m, 1000 m or 500 m. The throughput of the SINR-based algorithm is slightly better than that of the pathloss-based one. If SINR is difficult to implement, pathloss-based algorithm can be used with fairly good results. As expected, distance-based algorithm introduces the least throughput improvement, but it is easy to implement and it involves the least signalling overhead.

Note that in Figures 4.9-4.15, the beginning of the horizontal axis ($P_{rel} = 0$ W) corresponds to the no-relaying case.

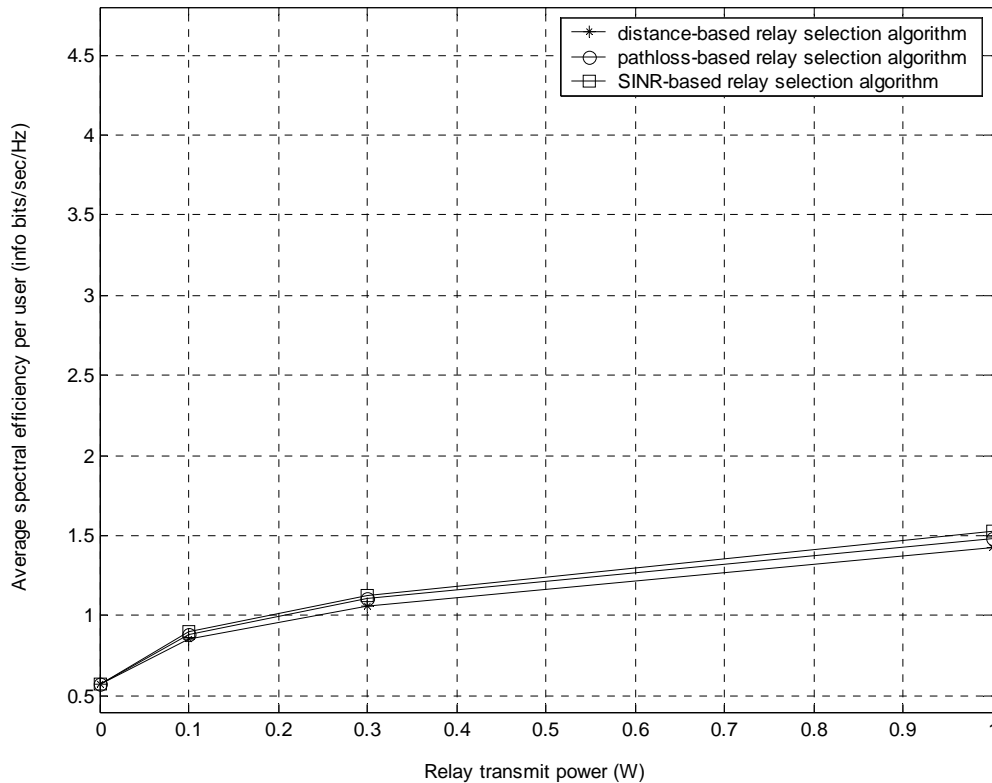


Figure 4.9: Average spectral efficiency comparison for distance-, pathloss- and SINR-based relay selection algorithms ($R = 2000$ m, $N = 4$).

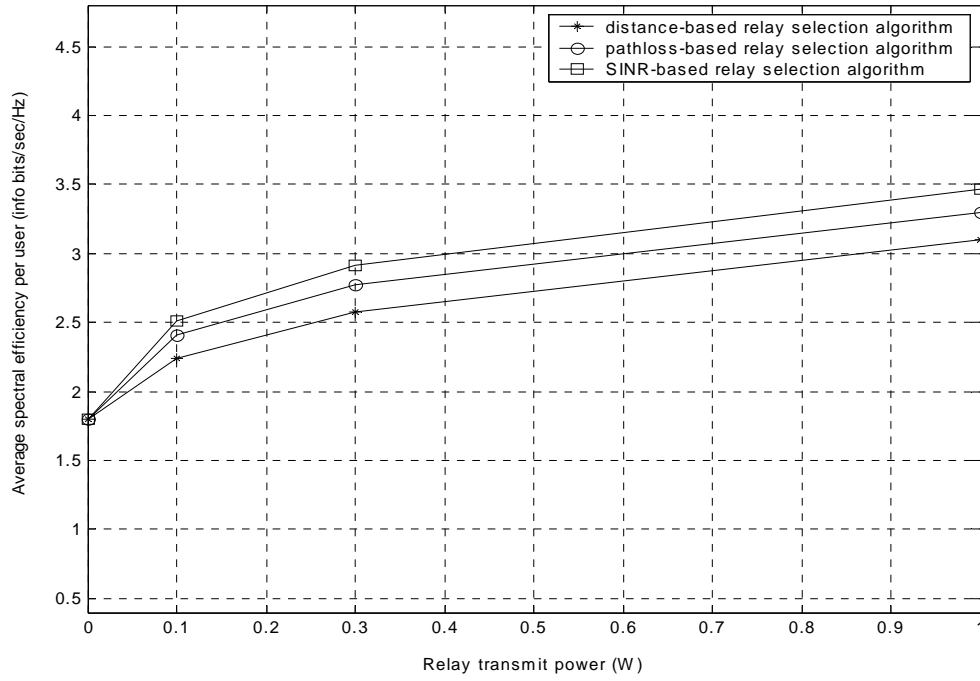


Figure 4.10: Average spectral efficiency comparison for distance-, pathloss- and SINR-based relay selection algorithms ($R = 1000$ m, $N = 4$).

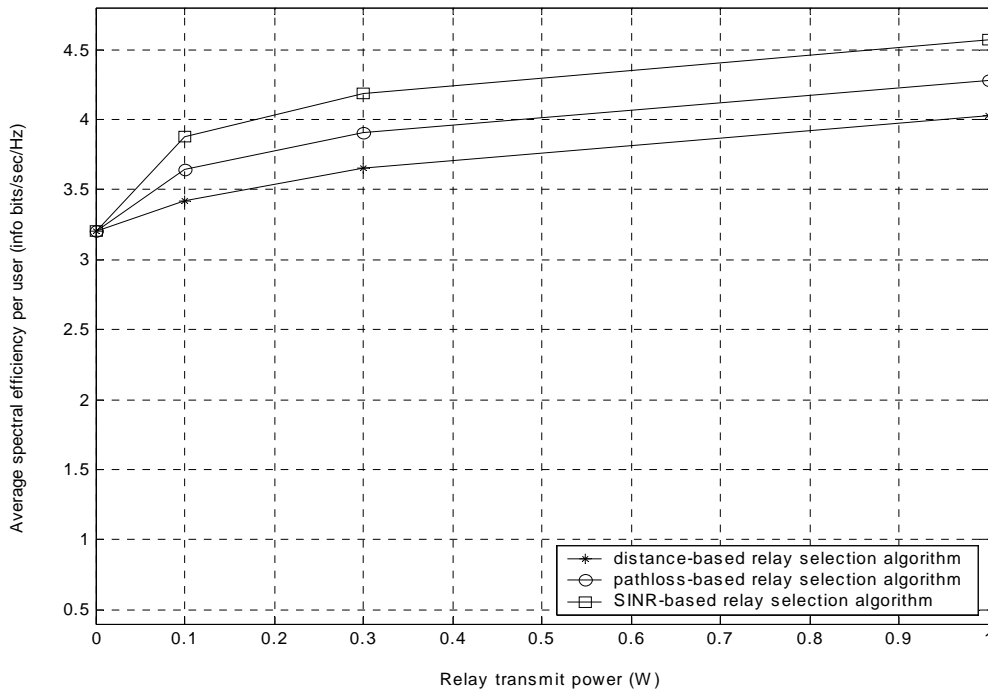


Figure 4.11: Average spectral efficiency comparison for distance-, pathloss- and SINR-based relay selection algorithms ($R = 500$ m, $N = 4$).

4.5 Average Spectral Efficiency Comparison for with and without Diversity

Figures 4.12, 4.13 and 4.14 show the average spectral efficiency increase provided through diversity for all the three cell sizes. Diversity is brought in to offer more throughput gain, though it does not offer much enhancement. For instance, it is observed from Figure 4.14 that for $R = 500$ m, when the relay transmit power is 1 W, the average throughput gain is 1.53% ($4.57 \rightarrow 4.64$ bits/sec/Hz). This is because only around 60% of the UEs communicating with a relay benefit from a secondary link (from BS to UE) for diversity. Usually the secondary links are much weaker than the primary links (from relay to UE). So, this type of diversity does not provide significant throughput increase.

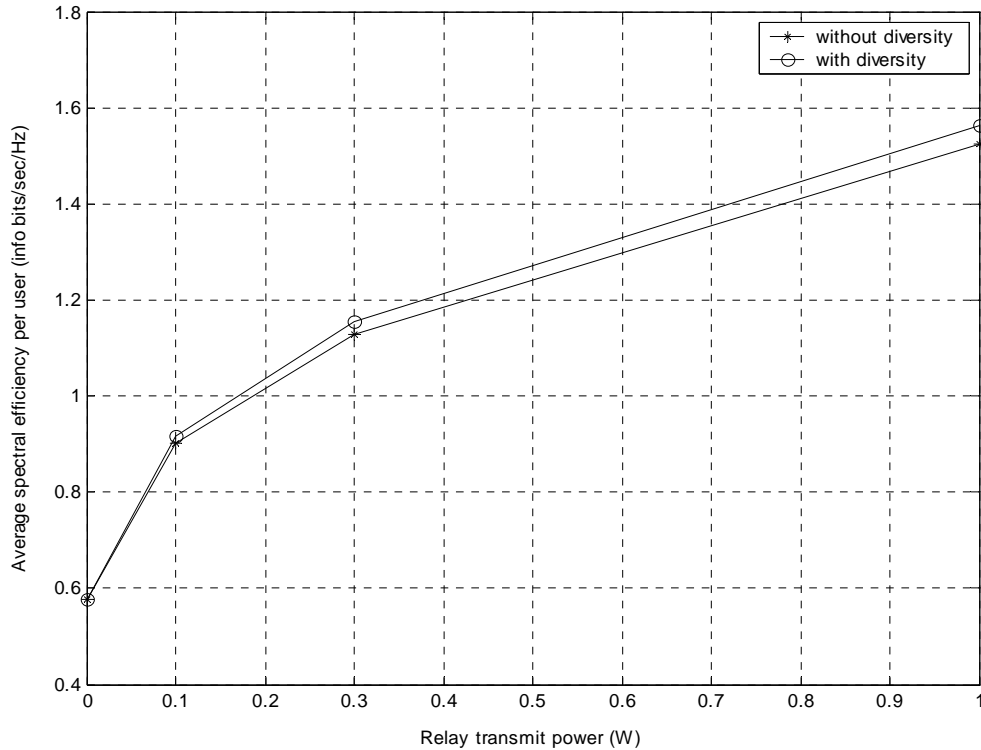


Figure 4.12: Average spectral efficiency comparison for with and without diversity (SINR-based relay selection algorithm, $R = 2000$ m, $N = 4$).

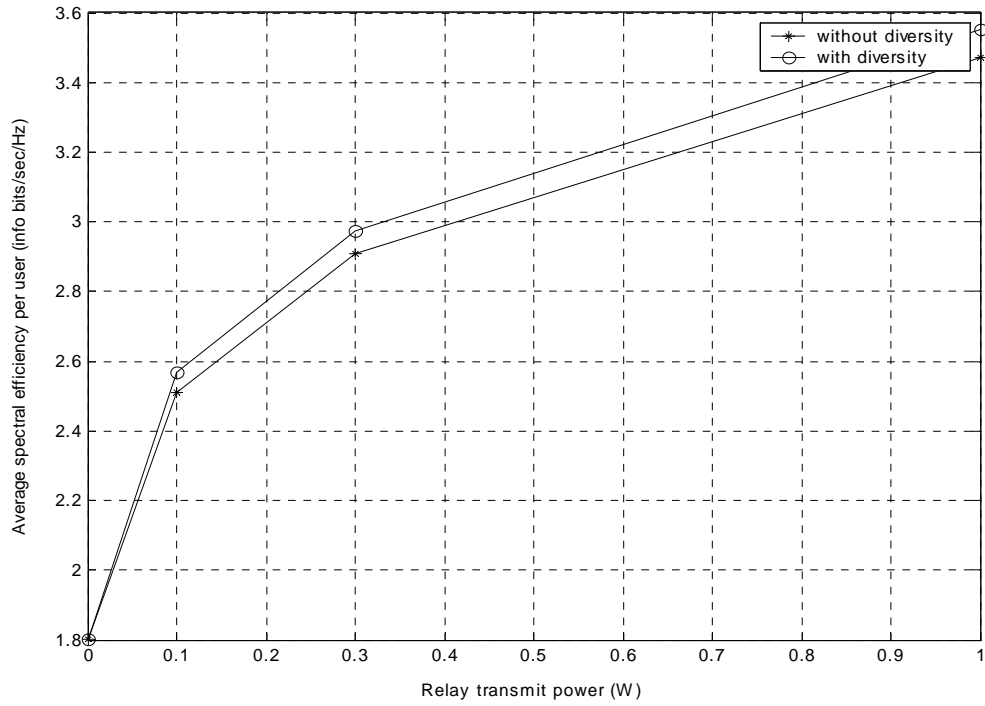


Figure 4.13: Average spectral efficiency comparison for with and without diversity (SINR-based relay selection algorithm, $R = 1000$ m, $N = 4$).

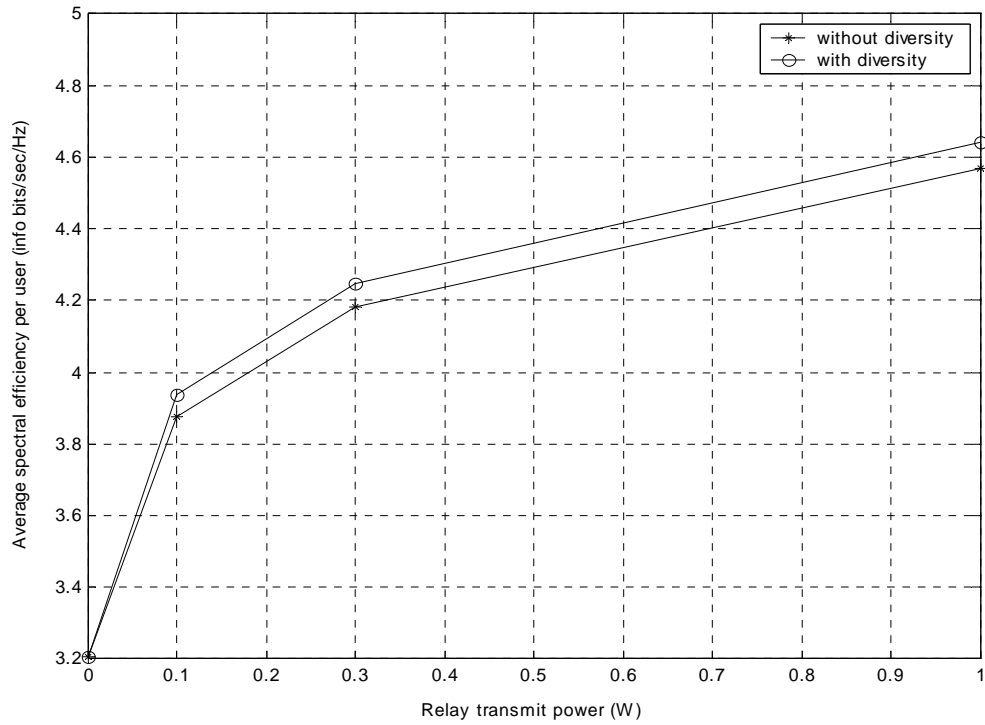


Figure 4.14: Average spectral efficiency comparison for with and without diversity (SINR-based relay selection algorithm, $R = 500$ m, $N = 4$).

4.6 Effect of Background Noise

Figure 4.15 shows how severe the noise can affect the overall performance ($R = 1000$ m). We observe from Figure 4.15 that the difference between with-noise and without-noise cases for no relay scheme is getting smaller with the increased relay power. For no-relaying case this difference is $3.65 - 1.8 = 1.85$ bits/sec/Hz, while this value is $4.8 - 3.48 = 1.32$ bits/sec/Hz when $P_{rel} = 1$ W.

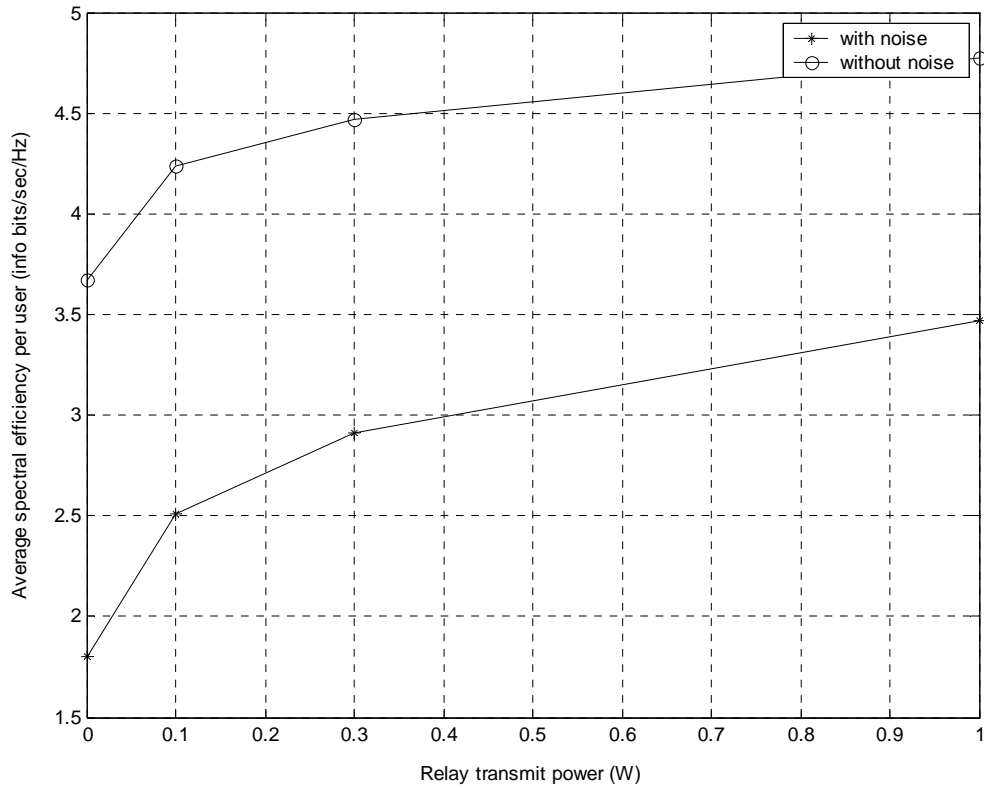


Figure 4.15: Average spectral efficiency comparison for with and without background noise (SINR-based relay selection algorithm, $R = 1000$ m, $N = 4$).

4.7 Effect of Bandwidth (i.e., Noise Power)

Figure 4.16 investigates how the transmission bandwidth (i.e., noise power) will affect the system throughput. From this figure we can see that when the bandwidth increases and thus the noise power gets higher, the average spectral efficiency decreases. It is also observed that when the bandwidth is 100 KHz, the throughput is increased by 28.7% (3.48 \rightarrow 4.7 bits/sec/Hz). And we can get much higher throughput increase of 173% (0.51 \rightarrow 1.39 bits/sec/Hz) when the bandwidth is 100 MHz. Since the transmission band used in the future's cellular network is likely to become wider, applying relaying technology is suitable in a wideband system.

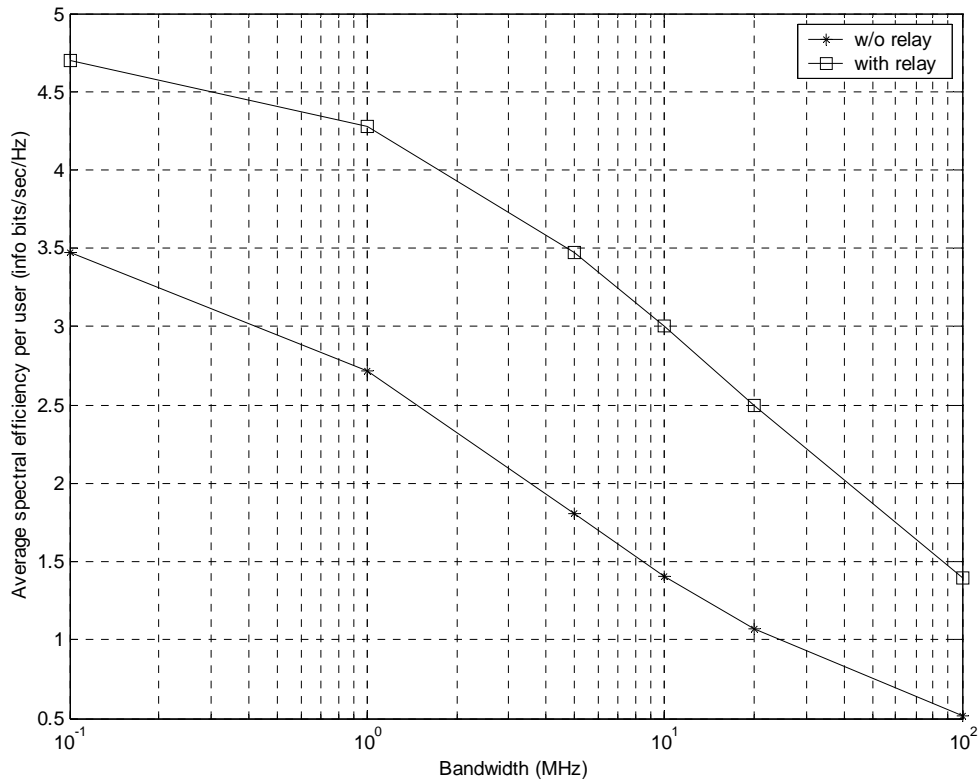


Figure 4.16: Average spectral efficiency for different bandwidth values (SINR-based relay selection algorithm, $P_{rel} = 1$ W, $R = 1000$ m, $N = 4$).

4.8 Effect of Pathloss Exponent

The pathloss exponent n used in all the previous simulations is 4. In order to investigate how the pathloss exponent n influences system performance, we subsequently examined the throughput gains for the following n values: 2.5, 3, 3.5, 4, 4.5, and 5. Figures 4.17-4.19 show the average spectral efficiency for different propagation exponent values in 2000 m, 1000 m and 500 m cells. As can be observed from the simulation results shown in these Figures, there is a consistent throughput gain for all n values. The following is a mathematical analysis of the affect of n on system performance.

As stated in Section 3.2, $SINR$ can be calculated as:

$$SINR = \frac{P_S}{P_I + P_N} = \frac{k(n) \times \frac{P_{t1}}{d^n}}{k(n) \times \sum_i \frac{P_{t2}}{d_i^n} + P_N},$$

where d is the distance from the source (BS or relay) to UE. d_i is the distance from the interferer (BS or relay) to UE. The value of k varies with the variation of n , and its variation rate is much less than that of d^n when n varies. P_{t1} and P_{t2} are the transmit powers of the BSs and relays, which can be 10 W or 1 W. When n is small, P_S and P_I dominate and P_N is negligible, so the results are similar to the no-background noise case. When n gets larger, P_N becomes dominant, and hence $SINR$ decreases.

To further analyze the above situation, let us set $P_N = 0$, then

$$SINR = \frac{P_S}{P_I} = \frac{k(n) \times \frac{P_{t1}}{d^n}}{k(n) \times \sum_i \frac{P_{t2}}{d_i^n}} = \frac{1}{\frac{P_{t2}}{P_{t1}} \times \sum_i \left(\frac{d}{d_i}\right)^n},$$

where $\frac{P_{r2}}{P_{r1}} = 0.1, 1$ or 10 . Since $\frac{d}{d_i} < 1$, when n increases, the denominator decreases, and

hence $SINR$ increases. The simulation results given in Figures 4.17-4.19 correspond to the above analysis.

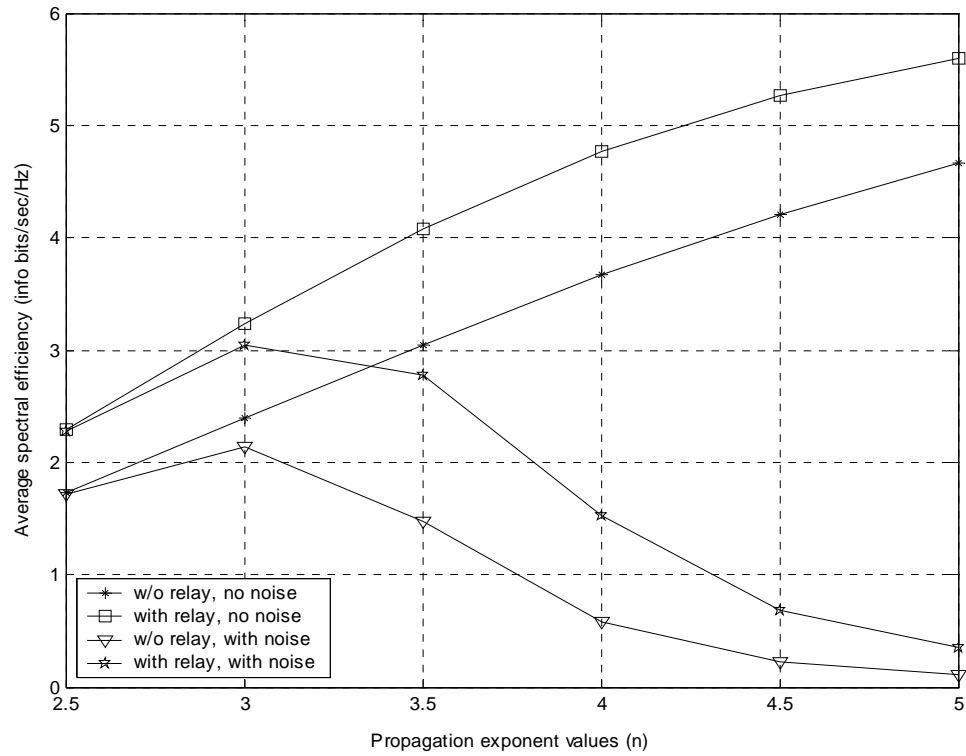


Figure 4.17: Average spectral efficiency for different propagation exponent (n) values (SINR-based relay selection algorithm, $P_{rel} = 1$ W, $R = 2000$ m, $N = 4$).

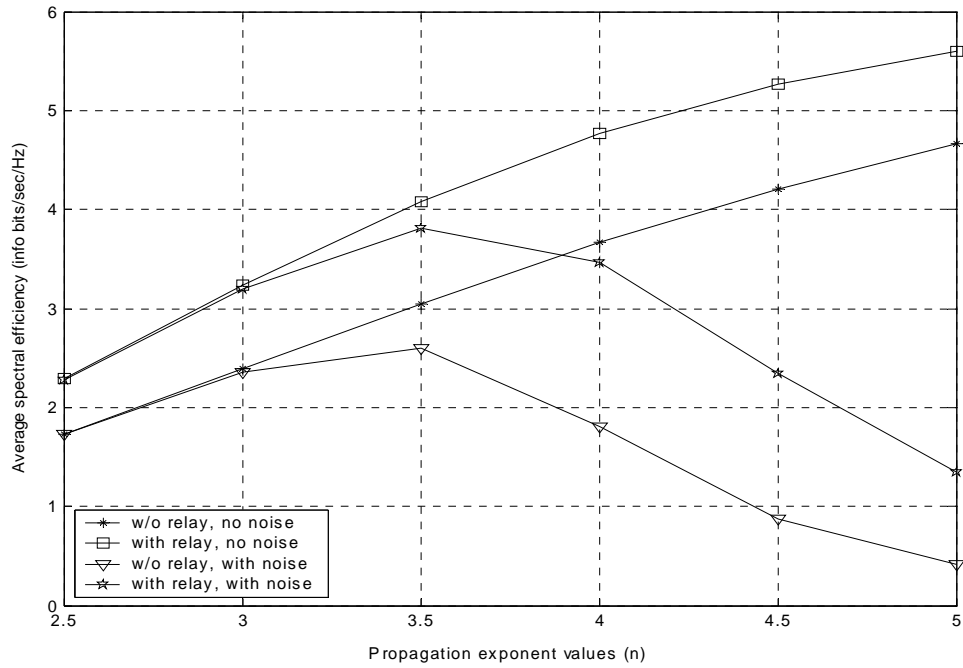


Figure 4.18: Average spectral efficiency for different propagation exponent (n) values (SINR-based relay selection algorithm, $P_{rel} = 1$ W, $R = 1000$ m, $N = 4$).

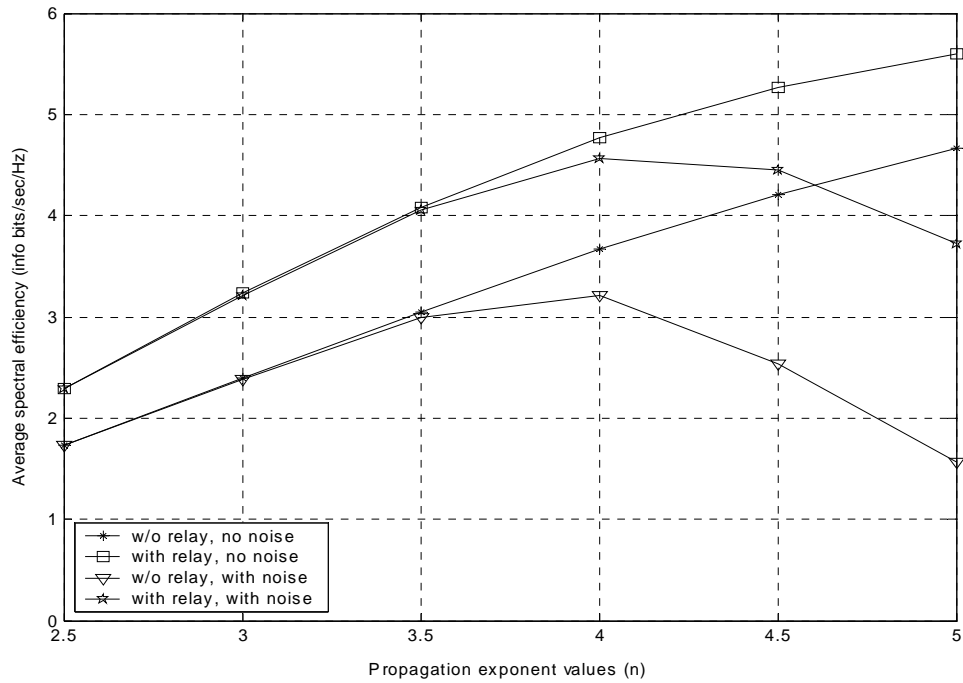


Figure 4.19: Average spectral efficiency for different propagation exponent (n) values (SINR-based relay selection algorithm, $P_{rel} = 1$ W, $R = 500$ m, $N = 4$).

4.9 Adaptive Modulation and Coding Histograms

Figures 4.20 to 4.25 show how often various combinations of the modulation and coding schemes are used. The results are shown for large, medium and small cells: Figures 4.20 and 4.21 are for 2000 m cells, Figures 4.22 and 4.23 are for 1000 m cells, and Figures 4.24 and 4.25 are for 500 m cells.

In all figures for with relaying case, the combinations of 64-QAM with different code rates are used more often than they are in the without relaying case; this is due to the help provided by relays.

In these figures, “% of successful links” means percentage of UEs whose received *SINR* value is greater than 4 dB so that it can support the combination of QPSK and Rate $\frac{1}{2}$, which yields the lowest throughput. This value can be regarded as the coverage performance with the required received signal threshold of 4 dB. See Table 2.

Table 2: Coverage results

Cell Size (m)	Coverage(%)		
	without Relay	with Relay	with Relay and Diversity*
2000	22.16	55.33	57.28
1000	60.14	92.83	94.04
500	84.86	98.56	98.86

On the contrary, “% of failing links” means percentage of UEs whose received *SINR* is less than 4 dB which corresponds to zero throughput. This value can be viewed as the outage performance. Table 3 shows the outage results for different cell sizes.

Table 3: Outage results

Cell Size (m)	Outage(%)		
	without Relay	with Relay	with Relay and Diversity*
2000	77.84	44.67	42.72
1000	39.86	7.17	5.96
500	15.14	1.44	1.14

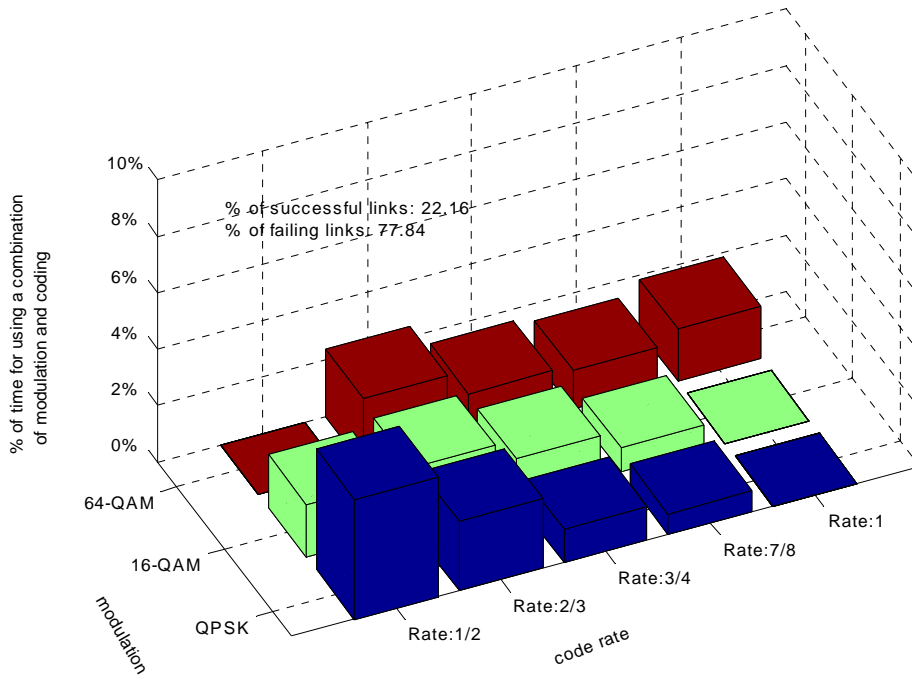


Figure 4.20: Percentage of time using a combination of modulation and coding (without relaying, SINR-based relay selection algorithm, $R = 2000$ m, $N = 4$).

* The data in this column is read from the histograms in Appendix C.

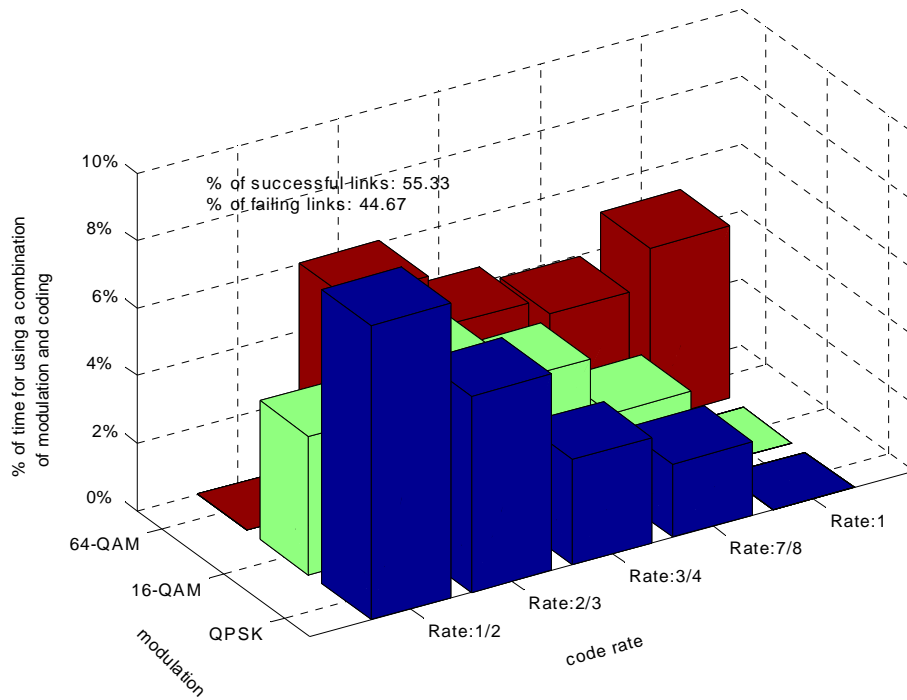


Figure 4.21: Percentage of time using a combination of modulation and coding (with relaying, $P_{rel} = 1$ W, SINR-based relay selection algorithm, $R = 2000$ m, $N = 4$).

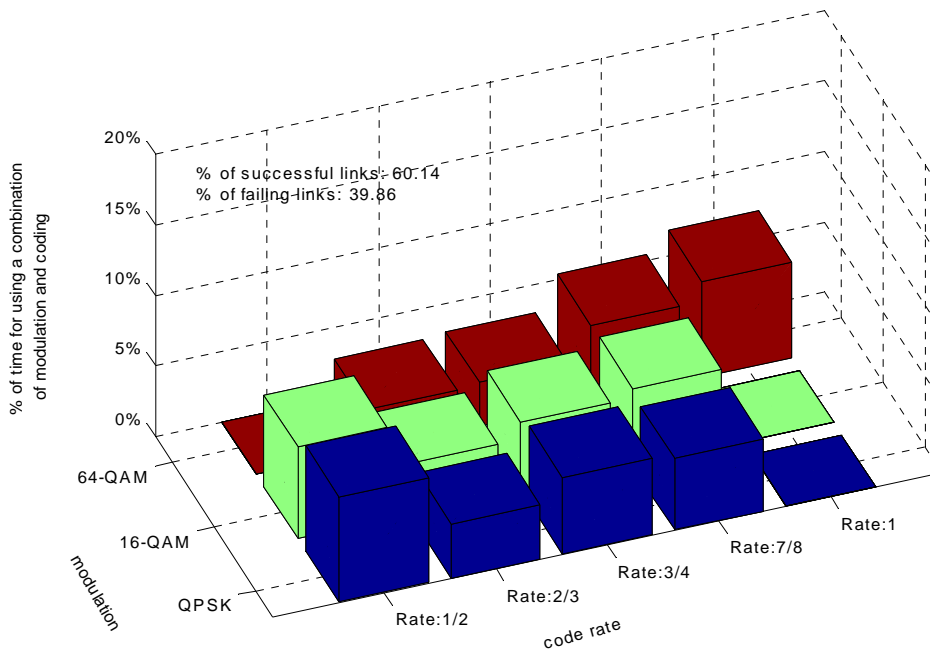


Figure 4.22: Percentage of time using a combination of modulation and coding (without relaying, SINR-based relay selection algorithm, $R = 1000$ m, $N = 4$).

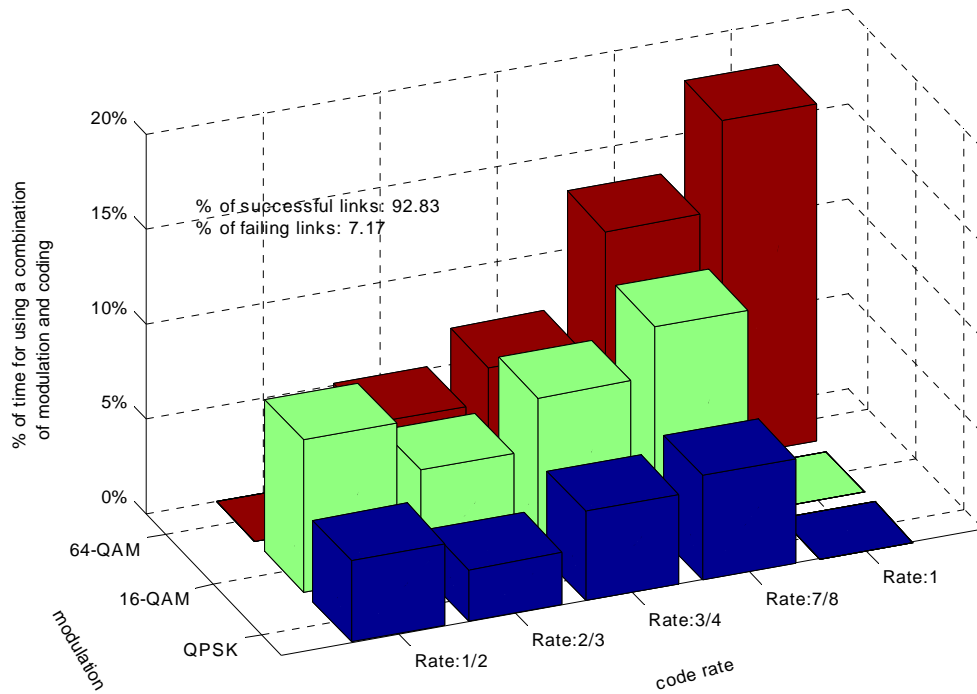


Figure 4.23: Percentage of time using a combination of modulation and coding (with relaying, $P_{rel} = 1$ W, SINR-based relay selection algorithm, $R = 1000$ m, $N = 4$).

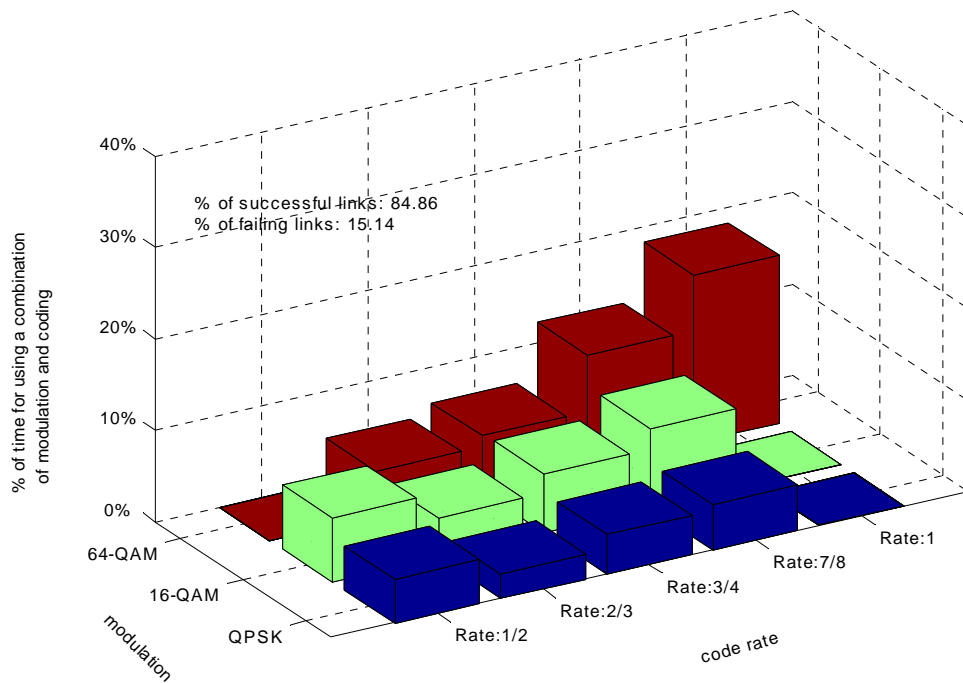


Figure 4.24: Percentage of time using a combination of modulation and coding (without relaying, SINR-based relay selection algorithm, $R = 500$ m, $N = 4$).

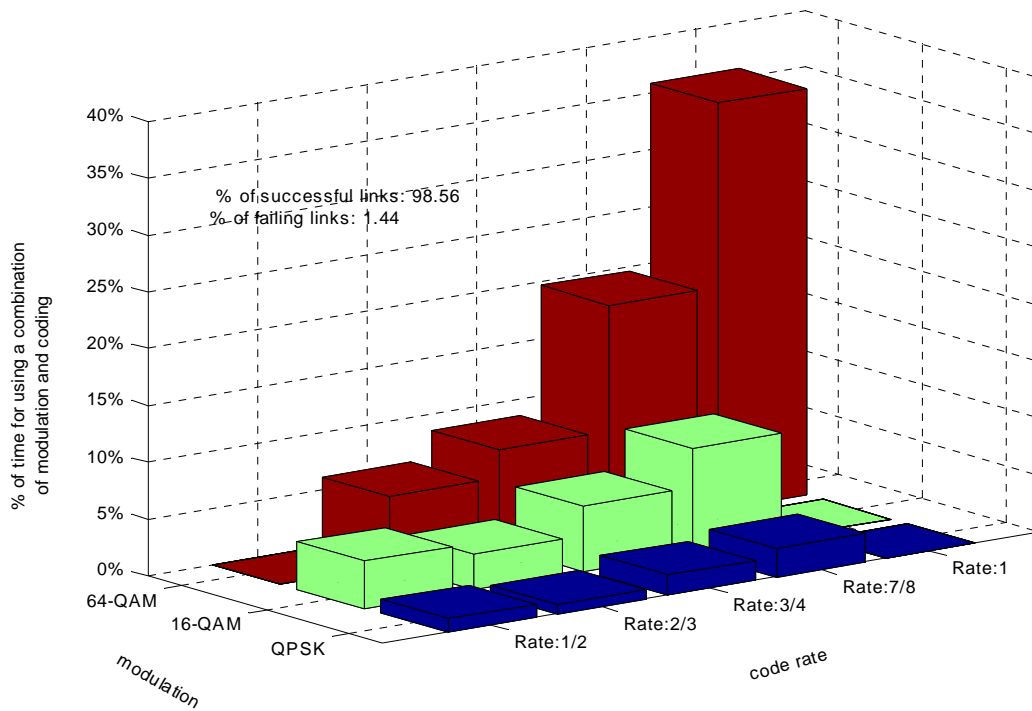


Figure 4.25: Percentage of time using a combination of modulation and coding (with relaying, $P_{rel} = 1$ W, SINR-based relay selection algorithm, $R = 500$ m, $N = 4$).

4.10 Coverage Extension

Digital fixed relays can also help extend the system coverage. Figures 4.26 and 4.27 use two different standpoints, average spectral efficiency and outage, to show the coverage extension brought in by digital fixed relays in large, medium and small cells. For example, in Figure 4.26, an average spectral efficiency of 3.2 bits/sec/Hz can only be achieved in a small cell (500 m) without relays, while the same amount of average spectral efficiency can be achieved in a medium cell (1000 m) with the help of relays. In other words, the system coverage with relays is four times as much as the coverage without relays, because the coverage area is proportional to the square of the radius.

Similarly, in Figure 4.27, the outage percentage around 40% can only be achieved in a medium cell (1000 m) without relays, but it can be achieved in a large cell (2000 m) with relays. This means that with the help of relays, the system outage is largely reduced.

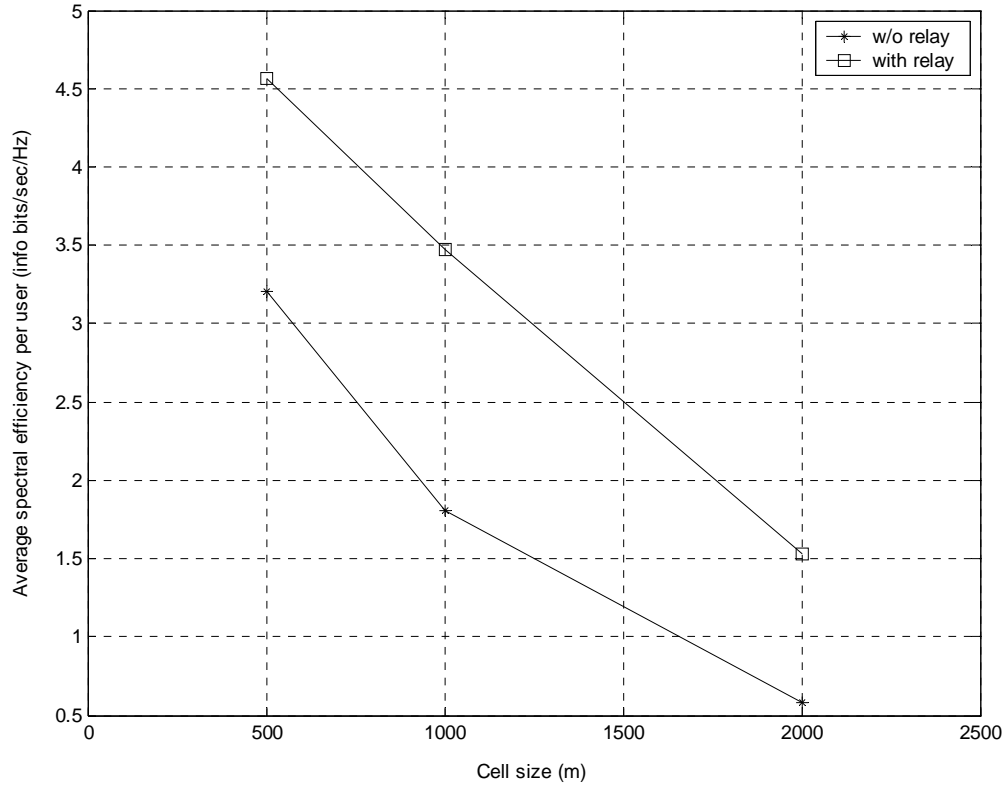


Figure 4.26: Average spectral efficiency for different cell sizes (SINR-based relay selection algorithm, $P_{rel} = 1$ W, $N = 4$).

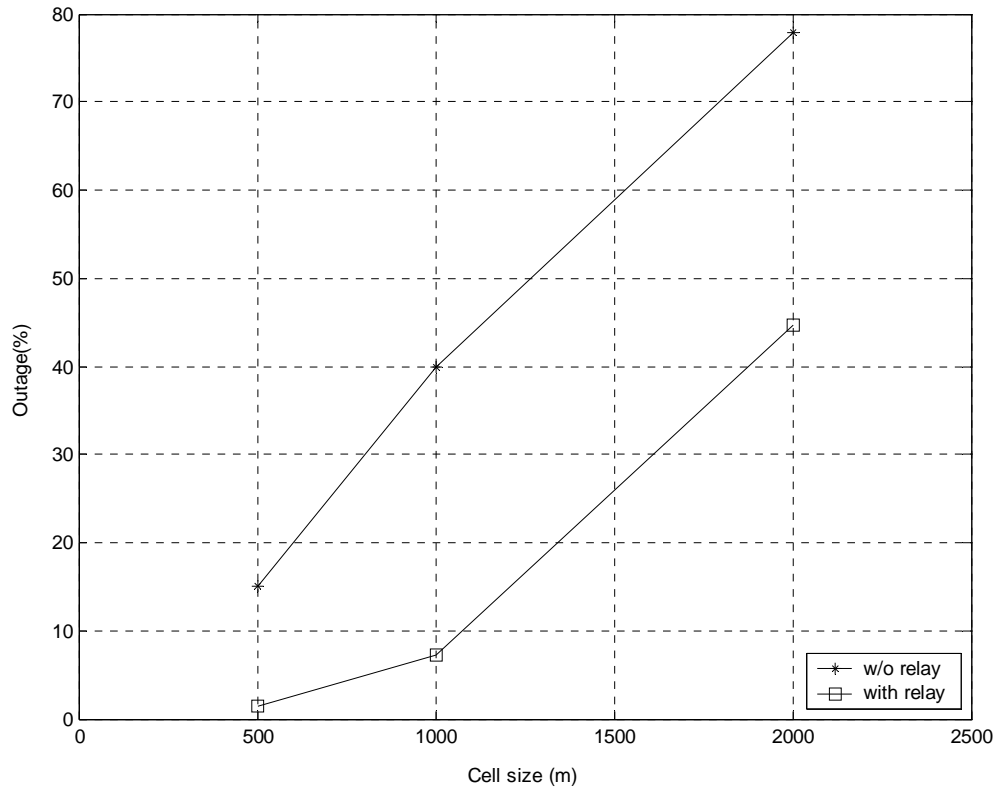


Figure 4.27: Outage results for different cell sizes (SINR-based relay selection algorithm, $P_{rel} = 1$ W, $N = 4$).

Chapter 5 Simulation Results, Part II: $N = 1$ Case

This chapter shows the results for cluster size $N = 1$ case. The simulation model for this case is established in Section 3.3. Some new aspects of the system are investigated for this case, including the coverage performance at various $SINR$ levels with respect to interference suppression factor, and the effect of changing relay positions.

5.1 Average Spectral Efficiency with respect to Interference Suppression Factor

Figures 5.1, 5.2 and 5.3 show the average spectral efficiency for the following values of the interference suppression factor (ISF): 0, 0.1, 0.2 and 1. From these three figures we can see that there are always throughput gains when the relays are incorporated. When $ISF = 1$, i.e., there is no interference suppression at all, and the average throughput is significantly low as we expected. When $ISF = 0$, i.e., there is no interference from co-channel interferers and only thermal noise exists, the throughput in 2000 m and 1000 m cells is still quite low because larger cells are noise-limited systems. So we need to increase $EIRP$ (Effective Isotropic Radiated Power) value to increase the throughput. However, in 500 m cells, when $ISF = 0$, the throughput is quite high, which suggests that smaller cells are interference-limited systems.

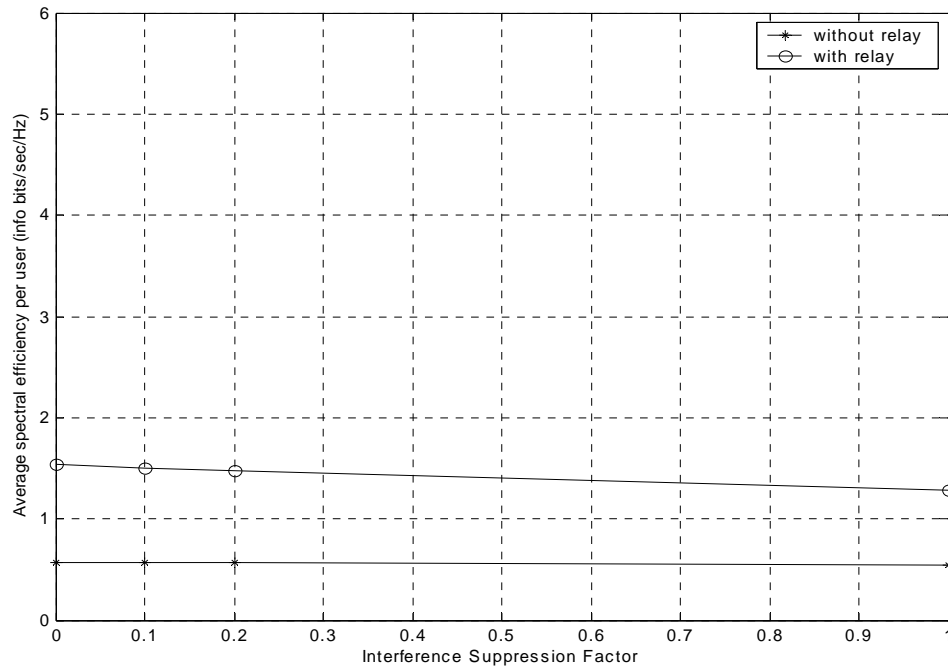


Figure 5.1: Average spectral efficiency with respect to interference suppression factor (SINR-based algorithm, $P_{rel} = 1$ W, $R = 2000$ m, $N = 1$, no diversity).

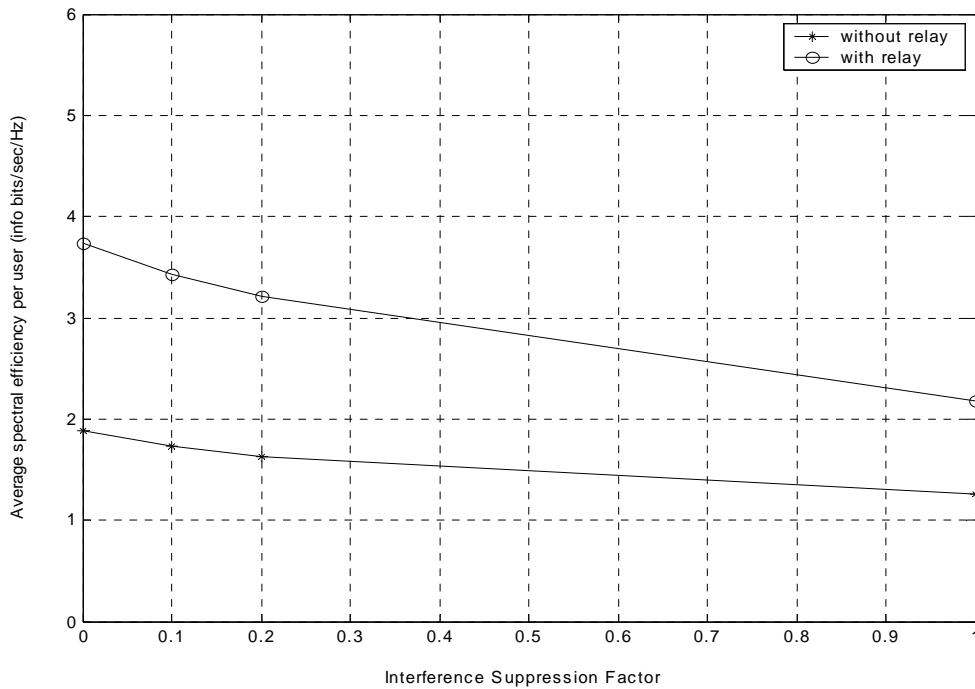


Figure 5.2: Average spectral efficiency with respect to interference suppression factor (SINR-based algorithm, $P_{rel} = 1$ W, $R = 1000$ m, $N = 1$, no diversity).

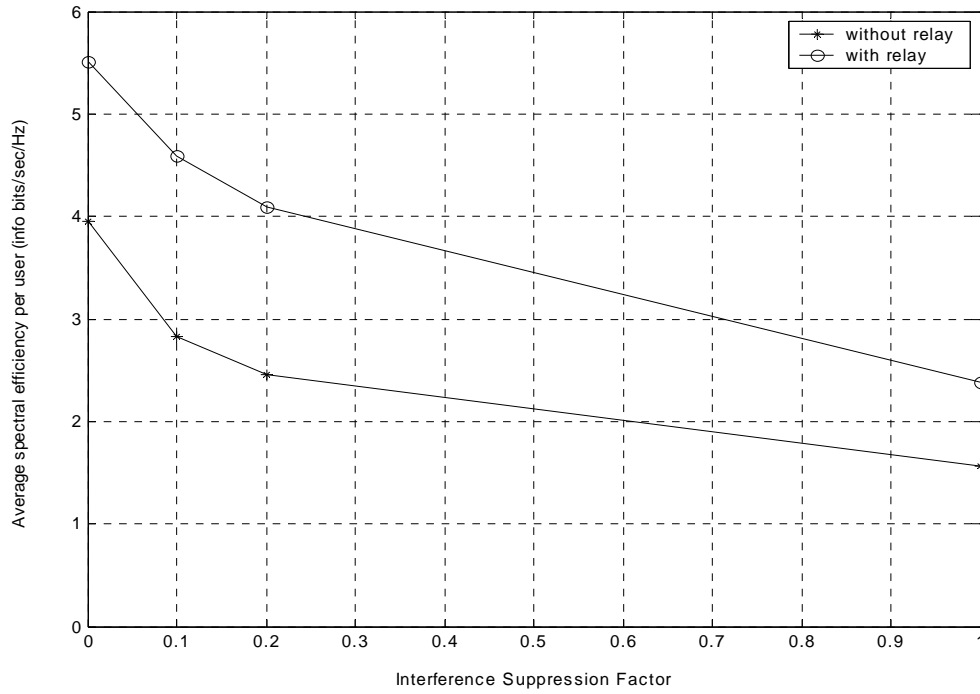


Figure 5.3: Average spectral efficiency with respect to interference suppression factor (SINR-based algorithm, $P_{rel} = 1$ W, $R = 500$ m, $N = 1$, no diversity).

5.2 Coverage at Various SINR Levels with respect to Interference Suppression Factor

Figures 5.4, 5.5 and 5.6 show the coverage performance, i.e., the probability of SINR being greater than the values given in the horizontal axis (4, 6, 8, ... , 26 dB) for 2000 m, 1000 m and 500 m cells, respectively. All the three figures indicate that when there are relays in the systems, the coverage can be greatly enhanced.

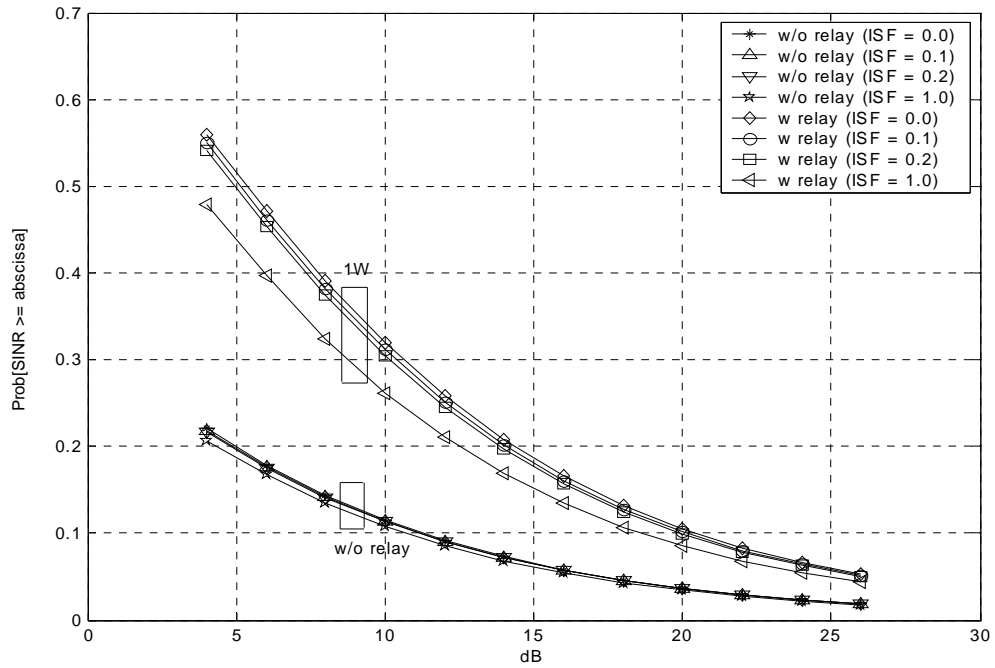


Figure 5.4: Coverage at various $SINR$ levels with respect to interference suppression factor (SINR-based algorithm, $P_{rel} = 1$ W, $R = 2000$ m, $N = 1$, no diversity).

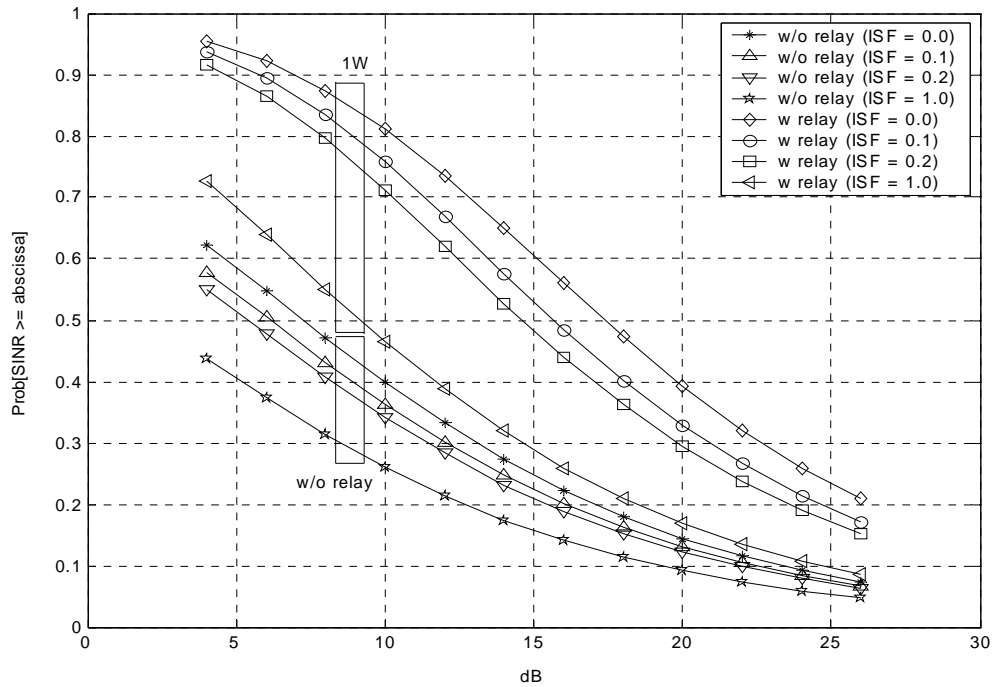


Figure 5.5: Coverage at various $SINR$ levels with respect to interference suppression factor (SINR-based algorithm, $P_{rel} = 1$ W, $R = 1000$ m, $N = 1$, no diversity).

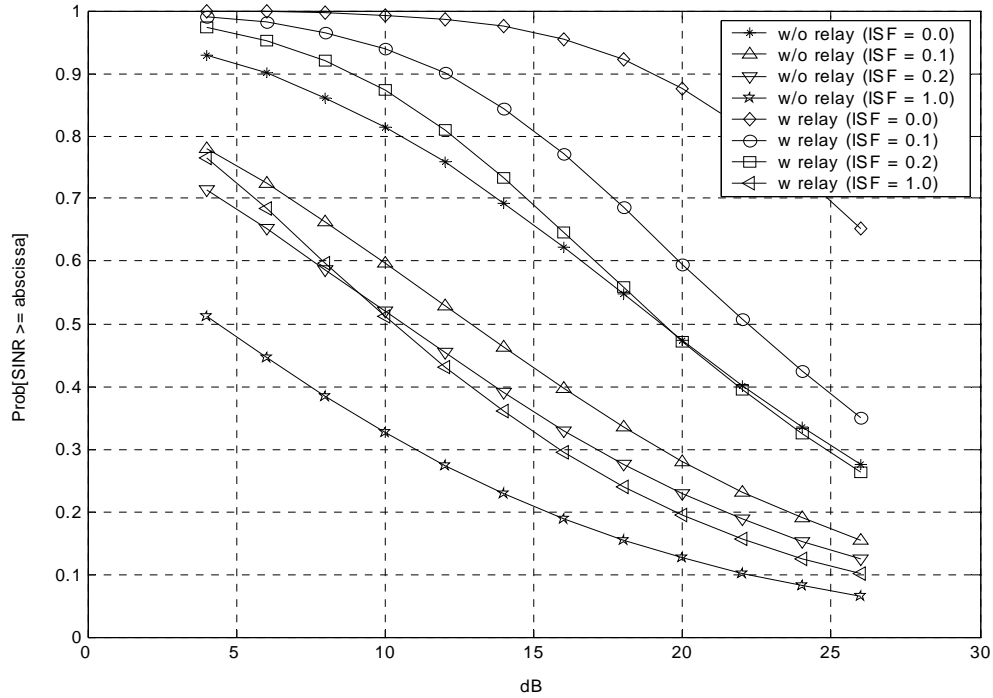


Figure 5.6: Coverage at various *SINR* levels with respect to interference suppression factor (SINR-based algorithm, $P_{rel} = 1$ W, $R = 500$ m, $N = 1$, no diversity).

5.3 Average Spectral Efficiency with respect to Relay Positions

Figure 5.8 shows the average spectral efficiency with respect to the relay positions for 1000 m and 500 m cells. As discussed in Section 2.3, the relays are placed on the segment between the centre and one corner of that cell. Here the relay position is indicated by a parameter m showing how far away the relay is from the BS. Please refer to Figure 5.7.

$$m = \frac{a}{R},$$

where a is the distance from the BS to the relay, R is the distance from the BS to one corner of the cell. In the simulation, the following m values are examined: 0, 0.1, 0.2, ...,

1. In addition, the results corresponding to the m values that are $2/3$, $3/4$ and $7/8$ are also given out in Figure 5.8. The results for the $m = 0$ case corresponds to the no relay case. The simulation results show that the best range for the relay position is $2/3$ to $3/4$ away from the BS, when the transmit power ratio of the BS and the relay is 10:1. It agrees with our relay position design in Section 2.3.

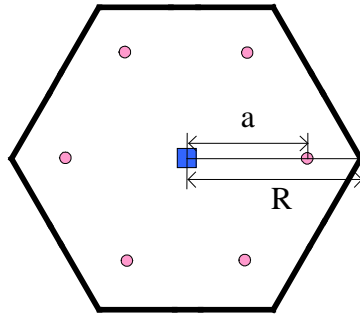


Figure 5.7: Relay position.

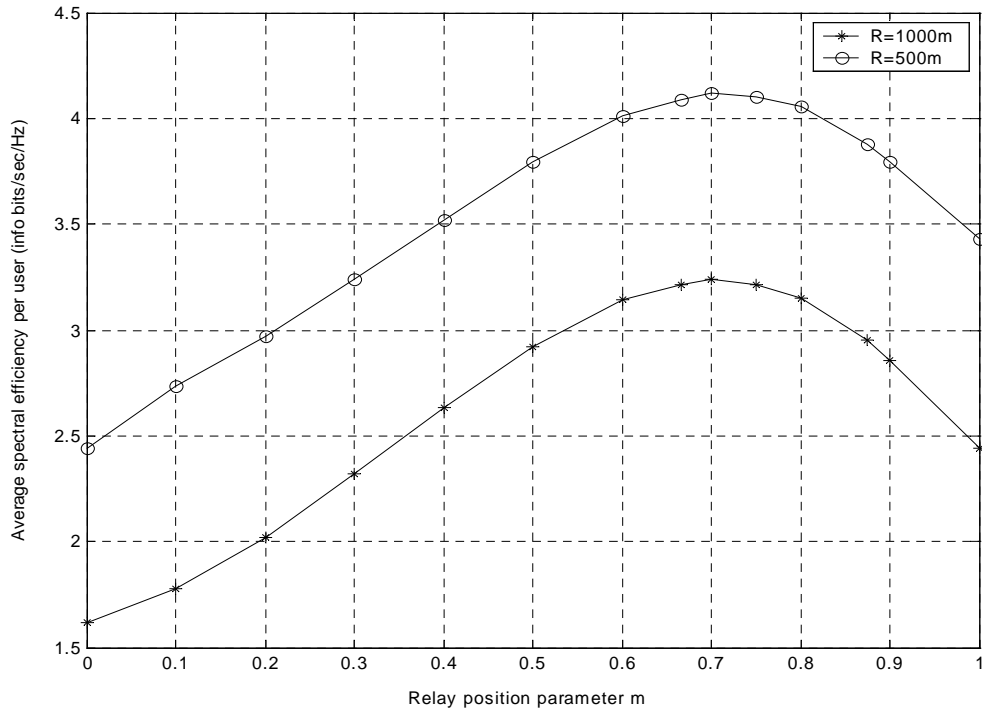


Figure 5.8: Average spectral efficiency with respect to relay positions (SINR-based relay selection algorithm, with relay, $P_{rel} = 1\text{ W}$, $N = 1$, $ISF = 0.2$).

Figures 5.9 and 5.10 show the relay usage situation when the relays are located at four different positions when $R = 1000$ m. It is observed that when relays are located at $1/2$ or $2/3$ away from the BSs, more users communicate with the relays and also the probability that ORB happens is correspondingly higher. When the relays are moved closer to or farther away from the BS, fewer users will communicate with the relays.

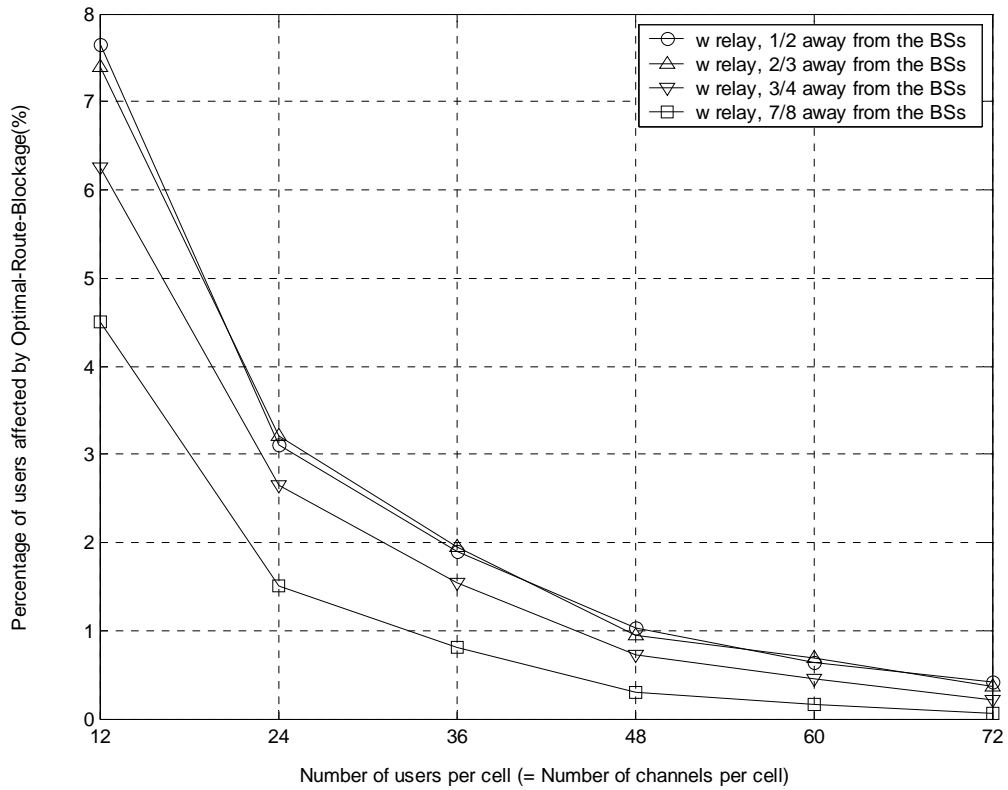


Figure 5.9: Percentage of users affected by Optimal-Route-Blockage (SINR-based relay selection algorithm, $R = 1000$ m, $ISF = 0.2$, $P_{rel} = 1$ W, $N = 1$).

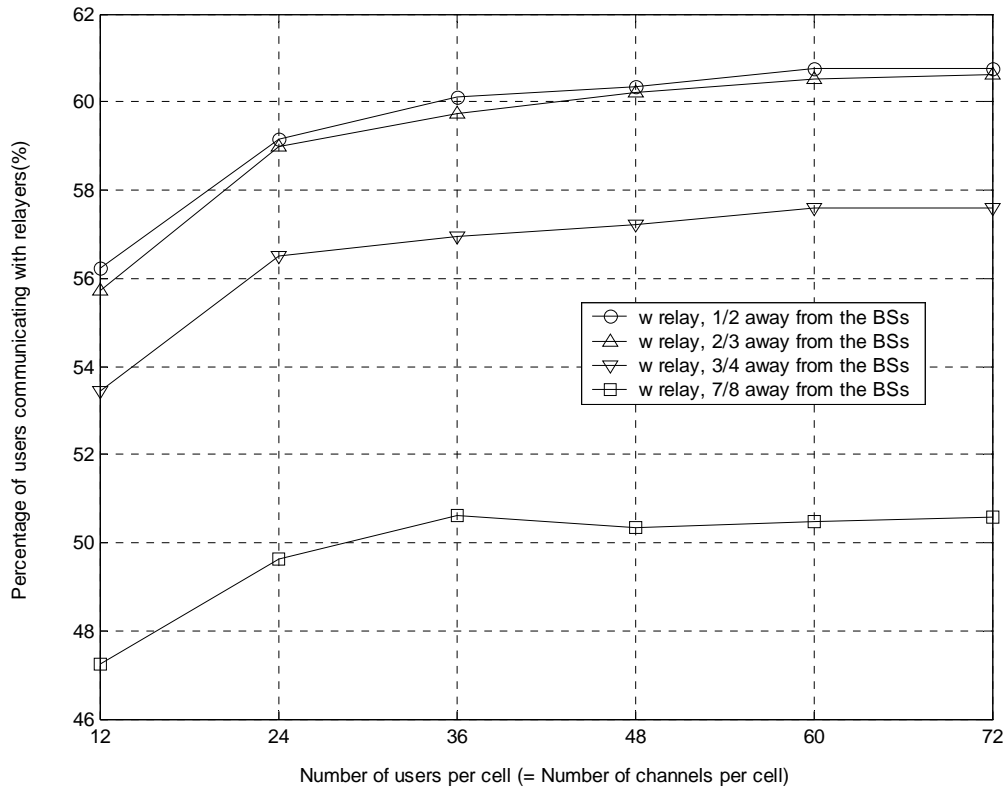


Figure 5.10: Percentage of users communicating with relays(SINR-based relay selection algorithm, $R = 1000$ m, $ISF = 0.2$, $P_{rel} = 1$ W, $N = 1$).

5.4 Coverage Extension

Same as Section 4.10, conclusion of coverage extension can be drawn in the case of $N = 1$. Please refer to Figures 5.11 and 5.12 for details, where the coverage extension brought in by digital fixed relays is shown in average spectral efficiency and outage viewpoints, in various ISF values and cell sizes. No matter what ISF value the system chooses, the coverage can always be extended with the help of relays.

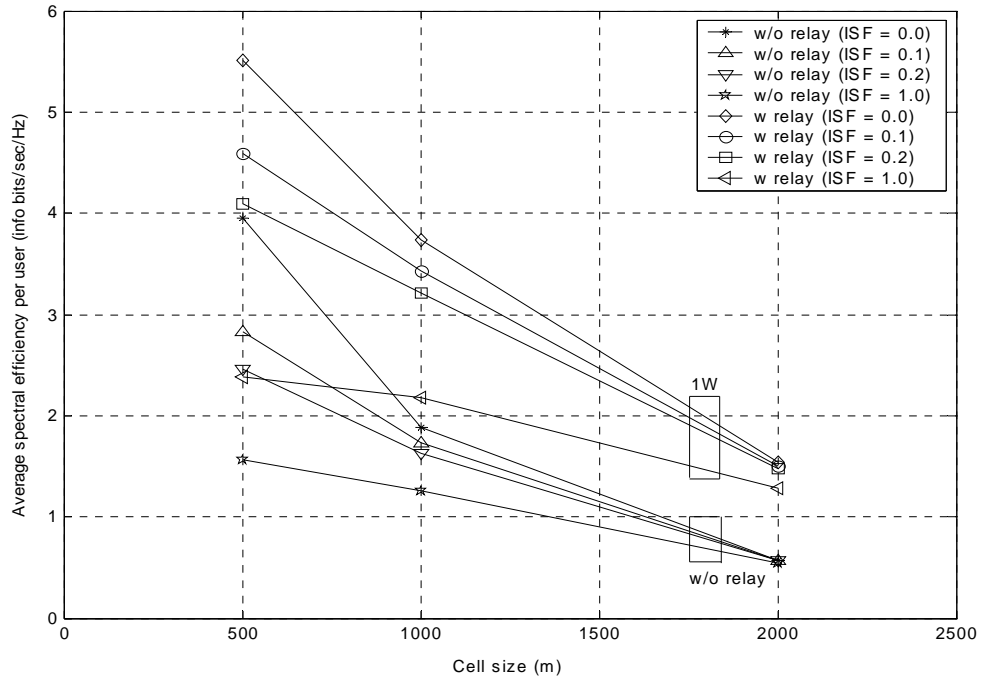


Figure 5.11: Average spectral efficiency for different cell sizes (SINR-based relay selection algorithm, $P_{rel} = 1 \text{ W}$, $N = 1$).

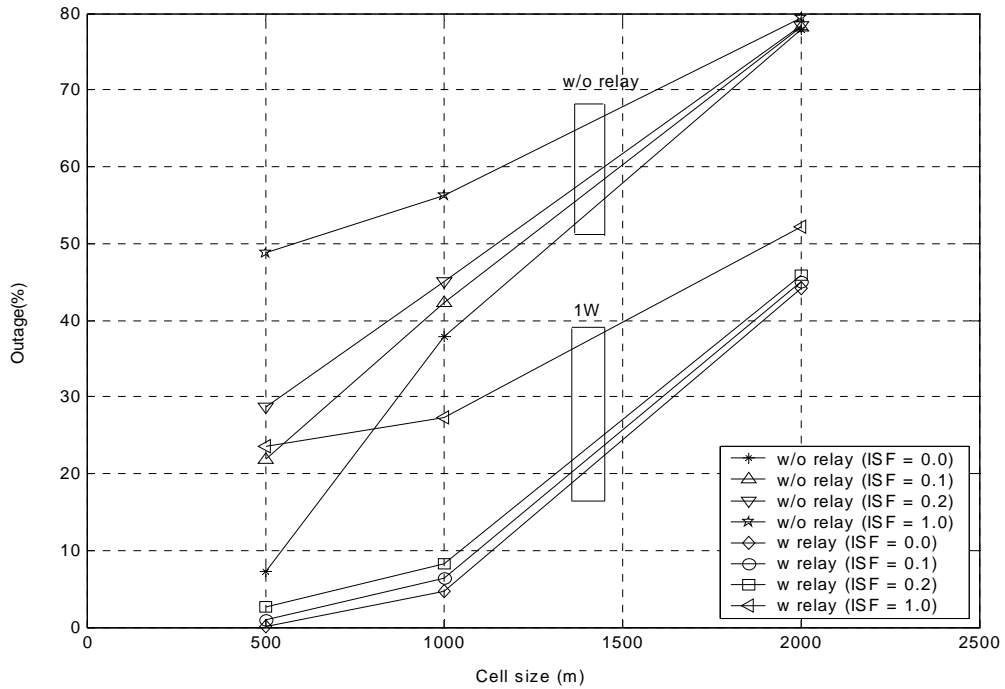


Figure 5.12: Outage results for different cell sizes (SINR-based relay selection algorithm, $P_{rel} = 1 \text{ W}$, $N = 1$).

Chapter 6 Conclusions and Discussions

6.1 Conclusions

This research studies the possible benefits that digital fixed relaying technology is able to provide for current and future cellular mobile networks. From the simulation results, we can conclude that digital fixed relaying is a simple yet effective approach to improve system throughput and high data rate coverage. Here are our observations:

First of all, in the new proposed network infrastructure, channel reuse is even denser due to the fact that the relaying channels are acquired through the reuse of existing channels, which will subsequently cause extra interference. However, simulation results still show that there are throughput improvements even if this extra interference is taken into account. Another point worth mentioning is the following: the simulation results indicate that with this relaying channel reuse design, ORB happens infrequently.

Secondly, the highest AMC combination utilized in this simulation is 64-QAM with code rate 1, corresponding to 6 bits/sec/Hz. As shown in the histograms 4.23 and 4.25 in Chapter 4, with the incorporation of relaying, the average received $SINR$ by a UE is increased and therefore, the majority percentage of UEs are using the highest AMC combination. As can be imagined, there must be UEs whose receiving $SINR$ is much higher than 26 dB, which are limited to use the combination of 64-QAM and code rate 1. And it can be anticipated that better results can be achieved when implementing higher AMC levels, for example 128-QAM and various code rate for these UEs. This is especially the case for small cells. So for nomadic applications in small cells, using higher AMC levels is recommended.

Thirdly, regarding the three relay selection algorithms, the advantages and disadvantages are analyzed thoroughly for each of them. The distance-based algorithm is the easiest to implement with the assistance of GPS (Global Positioning System) technology, but it brings in the least throughput increase; the SINR-based algorithm produces the greatest throughput improvement, however it involves more signalling overheads; the performance of the pathloss-based algorithm works in the middle.

Furthermore, as far as the relay position is concerned, we can tell from the simulation results that the best performance can be attained with the placement of relays at 2/3 to 3/4 away from the BS, when the transmit power ratio of the BS and the relay is 10:1. Nearer or farther from the BS will weaken the SINR values.

Moreover, two-path diversity is incorporated in the SINR-based algorithm and this proves that a further throughput increase can be obtained but at a very modest level. It is worth pointing out that diversity does not require any extra bandwidth or transmit power.

Two different cell cluster sizes, $N = 1$ and $N = 4$, are investigated as well. It can be concluded that digital fixed relaying technology works well in both cases.

Various values are applied to the pathloss propagation exponent n , i.e., 2.5, 3, 3.5, 4, 4.5 and 5. For all values of n , throughput improvements are observed consistently with the implementation of digital fixed relays.

6.2 Thesis Contributions

This section provides a summary of various highlights that contribute to this thesis.

- A proposal of a novel cellular infrastructure with the addition of digital fixed relays in the conventional cellular networks, along with three relay selection schemes and a

pre-configured relaying channel partition scheme to be used for relaying channel selection which can be applied to any cluster sizes. This is the primary contribution of this thesis.

- A series of simulations that support the intuitive idea provided in this thesis that digital fixed relaying technology coupled with the adoption of AMC scheme enhances the throughput and coverage of the cellular networks and realize the ubiquitous high data rate coverage in the entire network.
- A simulation comparison among different relay selection algorithms.
- A simulation to show that incorporating diversity can further increase the system throughput and coverage, though not much.
- A simulation to verify that digital fixed relays work well for both cluster size $N = 4$ and $N = 1$ cases and for various system parameters (propagation exponents, cell sizes, relay locations, etc.)

6.3 Future Research

This research opens up a series of interesting subjects for future work:

1. Load balancing is another possible benefit that digital fixed relays might be able to offer. When the traffic in a certain BS is overloaded, the relay may be able to divert an amount of traffic to the neighbouring BSs with extra resources, and thus the entire traffic load is well balanced.
2. The digital fixed relaying in this research is a two-hop technology, which raises a possible future research of exploring the advantages and disadvantages of digital

fixed relaying with more than two hops, i.e., the multi-hop digital fixed relaying technology.

3. The relaying channel partition scheme in this research is solely based on pessimistic assumptions: no existing radio channels can be reserved for relaying purpose. However, if sometimes the radio resources are abundant, one may consider reserving a part of radio channels for relaying channels, and ascertain the advantages and shortcomings it may generate.
4. The two-path diversity is employed in this research. Other diversity techniques may also be considered in future research to bring unique advantages to the system performance.
5. The study of digital fixed relaying for UEs when they are in mobility is another key research area.
6. Antenna techniques have advanced rapidly in recent years. The investigation of digital fixed relaying combined with different antenna techniques is recommended as well.
7. This research is focused on the benefits that digital fixed relaying can provide for circuit switched data, i.e., data transferred in continuous queues, but we notice that packet switched data has been highly demanded in modern cellular networks as well. Packet switched data happens when data are transferred in large packets or bursts, and it is suitable for large amounts of data transmission. The study of how digital fixed relaying can serve packet switched data transmission will definitely be a promising subject.

References

- [1] Y. D. Lin and Y. C. Hsu, "Multihop cellular: a new architecture for wireless communications", *IEEE INFOCOM'00*, pp. 1273-1282, 2000.
- [2] M. O. Hasna and M. Alouini, "Performance analysis of two-hop relayed transmissions over Rayleigh fading channels", *IEEE 56th Vehicular Technology Conference (VTC'02)*, pp. 1992-1996, 2002.
- [3] H. Wu, C. Qiao, S. De and O. Tonguz, "Integrated cellular and ad hoc relaying systems: iCAR", *IEEE Journal on Selected Areas in Communications (JSAC)*, vol. 19, no. 10, pp. 2105-2115, October 2001.
- [4] V. Sreng, "Coverage Enhancement through Two-Hop Relaying in Cellular Radio Systems", M.A.Sc. Thesis, supervisors: H. Yanikomeroglu and D. D. Falconer, Carleton University, 2002.
- [5] H. Yanikomeroglu, "Fixed and mobile relaying technologies for cellular networks", *Second Workshop on Applications and Services in Wireless Networks (ASWN'02)*, pp. 75-81, July 2002.
- [6] E. Armanious, D. D. Falconer, and H. Yanikomeroglu, "Adaptive modulation, adaptive coding, and power control for fixed cellular broadband wireless systems", *IEEE Wireless Communications and Networking Conference (WCNC'03)*, March 2003.
- [7] G. Cair, G. Taricco, and E. Biglieri, "Bit-interleaved coded modulation," *IEEE Trans. Info. Theory*, vol. 44, no. 3, pp. 927-946, May 1998.

- [8] V. Sreng, H. Yanikomeroglu, and D. D. Falconer “Capacity enhancement through two-hop relaying in cellular radio systems”, *IEEE Wireless Communications and Networking Conference (WCNC'02)*, 2002.
- [9] T. S. Rappaport, *Wireless Communications: Principles and Practice*, Prentice Hall PTR, 2002.
- [10] X. Tang, “Coverage Enhancement with Analog Fixed Relaying in Cellular Radio Networks”, M.A.Sc. Thesis, supervisor: D. D. Falconer, Carleton University, 2003.
- [11] C. Qiao, H. Wu, and O. Tonguz, “Load balancing via relay in next generation wireless systems,” Proc. of *Mobile and Ad Hoc Networking and Computing Conference*, 2000.
- [12] T. S. Rappaport, et. al, “Position Location Using Wireless Communications on Highways of the Future,” *IEEE Communications Magazine*, pp. 30-37, Oct. 1996.
- [13] J. H. Reed, et. al, “An Overview of the Challenges and Progress in Meeting the E-911 Requirement for Location Service,” *IEEE Communications Magazine*, pp. 30-37, Apr. 1998.
- [14] E. Zehavi, “8-PSK trellis codes for a Rayleigh channel,” *IEEE Trans. Commun.*, vol. 40, pp. 873-884, May 1992.
- [15] S. Y. Le Goff, “Signal Constellations for Bit-Interleaved Coded Modulation”, *IEEE Trans. Info. Theory*, vol. 49, no. 3, May 1998.
- [16] D. Walsh, “Relaying Using the Unlicensed Bands in Cellular CDMA Networks”, M.A.Sc. Thesis in progress, supervisor: H. Yanikomeroglu, Carleton University.

- [17] Branimir Vojcic, Raymond Pickholtz, Dezso Vekasky and Michael Souryal, “Throughput Analysis of Cellular Multihop Networks”, report submitted to Nortel Networks.
- [18] J. Boyer, “Multihop Wireless Communications Channels”, M.A.Sc. Thesis, supervisor: D. D. Falconer and H. Yanikomeroglu, Carleton University, 2001.
- [19] S. Hares, H. Yanikomeroglu, and B. Hashem, “A relaying algorithm for multihop TDMA TDD networks using diversity”, accepted to *IEEE Vehicular Technology Conference*, October 2003.
- [20] E. Armanious, “Link adaptation techniques for cellular fixed broadband wireless access”, M.A.Sc. Thesis, supervisor: H. Yanikomeroglu and D. D. Falconer, Carleton University, 2003.
- [21] A. Sendonaris, E. Erkip, and B. Aazhang, “User Cooperation Diversity – Parts I and II,” to appear in *IEEE Trans. on Communications*.
- [22] J. Boyer, D. D. Falconer, and H. Yanikomeroglu, “A theoretical characterization of the multihop wireless communications channel with diversity”, *IEEE Globecom*, 2001.
- [23] J. Boyer, D. Falconer, and H. Yanikomeroglu, “Multihop wireless communications channels”, submitted to *IEEE Transactions on Communications*, April 2003.
- [24] J. Boyer, D. D. Falconer, and H. Yanikomeroglu, “A theoretical characterization of the multihop wireless communications channel without diversity”, *IEEE Int.’l Symposium on Personal, Indoor, and Mobile Radio Communications (PIMRC)*, 2001.

- [25] S. Nanda, K. Balachandran, and S. Kumar, "Adaptation techniques in wireless packet data services", *IEEE Communications Magazine*, vol. 38, no. 1, pp. 54-64, Jan. 2000.
- [26] A. Goldsmith and S. G. Chua, "Adaptive coded modulation for fading channels", *IEEE Transactions on Communications*, vol. 46, no. 5, pp. 595-602, May 1998.
- [27] K. Balachandran, S. R. Kadaba, and S. Nanda, "Channel quality estimation and rate adaptation for cellular mobile radio", *IEEE Journal in Selected Areas Commun.*, vol. 17, no. 7, pp. 1244-1256, July. 1999.
- [28] M. Turkboylari and G. L. Stuber, "An efficient algorithm for estimating the signal-to-interference ratio in TDMA cellular systems", *IEEE Trans. Commun.*, vol. 46, no. 6, pp. 728-731, July 1998.
- [29] H. Yanikomeroglu, D. D. Falconer, and V. M. Sreng, "Coverage enhancement through two-hop peer-to-peer relaying in cellular radio networks", *World Wireless Research Forum (WWRF) meeting no. 7*, Dec. 2002.
- [30] V. Sreng, H. Yanikomeroglu, D. Falconer, "Coverage enhancement through peer-to-peer relaying in cellular networks", submitted to *IEEE Transactions on Wireless Communications*, Sept. 2002.
- [31] V. Sreng, H. Yanikomeroglu, D. Falconer, "Peer selection strategies in peer-to-peer relaying in cellular networks", accepted to *IEEE Vehicular Technology Conference*, Fall, 2003.
- [32] S. Hares, H. Yanikomeroglu, and B. Hashem, "Multihop relaying with diversity in peer-to-peer networks", accepted to *IEEE Globecom*, December 2003.

Appendix A - Geometric Characteristic of Co-channel BSs and Relays for Cluster Size $N = 3$ and $N = 7$ Cases

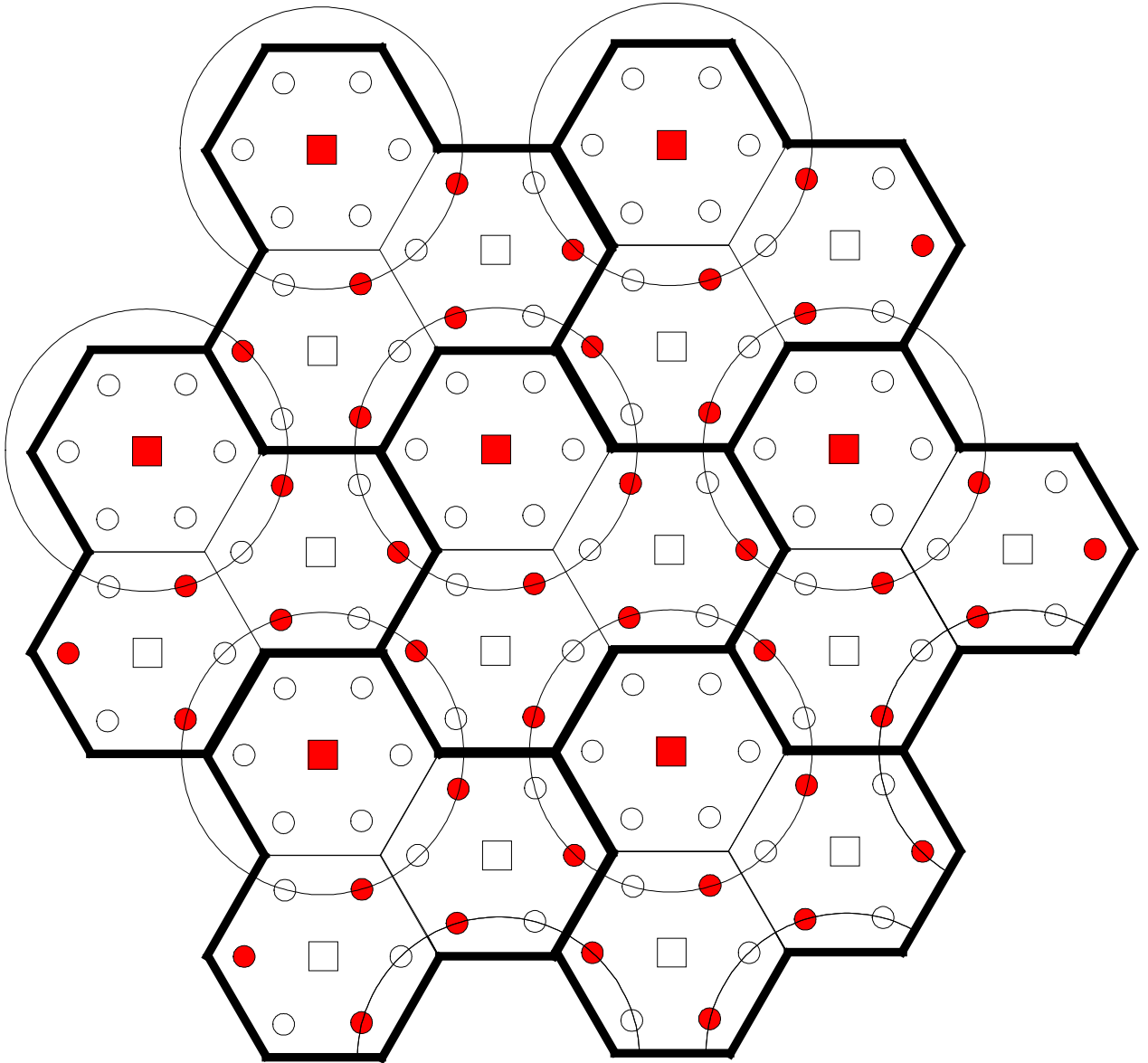


Figure A.1: Cluster size $N = 3$ case.

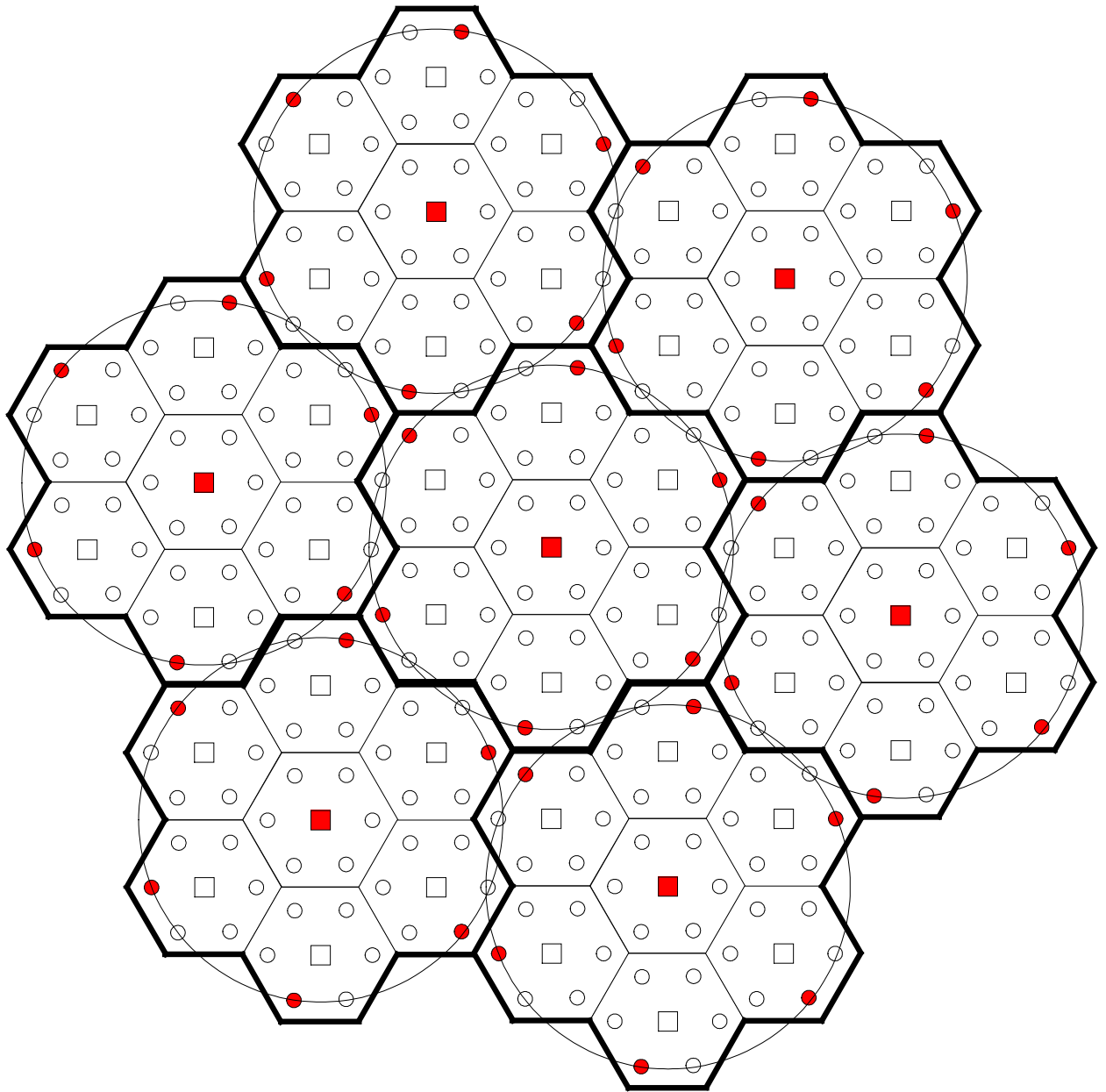


Figure A.2: Cluster size $N = 7$ case.

Appendix B - Proof of “the locus is a circle when meeting the condition the ratio of the distances of a moving point to two fixed points is a constant”

Let us suppose there is a moving point (x, y) and two fixed points (x_1, y_1) and (x_2, y_2) . If the ratio of the distances of (x, y) to (x_1, y_1) and (x_2, y_2) is a constant, it can be expressed as follows:

$$\frac{(x - x_1)^2 + (y - y_1)^2}{(x - x_2)^2 + (y - y_2)^2} = C \quad (1)$$

Which means

$$x^2 - 2x_1x + x_1^2 + y^2 - 2y_1y + y_1^2 = Cx^2 - 2Cx_2x + Cx_2^2 + Cy^2 - 2Cy_2y + Cy_2^2,$$

So

$$(C - 1)x^2 + (C - 1)y^2 + (2x_1 - 2Cx_2)x + (2y_1 - 2Cy_2)y + C(x_2^2 + y_2^2) - (x_1^2 + y_1^2) = 0. \quad (2)$$

We know from geometry that if the coefficients in front of the terms “ x^2 ” and “ y^2 ” are equal, and there is no “ xy ” term in the expression, then the locus meeting the above condition is a circle (if the coefficients in front of the terms “ x^2 ” and “ y^2 ” are different, the curve will be an ellipse, a hyperbola or a parabola). Expression (2) meets this requirement, therefore the locus representing (2) is a circle.

Now let us determine the center and radius of this circle. Continue with (2),

$$x^2 + y^2 + \frac{2x_1 - 2Cx_2}{C - 1}x + \frac{2y_1 - 2Cy_2}{C - 1}y + \frac{C(x_2^2 + y_2^2) - (x_1^2 + y_1^2)}{C - 1} = 0,$$

then

$$x^2 + \frac{2x_1 - 2Cx_2}{C-1}x + \left(\frac{2x_1 - 2Cx_2}{C-1}\right)^2 + y^2 + \frac{2y_1 - 2Cy_2}{C-1}y + \left(\frac{2y_1 - 2Cy_2}{C-1}\right)^2 = \left(\frac{2x_1 - 2Cx_2}{C-1}\right)^2 + \left(\frac{2y_1 - 2Cy_2}{C-1}\right)^2 - \frac{C(x_2^2 + y_2^2) - (x_1^2 + y_1^2)}{C-1},$$

therefore

$$\left(x + \frac{x_1 - Cx_2}{C-1}\right)^2 + \left(y + \frac{y_1 - Cy_2}{C-1}\right)^2 = \left(\frac{x_1 - Cx_2}{C-1}\right)^2 + \left(\frac{y_1 - Cy_2}{C-1}\right)^2 - \frac{C(x_2^2 + y_2^2) - (x_1^2 + y_1^2)}{C-1} \quad (3)$$

From (3) we can tell that the center of the circle is:

$$\left(-\frac{x_1 - Cx_2}{C-1}, -\frac{y_1 - Cy_2}{C-1}\right)$$

While the radius is:

$$\sqrt{\left(\frac{x_1 - Cx_2}{C-1}\right)^2 + \left(\frac{y_1 - Cy_2}{C-1}\right)^2 - \frac{C(x_2^2 + y_2^2) - (x_1^2 + y_1^2)}{C-1}}$$

In our case, the two fixed points are the BS (0, 0) and the rightmost relay (667, 0) respectively when $R = 1000$ m. So $x_1 = y_1 = y_2 = 0$, and $x_2 = 667$.

While $C = \sqrt{\frac{P_{BS}}{P_{rel}}} = \left(\frac{d_1}{d_2}\right)^2$, where P_{BS} is the BS transmit power, P_{rel} is the relay transmit

power, d_1 and d_2 are the distances between the BS and the UE and the relay and UE respectively. Assuming $P_{BS} = 10$ W and P_{rel} has different values in the following table,

we can come up with the corresponding values of C .

The next step is to calculate the center and radius of the circle, when $P_{BS} = 10$ W and P_{rel} is a variable based on the following table. Note: We only show the center and radius of the circle at the very right hand side. The centers and radii of other circles can easily be

figured out. Table B.1 shows the locus information based on various P_{rel} values when $R = 1000$ m.

Table B.1: Locus information based on various P_{rel} values ($R = 1000$ m)

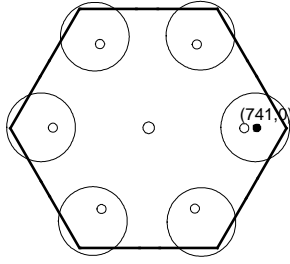
$P_{rel}(W)$	C	Center Coordinates	Radius
0.1	10	(741,0)	234
0.3	5.77	(807,0)	336
1	3.16	(976,0)	549
3	1.83	(1471,0)	1087
9	1.05	(14007,0)	13669
9.9	1.005	(134067,0)	134400
10	1	Note: This is a special case. The locus corresponding to the right most relay will be a straight line passing through (333,0), perpendicular to the X axis.	
10.1	0.995	(-132733,0)	133066
11	0.953	(-13524,0)	13854
30	0.58	(-921,0)	1209
100	0.32	(-314,0)	555

The following figures show the loci in different values of P_{rel} . The observations drawn from these figures are:

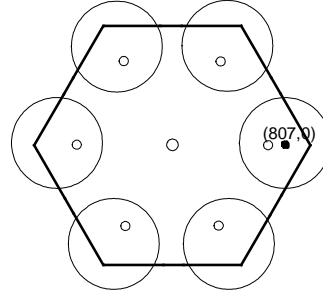
- 1) $P_{rel} \leq P_{BS}$, namely P_{rel} is between 0 and 10 W. The higher the P_{rel} is, the center of the circle will move away from the BS, the larger the radius will be, meaning the larger the circle will be. This clearly demonstrates that the higher the P_{rel} is, the larger coverage area it will be able to handle. A UE will receive a stronger signal from the BS anywhere outside the circle but inside the hexagon; but will receive a stronger signal from the relay anywhere inside the circle but outside the

hexagon. It is a special case when P_{rel} equals P_{BS} (10 W). The locus is a straight line perpendicular to the X-axis. As we know, a straight line can be regarded as a circle with its center infinitely far away from the BS and the radius is an infinite.

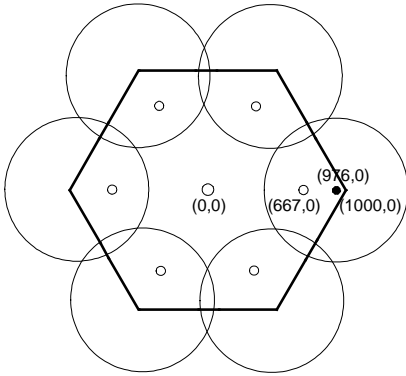
- 2) $P_{rel} \geq P_{BS}$, namely P_{rel} is no less than 10 W. The center of the circle moves to the other side of the relay creating this circle. The higher the P_{rel} is, the center of the circle will move towards the BS, the smaller the radius will be, meaning the smaller the circle will be. The coverage responsibility between the BS and the relay is on the contrary to the above scenario, e.g., a UE will receive a stronger signal from the BS anywhere inside the circle but outside the hexagon; but will receive a stronger signal from the relay anywhere outside the circle but inside the hexagon.



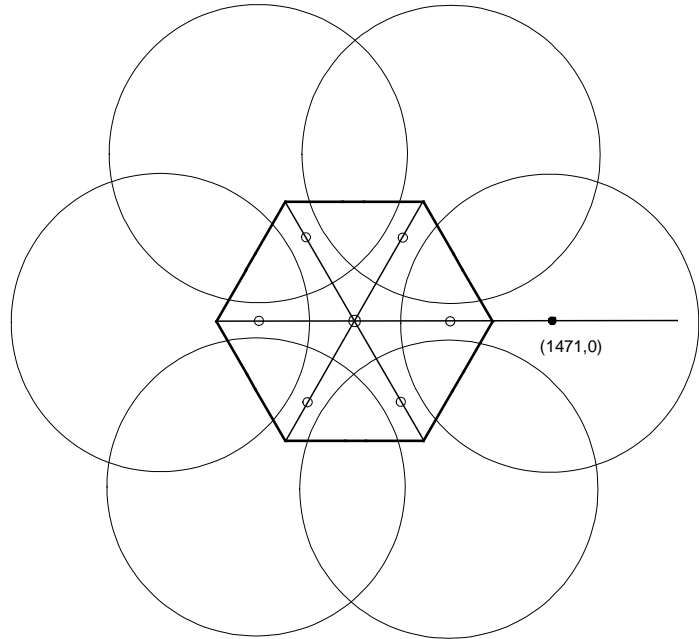
$$P_{BS} = 10 \text{ W}, P_{rel} = 0.1 \text{ W}, R_{circle} = 234 \text{ m}$$



$$P_{BS} = 10 \text{ W}, P_{rel} = 0.3 \text{ W}, R_{circle} = 336 \text{ m}$$

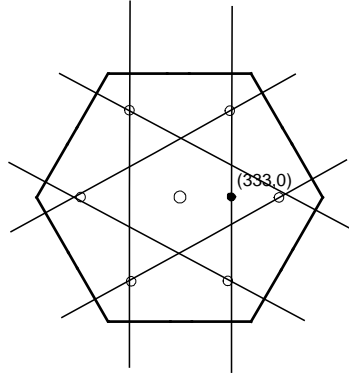


$$P_{BS} = 10 \text{ W}, P_{rel} = 1 \text{ W}, R_{circle} = 549 \text{ m}$$

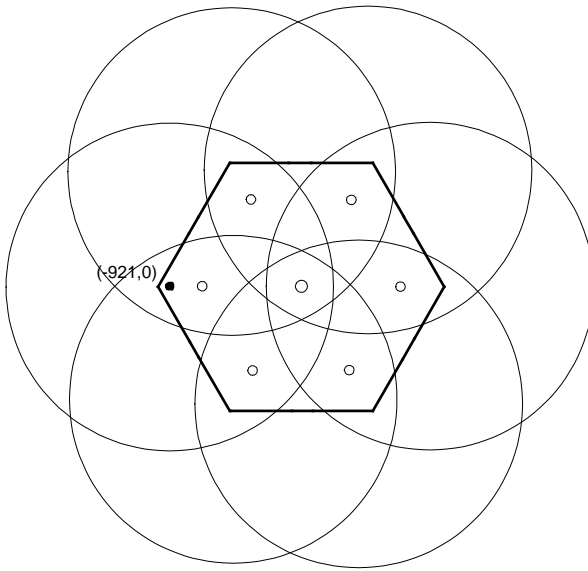


$$P_{BS} = 10 \text{ W}, P_{rel} = 3 \text{ W}, R_{circle} = 1087 \text{ m}$$

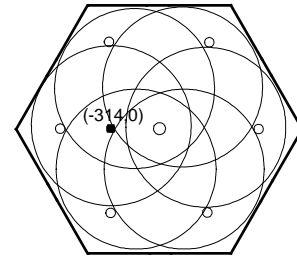
Figure B.1: Distance-based relay selection in various relay transmit power settings, $R = 1000 \text{ m}$.



$P_{BS} = 10 \text{ W}, P_{rel} = 10 \text{ W}, 6 \text{ straight lines.}$



$P_{BS} = 10 \text{ W}, P_{rel} = 30 \text{ W}, R_{circle} = 1209 \text{ m}$



$P_{BS} = 10 \text{ W}, P_{rel} = 100 \text{ W}, R_{circle} = 555 \text{ m}$

Figure B.1: Distance-based relay selection in various relay transmit power settings, $R = 1000 \text{ m}$ (Continued).

Appendix C – Diversity Results for Cluster Size $N = 4$ and $N = 1$ cases

More simulation results with the incorporation of diversity in $N = 4$ and $N = 1$ cases are provided in this section.

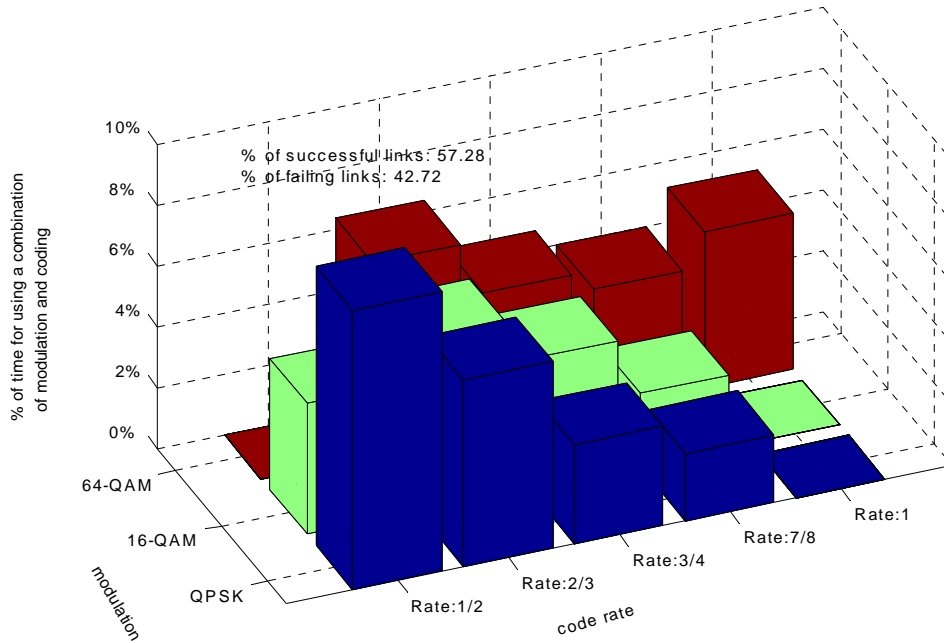


Figure C.1: Percentage of time using a combination of modulation and coding (with relaying, $P_{rel} = 1$ W, SINR-based relay selection algorithm, with diversity, $R = 2000$ m, $N = 4$).

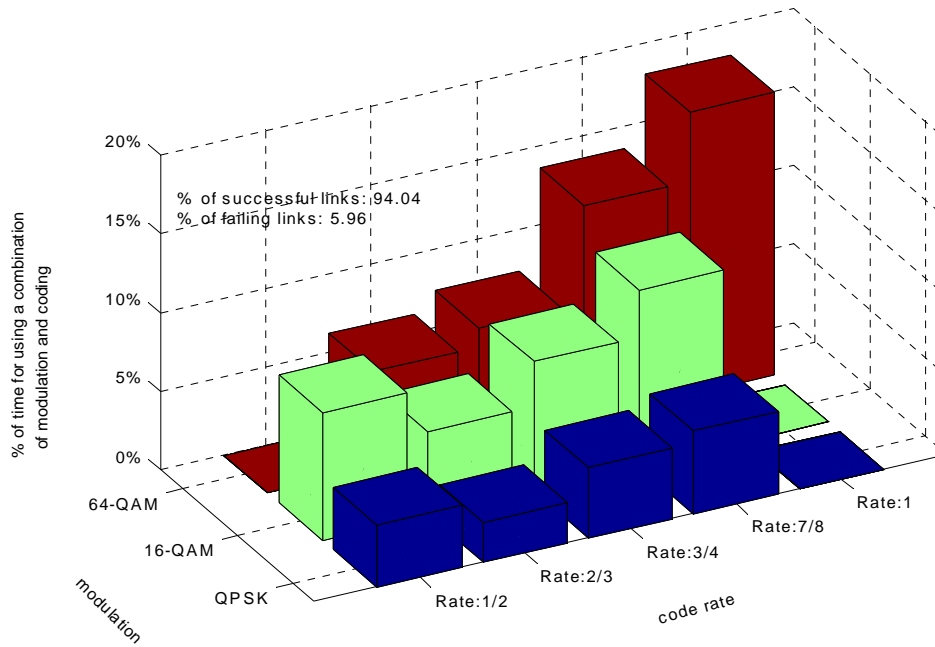


Figure C.2: Percentage of time using a combination of modulation and coding (with relaying, $P_{rel} = 1$ W, SINR-based relay selection algorithm, with diversity, $R = 1000$ m, $N = 4$).

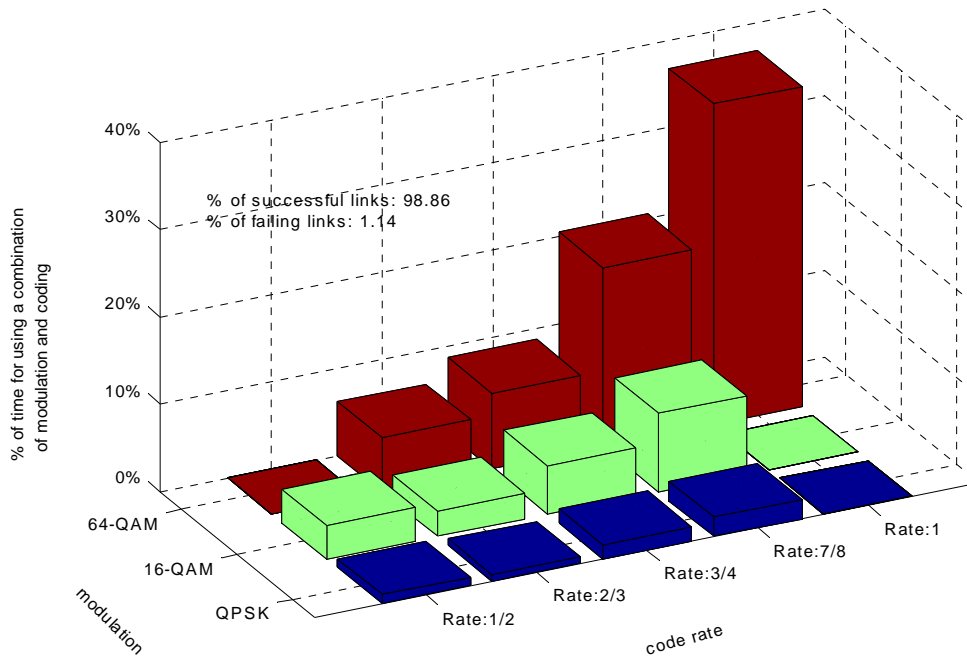


Figure C.3: Percentage of time using a combination of modulation and coding (with relaying, $P_{rel} = 1$ W, SINR-based relay selection algorithm, with diversity, $R = 500$ m, $N = 4$).

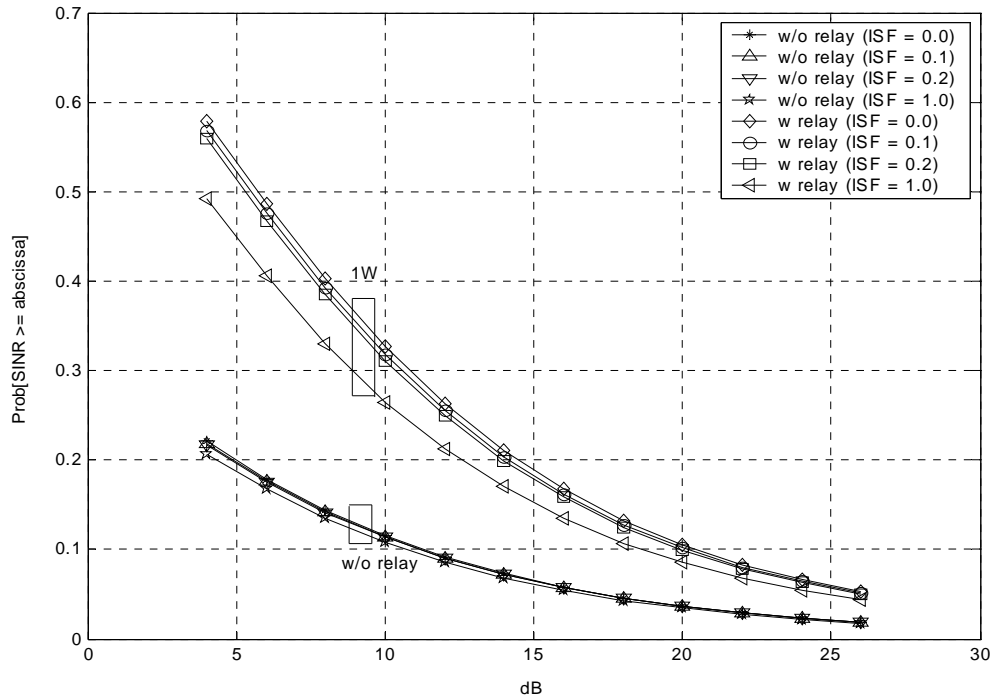


Figure C.4: Coverage at various $SINR$ levels with respect to interference suppression factor (SINR-based algorithm, $P_{rel} = 1$ W, $R = 2000$ m, $N = 1$, with diversity).

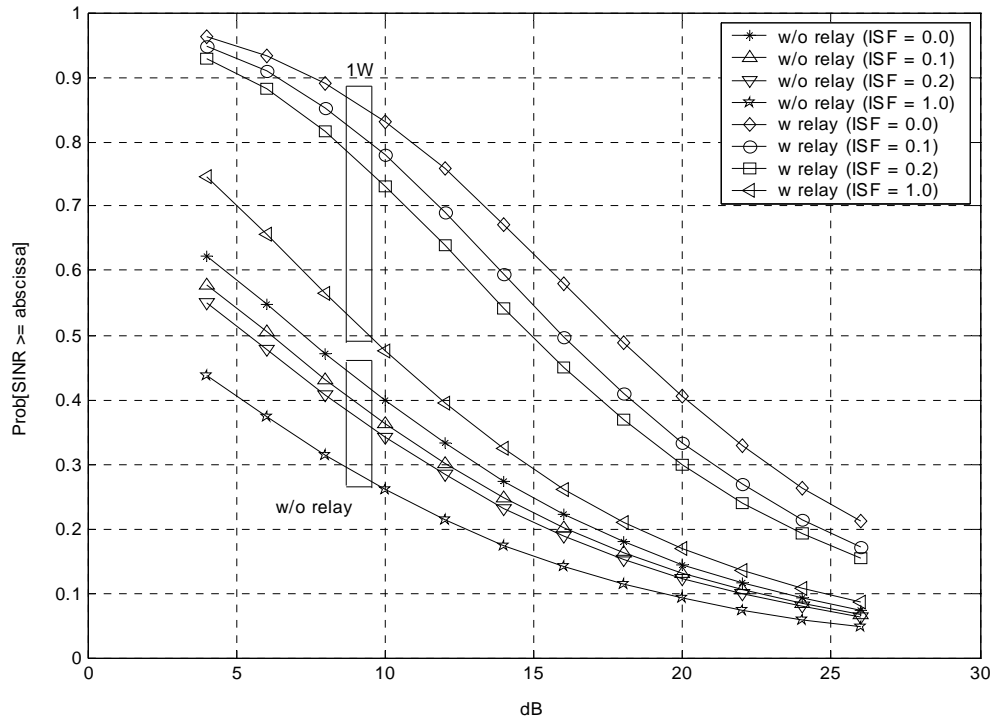


Figure C.5: Coverage at various $SINR$ levels with respect to interference suppression factor (SINR-based algorithm, $P_{rel} = 1$ W, $R = 1000$ m, $N = 1$, with diversity).

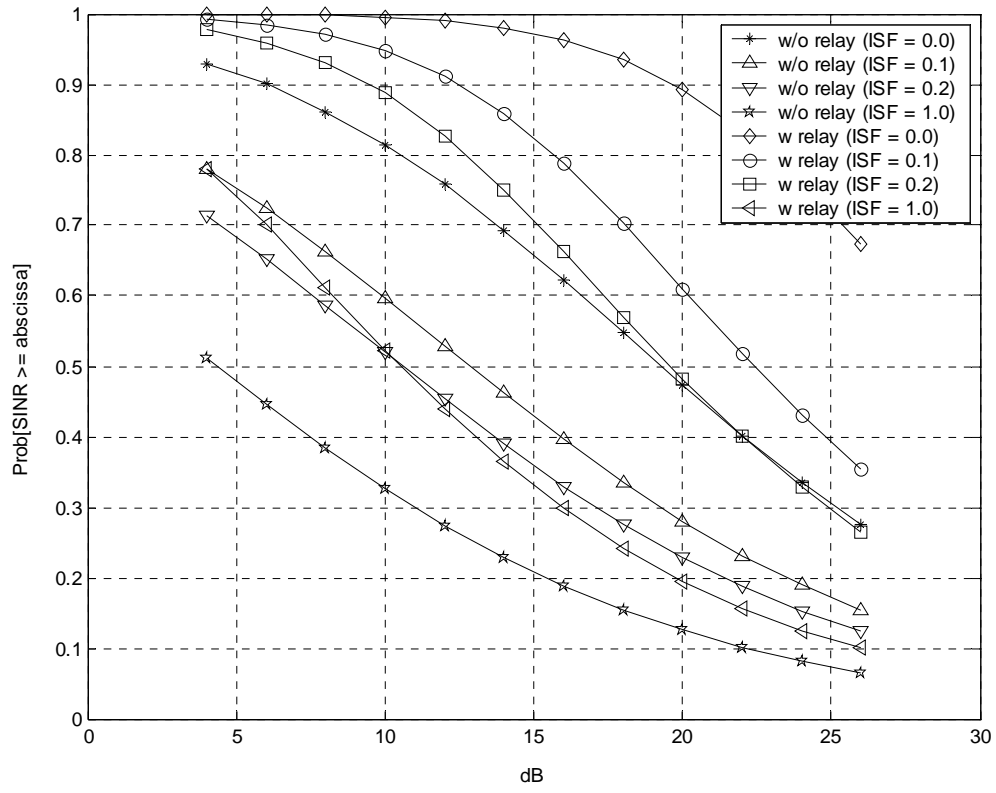


Figure C.6: Coverage at various *SINR* levels with respect to interference suppression factor (SINR-based algorithm, $P_{rel} = 1$ W, $R = 500$ m, $N = 1$, with diversity).